DEOXYGENATION OF HEPTANOIC ACID OVER COBALT SUPPORTED SILICA CATALYSTS

PLOYNISA PHICHITSURATHAWORN

A THESIS SUBMITTED IN PARTIAL FULFILLMENT OF THE REQUIREMENT FOR THE DEGREE OF MASTER OF SCIENCE IN PETROCHEMICALS AND HYDROCARBON CHEMISTRY

DEPARTMENT OF CHEMISTRY

FACULTY OF SCIENCE

KING MONGKUT'S INSTITUTE OF TECHNOLOGY LADKRABANG

2018

KMITL-2018-SC-M-015-001

Thesis Title	Deoxygenation of heptanoic acid over cobalt supported silica catalysts
Student Name	Ploynisa Phichitsurathaworn
Student ID	58605037
Degree	Master of Science (Petrochemicals and hydrocarbon chemistry)
Department	Chemistry
Year	2018
Thesis Advisor	Assoc. Prof. Dr. Tawan Sooknoi
Thesis Co-advisor	Dr. Kittisak Choojun

Abstract

In this thesis, the conversion of fatty acid to α–olefins over investigated via the deoxygenation of heptanoic acid to hexene using metal supported silica catalysts as a model reaction. Catalysts studied include monometallic catalysts (Co, Ni, Cu and Cr) and Co bimetallic catalysts (Co-Pt, Co-Au, Co-Pd, Co-Ru). The reduction temperature of Co bimetallic is lower than Co monometallic. The catalytic deoxygenation of heptanoic acid was tested in the continuous flow fixed-bed reactor process at 350 – 425 °C under H_2 atmosphere. It was found that 5%Co/SiO_2 shows high activity, as compared to other monometallic catalysts and gave hexene as a major product via reduction/ decarbonylation of heptanoic acid and minor products, such as, light hydrocarbons (C1-C5), hexane, heptene, heptanal, and 7-tridecanone were also observed. However, 5%Co/SiO_2 shows deactivation due to strong adsorption of feed (heptanoic acid) over Co active surface. The incorporation of Pt to Co based catalysts gives relatively high stability, as compared to the Co-Au, Co-Pd, Co-Ru over SiO_2 and monometallic Co/SiO_2, resulting the yield of hexene as a major product with some yield of hexane. Co-Pt/SiO_2 prepared by co-impregnation method shows higher stability than that prepared by sequential impregnation method. The stability is also increased with Pt content. The deoxygenation of heptanoic acid over cobalt supported silica catalysts proceeds via reduction of heptanoic acid to heptanal that is an intermediate for decarbonylation to hexene.

Keywords : Deoxygenation, Heptanoic acid, Cobalt, α-olefins

ACKNOWLEDGEMENT

The authors take this opportunity to acknowledge advisors Assoc.Prof.Dr. Tawan Sooknoi and co-advisor Dr. Kittisak Choojun, for the continually suggestion, graceful knowledge and useful discussion throughout this research.

I am grateful to Dr. Amnat Permsubsakul, Asst. Prof. Dr. Sutha Sutthiruangwong and Prof. Dr. Apanee Luengnaruemitchai for serving as the chairperson and the committee, and for valuable comments.

I would like to acknowledge the financial support from the Thailand Research Fund, granted to Assoc. Prof. Tawan Sooknoi (BRG5680007). I also appreciate the supports from the Department of Chemistry, Faculty of Science, King Mongkut's Institute of Technology Ladkrabang for the equipments, chemicals and facilities.

I would like to extend my thanks to Mr. Boonyawat Wuttitham, Mr. Thanasak Solos, Mr. Ayut Witsuthammakul, Mr. Porn-a-nan Arsa and Mr. Pratya Promchana for their help and advices in working the data analysis, support and encouragement.

I would like to extend my sincere appreciation to all teachers, friends and the member of this research group for their constant guidance, advice, support and encouragement.

Finally, I deeply appreciate and thank my parents and family for their love and supports.

Ploynisa Phichitsurathaworn

CONTENTS

LIST OF TABLES

Table Page

LIST OF FIGURES

Figure Page

CHAPTER 1
Introduction

1.1 Motivation

Linear alpha olefins (LAOs) is one of the important chemicals widely used in industry. LAOs is commonly used as a co-monomer in the production of polyethylene in order to modify the properties of polyethylene. Moreover, it is also applied in detergent, synthetic lubricant, and plasticizer manufactures [1].

Industrially, linear alpha olefins are commonly produced by two main routes. The first pathway is the oligomerization of ethylene and by Fischer-Tropsch synthesis. Another route that is commercially in a small scale, is the dehydration of alcohols [2]. However, these two processes depend on the non-renewable feedstock which is mostly from petrochemicals. Thus, the shortage of those non-renewable feedstocks is threatening the production in far future. To tackle this problem, the decarbonylation of fatty acids is an interesting alternative approach since fatty acids is derived from renewable sources.

Fatty acids, which are considered as the derivative of the biomass, can be easily obtained from the hydrolysis of triglycerides in vegetable oils and animals fats. The use of fatty acid as chemical feedstocks is of interest in an agricultural country like Thailand. Conversion of fatty acids to oxygen-free hydrocarbons can be converted using catalysts via several reactions, such as, dehydration [3], ketonization [4], decarbonylation [5,6], and decarboxylation [6,7]. All of those reactions are classified as deoxygenation that involves the production of CO_2 and/or CO from fatty acids and release a linear alkane or alkene. Metals over silica support, such as, platinum [8], palladium [9] and rhodium [5], are normally used as a catalyst for this conversion. However, the yield of alkane is higher than the yield of alkene due to rapid hydrogenation of the olefins primarily formed [10]. Furthermore, those metals are somewhat expensive.

We, thus, investigate the use of cheaper cobalt supported on silica support as a catalyst for the deoxygenate reaction of heptanoic acid (a model compound of fatty acids) via the reduction of fatty acid to aldehyde and then decarbonylation yielding

alpha olefin. The cobalt catalyst could also promote the decarbonylation of fatty acid resulting the higher amount of alkene rather than the alkane product.

1.2 Objectives of the study

1.2.1 To obtain linear alpha olefins from the deoxygenation of model fatty acid over cobalt supported silica catalysts.

1.2.2 To understand the reaction pathway for deoxygenation of fatty acid to alpha olefin over cobalt supported silica catalysts.

1.2.3 To obtain optimum conditions for the deoxygenation of fatty acid over the cobalt supported silica catalysts.

1.3 Scopes of the study

1.3.1 Preparation of Co, Cu, Ni, and Cr supported silica catalysts by wet impregnation over different types of secondary metal and preparation method, including Co-Pt/SiO_2, Co-Pd/SiO_2, Co-Ru/SiO_2, Co-Au/SiO_2, Co-Pt/SiO_2 (SIP).

1.3.2 Characterization of supported metal catalysts by the following techniques:

1.3.2.1 Brunauer Emmett Teller technique (BET)

1.3.2.2 X-ray Fluorescence (XRF)

1.3.2.3 Scanning Electron Microscopy with Energy Dispersive X-ray Analysis (SEM-EDX)

1.3.2.4 H_2-Temperature programmed reduction by hydrogen gas (H_2-TPR)

1.3.2.5 Transmission Electron Microscopy (TEM)

1.3.2.6 Thermogravimetric Analysis (TGA)

1.3.3 Investigation of the deoxygenation activity of prepared catalysts in the continuous fix bed reactor under hydrogen gas at atmospheric pressure for

1.3.3.1 Effect of types of metal (Ni, Co, Cr, Cu)

1.3.3.2 Effect of temperature (350 – 425 ^{o}C)

1.3.3.3 Effect of cobalt loading (2 – 15 wt.%)

1.3.3.4 Effect of secondary metal incorporated Co catalysts (Pt, Pd, Ru, Au)

1.3.3.5 Effect of preparation method for bimetallic Co-Pt catalyst (co-impregnation and sequential impregnation)

1.3.3.6 Effect of platinum loading (0.25 – 0.75 wt.%) on Co/SiO_2 catalyst

1.3.3.7 Effect of contact time (12 – 34 g•h/mol)

1.3.4 Analysis and quantification of liquid products from the reactions by online gas chromatograph equipped with a flame ionization detector (GC-FID).

1.4 Expected results

The new approach can be obtained for the production of long chain alpha olefin rather than alkane from renewable feed stocks.

CHAPTER 2

Theory and literature reviews

2.1 Fatty acids

Fatty acids refer to aliphatic monocarboxylic acid with four or more carbon atoms and a carboxylic (-COOH) group. Fatty acids are the main component in vegetable oils and derivative fats. They are categorized either as a saturated (without double bond) or unsaturated (with one or more double bonds) hydrocarbon chain [11, 12, 13, 14].Natural fatty acids can be obtained from the hydrolysis of triglycerides from several sources, such as, hard animal fats (tallow), coconut, palm kernel, and soybean oils. Natural fatty acids commonly have an unbranched chain with even number of carbon atoms (mostly 16-22) which can be either saturated or unsaturated molecules. Most of the naturally-occurring unsaturated fatty acids are *cis*-isomers. The *trans*-isomers are usually not found in nature but they are the result of the processing. Southeast Asia is the major source of fatty acids since they produce a lot of coconut, palm, and palm kernel oils [15]. The difference in the number of carbon atoms can differentiate physical properties of different fatty acids as shown in **Table 2.1**.

Table 2.1 Saturated fatty acid and their physical properties [16]

Chain length	Systematic Name	Trivial name	Acid		Methyl ester	
			m.p./ °C	b.p./ °C	m.p./ °C	b.p./ °C
1	Methanoic	Formic	8.4	101	-	32
2	Ethanoic	Acetic	16.6	118	-	57
3	Propanoic	Propionic	-20.8	141	-	80
4	Butanoic	Butyric	-5.3	164	-	103
5	Pentanoic	Valeric	-34.5	186	-80.7	127
6	Hexanoic	Caproic	-3.2	206	-69.6	151
7	Heptanoic	Enanthic	-7.5	223	-55.7	174
8	Octanoic	Caprylic	16.5	240	-36.7	195
9	Nonanoic	Pelargonic	12.5	256	-34.3	214
10	Decanoic	Capric	31.6	271	-12.8	228

Table 2.1(continued) Saturated fatty acid and their physical properties

Chain length	Systematic Name	Trivial name	Acid		Methyl ester	
			m.p./ °C	b.p./ °C	m.p./ °C	b.p./ °C
11	Hendecanoic	-	29.3	284	-11.3	250
12	Dodecanoic	Lauric	44.8	130	5.1	262
13	Tridecanoic	-	41.8	140	5.8	-
14	Tetradecanoic	Myristic	54.4	149	19.1	114
15	Pentadecanoic	-	52.5	158	19.1	127
16	Hexadecanoic	Palmitic	62.9	167	30.7	136
17	Heptadecanoic	Margenic	61.3	175	29.7	148
18	Octadecanoic	Stearic	70.1	184	37.8	156
19	Nonadecanoic	-	69.4	-	38.5	191
20	Eicosanoic	Arachidic	76.1	204	46.4	188
21	Heneicosanoic	-	75.2	-	-	207
22	Docosanoic	Behenic	80.0	-	51.8	206
23	Trocosanoic	-	79.6	-	59.3	-
24	Tetracosanoic	Lignoceric	84.2	-	57.4	222
25	Pentacosanoic	-	83.5	-	59.5	-
26	Hexacosanoic	Cerotic	87.8	-	63.5	237
27	Heptacosanoic	-	87.6	-	64.6	-
28	Octacosanoic	Montanic	90.9	-	67.5	-
29	Nonacosanoic	-	90.4	-	68.8	-
30	Triacontanoic	Melissic	93.6	-	71.5	-

In this thesis, heptanoic acid is selected as a model compound described below.

2.1.1 Heptanoic acid

Heptanoic acid (**Figure 2. 1**), also called enanthic acid, is the acid with seven carbon atoms. Heptanoic acid is the oily liquid with unpleasant smell. It contributes to the odor of some rancid oils. It presents as light yellow liquid and slightly soluble in water. In contrast, it is very soluble in ethanol and ether. Heptanoic acid has been naturally found in oily seed [17]. Alternatively, heptanoic acid can be derived from the

methyl ester of ricinoleic acid (which is a constituent of caster bean oil) from a process comprising of hydrolyzation and oxidation, respectively [18]. The bio-transformation of ricinoleic acid has also been reported with multi-step enzymatic activations [19]. Heptanoic acid is used in organic synthesis, manufacture of perfume, lubricating, grease, rubber and dry, latex, plastic, and food additives [20]. Additionally, the salts of heptanoic acid (i.e., heptanoates) are a corrosion inhibitor, and are a representative precursor for drugs, such as, esterify steroid [21].

Figure 2.1 Molecular structure of heptanoic acid

2.2 Chemical reaction of fatty acids

2.2.1 Reaction of carboxyl group of fatty acids

2.2.1.1 Deoxygenation

Deoxygenation is a chemical reaction involving the removal of oxygen atoms from the starting molecule [22]. It is a novel method for the production of long chain hydrocarbons (diesel, olefin) from renewable sources, and is currently being investigated worldwide. The deoxygenation can be divided in to two types, decarbonylation and decarboxylation. Figure 2.2 (a) and (b) are shown the products from decarbonylation which are CO, water and alkenes; whereas, decarboxylation yields CO_2, water, and alkanes. Therefore, the decarbonylation of fatty acid is capable of producing long chain olefins, given that hydrogen transfer/hydrogenation of the formed long chain olefins is limited. Both deoxygenation and decabonylation are thermodynamically favorable above 300 °C [23]. It is well known that the decarboxylation of carboxylic acids to the corresponding hydrocarbons occurs in the gas phase over heterogeneous metal catalysts [24]. This process has been applied in the production of liquid fuel from a free fatty acid.

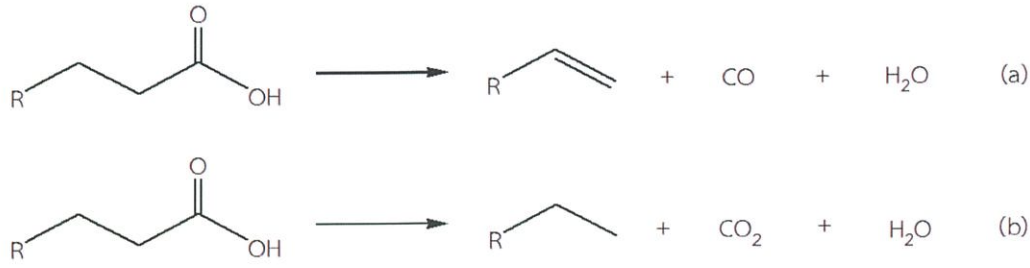

Figure 2.2 Hydrocarbon production from fatty acid via (a) decarbonylation and (b) decarboxylation [25].

2.2.1.2 Ketonization

Ketonization (also known as ketonic decarboxylation) is a reaction where two equivalents of carboxylic acid are converted into a symmetric ketone, with the expulsion of one equivalent of water and carbon dioxide each as shown in Figure 2.3. A large variety of oxides, such as Cr_2O_3, Al_2O_3, PbO_2, Bi_2O_3, TiO_2, ZrO_2, CeO_2, iron oxides, SiO_2, manganese oxides, and MgO, can catalyze the ketonization of carboxylic acids. Claisen condensation to form β-keto acid followed by decarboxylation, and a concerted mechanism involving two monodentate carboxylates have been proposed [74]. Another possible mechanism consists of reaction of an adsorbed acyl carbenium ion (RCO^+) with an adsorbed carboxylate to give ketonization products. Some authors have proposed that the formation of ketones on oxides is a sequential reaction going through a "ketene intermediate" [75].The surface ketene intermediate reacts with an adsorbed carboxylate to ultimately form the ketone, eliminating CO_2, but the details of coupling step are not clear. The mechanism of ketonization of carboxylic acid over SiO_2 was proposed [68]. It has been found that the nearby acid-base pair induces dissociative adsorption of the carboxylic acid molecules resulting in the formation of surface carboxylate species. The adsorption process proceeds spontaneously. After surfacing the acid-base pairs of catalyst, the new portions of carboxylic acid molecules interact with another adsorbed species in Eley-Riedel mode, converting into acyl cations. The adsorbed carboxylate species are attacked from the methyl group side by the acyl cation resulting in the formation of an acetone molecule and CO_2 by bimolecular electrophilic substitution reaction [26].

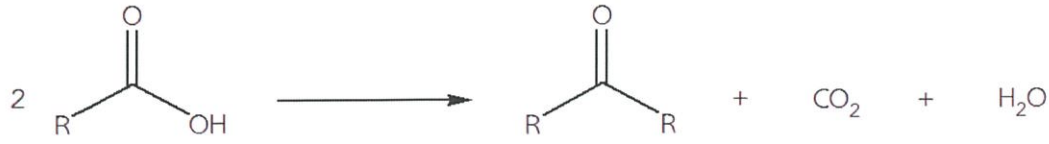

Figure 2.3 Decarboxylative ketonization of acetic acid to acetone

2.2.1.3 Esterification

Esterification refers to the conversion of acids (RCOOH) into esters (RCOOR) as shown in **Figure 2.4 and 2.5**. The esters can be used as alternative fuels, i.e., the biodiesel from the transesterfication of triglycerides with alcohols [27]. Fatty acid methyl esters (also known as FAMEs) are generally referred to as the first generation of the biodiesel [28]. Some physical characteristics of the methyl esters from fatty acids are shown in **Table 2.1**.

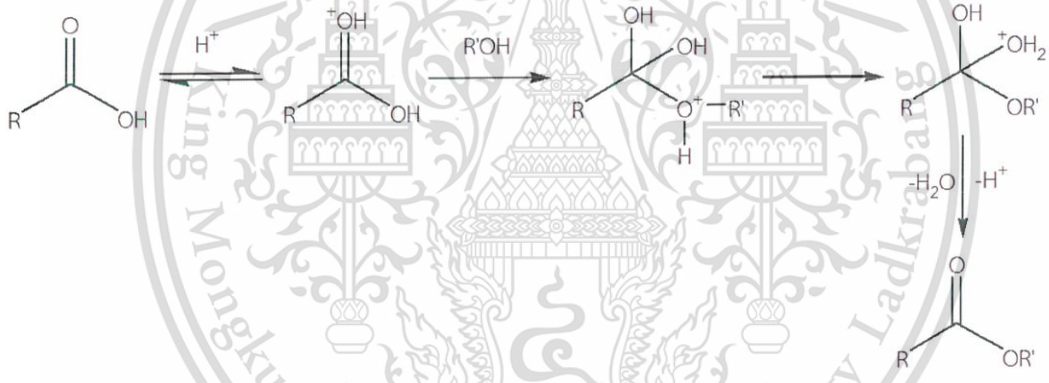

Figure 2.4 Acid-catalyzed esterification [Adapted from 29]

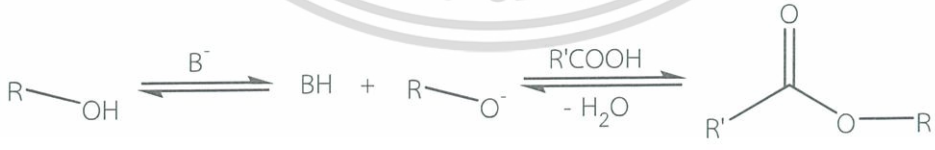

Figure 2.5 Base-catalyzed esterification [Adapted from 30]. The letter B stands for a basic site.

The reaction is catalyzed either by acid catalysts, such as, H-ZSM5 or basic catalysts, i.e, aqueous NaOH or MgO [31]. However, the use of homogeneous basic catalysts generates a large amount of liquid waste. On the other hand, the use of some heterogeneous basic catalysts gives rise to the saponification of the acids; thereby,

producing soap as a by product. Saponification is due to the presence of a free fatty acid (FFA) in large excess. Therefore, alternative catalysts with high reactivity but limited production of the undesirable soap are sought [32].

2.2.2 Reaction associated with double bonds of fatty acid

2.2.2.1 Hydrogenation

Hydrogenation of fatty acid is the addition of molecular hydrogen in molecule of fatty acid to break a double bond; thereby, saturating the acids are obtained (**Figure 2.6**). However, saturated fatty acids which are too waxy to be used in food production. The hydrogenation process has a side reaction, such as the double bond isomerization at about 180 to 270 °C was observed in the system of nickel supported on inert material as catalyst [33]. The hydrogenation of fatty acids finds some use in the production of magarine. In other applications, however, it is more useful to limit the hydrogenation; thereby, retaining the unsaturation of the fatty acids. For example, olefins have high heating value than alkanes when used as fuels. Also, olefins are essential chemicals in synthesis polymer [34].

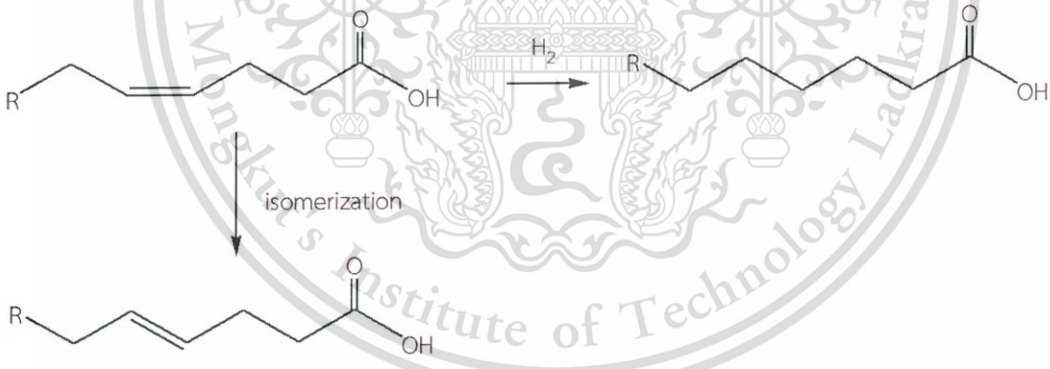

Figure 2.6 Direct hydrogenation and isomerization of an unsaturated fatty acid [25].

2.3 Long chain olefins

Linear alpha olefins (LAOs) have a variety of uses in industry and are usually used as starting materials in the production of plastics. Olefin is simply a common name for the alkene family of organic compounds, which all share the common double-bond functional group. Linear alpha olefins refer to the family of un-branched alkenes that have their double –bonds on the first or 'alpha' carbon atom in their

carbon chain. The smallest example is ethylene, which can be produced from the thermal cracking of naptha or natural gas [35]. Ethylene can further oligomerize into long chain α-olefins, or react with another olefin to form longer chain olefins via metathesis by an organometallic catalyst [36]. The reaction of ethylene (C_2H_4) reacts with itself over a transition metal co-catalyst system can produce longer chain olefins, in this case 1-hexene and 1-octene. Trimerization refers to the combination of three ethylene molecules to create 1-hexene; while, tetramerization involves the reaction of four ethylene molecules to form 1-octene. 1-Hexene and 1-octene which are mainly used in polyethylene production, manufacturing of surfactants lubricants and alcohol production. The demand of these compounds is very high in North America, Western Europe and Asia. There are several current industrial processes producing linear alphaolefins [37]. Some examples on the use of long chain olefins are listed in **Table 2.2**.

Table 2.2 The use of long chain olefins in industrial application [21].

Long chain olefins in range of C_4-C_8	■ Precursor in the production of linear aldehyde ■ Manufacturing of linear alcohol for plasticizer ■ Production of short chain carboxylic acid ■ Synthesis of poly α-olefins used as synthetic lubricant ■ Use as surfactant in a blend with the others long chain olefins
Long chain olefins in range of C_{10}-C_{14}	■ Production of linear alkyl benzene surfactant ■ Use as the drilling fluid base stock to replace diesel or kerosene
Long chain olefins in range of C_{16}-C_{18}	■ Hydrophobes in oil-soluble surfactant ■ Lubricating fluids ■ Synthetic drilling fluids ■ Production of maleic acid for paper sizing chemicals
Long chain olefins in range of C_{20}-C_{30}	■ Chemical feedstock for heavy linear alkyl benzene ■ Chemical feedstock for low molecular weight polymer

2.4 Literature reviews

Catalytic deoxygenation is chemical reaction in an industrial process and has also been widely applied in organic synthesis on a smaller scale. It has been studied in broad reaction conditions over various types of catalysts. Factors, such as, types of metal, reactants, dispersion of metal, temperature, including the concentration of the reactants were reported.

Mathias Snåre *et al.* [38] studied types of metals that can activate deoxygenation of fatty acid to diesel-like hydrocarbons. Stearic acid was used to the model compound and the reaction was tested in a semibatch reactor under constant temperature (300 °C) and pressure (6 bar). The result showed that carbon supported palladium catalyst (Pd/C) converted stearic acid completely with >98% selectivity toward deoxygenated C17 products. Whereas, other metals can be deoxygenation was in the descending order of Pd > Pt > Rh > Ir >Ru > Os > Ni. Apart from deoxygenation reactions, other reactions, such as hydrogenation, dehydrogenation, cyclization, ketonization, dimerization, and cracking, were observed in various extents depending on the catalysts. After that the same group also [39] investigated types of reactants for deoxygenation, such as, monounsaturated fatty acid, oleic acid, the diunsaturated fatty acid, linoleic acid and monounsaturated fatty acid ester, methyl oleate over a Pd/C catalyst under constant pressure (15 bar) and temperature (300 °C) with Ar and H_2-mixture in a semi-batch reactor. The result showed unsaturated acids or esters converted completely after 6 h but the diunsaturated linoleic acid exhibited the lowest conversion level (34%) after 6 h. While, monounsaturated oleic acid and methyl oleate displayed higher conversion after 6 h, 78% and 84%, respectively. Linoleic acid gave lower the conversion, as compared to another feeds, since an additional hydrogenation step, from diunsaturated to monounsaturated, is included. Moreover, in all cases the catalyst deactivation by coke formation was more pronounced within 90 min. Furthermore, the formation of higher products was substantially higher for the two acids as compared to the methyl ester. This could be the result of the metal dispersion.

The effect of metal dispersion was investigated by Irina Simakova *et al.* [40]. The studied catalytic deoxygenation of palmitic and stearic acids mixture over 1%Pd supported on synthetic carbon (Sibunit) with 18, 47, 65, 72% dispersion in a semibatch reactor and dodecane was used as a solvent at 300 °C under the overall pressure of

17.5 bar of 5 vol% hydrogen in helium. It was found that 47% dispersion gave the highest reaction rate. The main liquid phase products were *n*-heptadecane and *n*-pentadecane, which were formed in parallel. The large Pd particles (6 nm, 18% dispersion) are not active due to low surface area. At the same time, highly dispersed (72%) Pd species had lower activity, as compared to 2.3 nm particle size (47% dispersion), because of its strong interaction between the Pd with the support. In addition, effect of temperature was also studied from 260-300 °C over 1 wt.% Pd/C (dispersion 47%). The result shows that at 260 °C the reaction rate was much slower than that at higher temperatures. The complete conversion of palmitic acid was achieved at 300 °C, whereas at 260 °C only 50% conversion of palmitic acid was obtained. The liquid phase products were heptadecane and pentadecane, which were formed in a parallel and independent on temperature.

P. Mäki-Arvela *et al*. [41] investigated feed concentration and products towards the catalyst deactivation. The catalytic deoxygenation of lauric acid in dodecane at temperature 270 °C, pressure 10 bar, volumetric liquid flow rate 1.0 mL/min, catalyst mass 0.4 g was studied in the continuous fixed bed reactor using Pd/C as a catalyst. It was found that the catalyst deactivation is dependent on the lauric acid concentration (0.22, 0.35 and 0.44 mol/L). The initial conversion reached 100% when 0.35 mol/L lauric acid was used, whereas 0.44 mol/L of the acid gave only 71%. The conversion on time profile fall to 3% in 30 min. in all cases due to the poisoning by the product gases, CO and CO_2 and coking. The selectivity toward the desired products, undecane and undecene were very high under all conditions, being above 95%. Corresponding with Siswati Lestari *et al*. [42], they found deoxygenation of stearic acid at 360 °C under 10 bar argon or 5 vol% hydrogen in argon over Pd/C (Sibunit) in a fixed-bed reactor (down flow). The results showed catalyst performance, giving about 15% conversion level of stearic acid. The main liquid-phase product was heptadecane; while, the main gaseous products were CO and CO_2. The cause of catalyst deactivation was suggested to be coking.

Juan A. Lopez-Ruiz *et al*. [43] studied the decarbonylation and decarboxylation of heptanoic acid over carbon-supported Pt nanoparticles in a continuous flow fixed bed reactor at 573 K and 37 bar. At very low conversions, approaching zero, the product selectivity was decarbonylation as the primary reaction, producing mostly hexenes and CO. As conversion increased from 1% to 5% at 37 bar, substantial

amounts of hexane and CO_2 were observed because of side reactions, such as, water-gas shift (WGS) and hydrogenation instead of direct decarboxylation. During the reaction, Pt metal particles were sintering causing the deactivation.

It is well known that cobalt complexes can be decarbonylation in homogenuous catalysts. For examples, Michael Dennis *et al.* [44] investigated the final step in hydrocarbon biosynthesis involves the loss of CO from a fatty aldehyde. Reactions were tested with octadecanal at 60 °C for 45 min. Co-protoporphyrin IX itself caused decarbonylation of octadecanal to alkane about 28 pmol. Fe-protoporphyrin IX chloride showed 8% of the decarbonylation activity observed with Co protoporphyrin IX chloride, whereas the metal ion, protoporphyrin alone, or the other metal porphyrins examined Mn-, Sn-, and Zn-protoporphyrin IX chlorides did not generate detectable amounts of alkane from octadecanal. Shuo Yuan *et al.* [45] studied fluorophenyl carbonyl cobalt(I) complexes ($PhF(PMe_3)_3Co(CO)$) synthesized by the reaction of fluoro-benzaldehydes with $CoMe(PMe_3)_4$ via C–H bond activation and decarbonylation reaction. Furthermore, they found that $CoMe(PMe_3)_4$ (37.8 mg, 0.1 mmol) could be used as a catalyst for the catalytic decarbonylation of 2,4,5-trifluorobenzaldehyde (1.6mg, 1.0 mmol) with triethylsilane (0.14 g, 1.2 mmol) as a hydrogen source in 2 mL of THF as solvent under N_2 atmosphere. The reaction mixture was stirred at 50 °C for 6 h. It gave 94% yield fluorobenzene. This suggests that cobalt complexes can be activate to decarbonylation.

G. Leendert Bezemer *et al.* [46] studied influence of cobalt particle size in the range of 2.6-27 nm on the performance in Fischer- Tropsch synthesis. The turnover frequency (TOF) for CO hydrogenation was independent of cobalt particle size at it's larger than that 6-8nm. At 35 bar, the TOF decreased from 23×10^{-3} to 1.4×10^{-3} s^{-1}; while, the C_{5+} selectivity decreased from 85 to 51 wt.% when the cobalt particle size was reduced from 16 to 2.6 nm. This demonstrates that the minimal required cobalt particle size for Fischer-Tropsch catalysis is larger than 6-8nm, so can be explained by classical structure sensitivity. Other explanations raised in the literature, such as, formation of CoO or Co carbide species on small particles during catalytic testing. It is argued that the cobalt particle size effects can be attributed to nonclassical structure sensitivity in combination with CO-induced surface reconstruction. The influences of particle size may be important for the design of new Fischer-Tropsch catalysts. The presented data have a large consequence for the preparation of active cobalt-based

Fischer-Tropsch catalysts. One should aim for catalysts with average cobalt particle sizes close to the optimum values of 6-8 nm as larger particles display a lower activity and smaller particles both a lower activity and a lower selectivity.

Tatsumi Ishihara *et al*. [47] investigated alloy catalysts of iron, cobalt, and nickel for carbon monoxide hydrogenation. Alloying of these metal components mostly enhanced the catalytic activity and suppressed methanation. The alloy catalyst of 50Co50Ni yielded a large amount of gasoline compounds; and the cobalt-rich iron-cobalt system was selective for olefin formation. The increase in iron content lowered the overall catalytic activity and accelerated methanation. The alloying of iron, cobalt, and nickel brings about changes in the adsorption state of hydrogen and carbon monoxide, which strongly affects catalytic activity and selectivity. These indicates that the alloy of the appropriate metallic composition greatly changed the adsorption properties of carbon monoxide and hydrogen, and enabled the control of product selectivity for desired products.

CHAPTER 3

Experimental

3.1 Reagents

Details on the reagents used in this thesis are summarized in **Table 3.1**.

Table 3.1 A list of reagents

Chemical	Grade of purity	Manufacturer
Air zero grade gas	99.99 %	PRAXAIR
Nitrogen gas	99.99 %	PRAXAIR
Hydrogen gas	99.99 %	PRAXAIR
10% Hydrogen gas in Argon	10 %	PRAXAIR
Helium gas	99.99 %	PRAXAIR
Acetic acid	99.70%	J.T. Baker
Heptanoic acid	99.50 %	ALDRICH
Octane	99%	Sigmar aldrich
Cobalt(II) nitrate hexahydrate ($Co(NO_3)_2{\cdot}6H_2O$)	≥ 99.80 %	Rankem
Copper(II) nitrate trihydrate ($Cu(NO_3)_2{\cdot}3H_2O$)	99.5%	QREC
Nickel(II) nitrate hexahydrate ($Ni(NO_3)_2{\cdot}6H_2O$)	99%	CARLO ERBA
Chromium(III) nitrate nonahydrate ($Cr(NO_3)_3{\cdot}9H_2O$)	97.00%	FLUKA
Tetraammineplatinum (II) nitrate	99.995%	Sigmar aldrich
Palladium (II) acetate	98%	Sigmar aldrich
Dichloro (*p*-cymene) ruthenium (II) dimer	100%	Sigmar aldrich
Gold (III) chloride trihydrate	99.9%	Sigmar aldrich
Silicon dioxide (SiO_2)	99.00%	CARLO ERBA
37% Hydrochloric acid (HCl)	36.90%	CARLO ERBA
70% Nitric acid (HNO_3)	69.90%	CARLO ERBA
Deionized water		

3.2 Apparatus and instruments

1. Alumina crucible
2. Graduate pipette and red bulb
3. Laboratory glassware
4. Protector laboratory hood, Science Technology
5. Mass flow controller, BROOKS INSTRUMENT LLC, Model SLA5350SB1AB1B2A1D3N4AA
6. Sieve, AASHO N-92, U.S.A standard sieve
7. Glass bead
8. Glass wool
9. Glass tube
10. Quartz wool
11. Quartz tube
12. Quartz tube
13. Glass syringe, SGE Analytical Science
14. Syringe pump, KDS-100, KD-scientific
15. Gas chromatography, Varian 3800
16. Capillary column, MXT-1
17. Digital Round-Top Stirring Hot Plate, 3810001, IKA
18. Hot air oven, UM500, Memmert
19. Tube furnace with a programmed temperature controller, VCTF4, Vecstar
20. Tube furnace with a programmed temperature controller, VIF, Utsakan
21. Muffle furnace with a programmed temperature controller, FHP-05, Wisethem
22. Temperature programmed reduction (TPR), TCD2-NIFED
23. Surface area and pore size analyzer, Autosorb-1, Quantachrome
24. Thermogravimetric analyzer, Pyris, Perkin Elmer
25. Scanning electron microscope, EVO®MA10, ZEISS
26. Weavelength dispersive X-ray fluorescence spectrophotometer, Bruker, Tiger
27. Transmission electron Microscope, FEI Tecnai G^2 20, 200kv

3.3 Catalyst preparation

3.3.1 Silica support (SiO_2)

Silica was calcined in muffle oven by ramping to 600 °C with the heating rate of 5 °C/ minutes and holding for 1 hour.

3.3.2 Preparation of 5%wt Cobalt on silica catalysts (5%Co/SiO_2)

The 5%wt cobalt on silica support was prepared by wet impregnation method. In the first step, 2.5049 g. of cobalt nitrate hexahydrate ($Co(NO_3)_2.6H_2O$) was dissolved in deionized water 21 mL. After that, 9.6019 g of SiO_2 was impregnated with this solution. The solid was dried in oven at 70 °C for 6 hours. Then, the dried catalyst was calcined in tube furnace by ramping to 600 °C for 1 hour with the heating rate of 5 °C/min.

3.3.3 Preparation of 5%wt Nickel on silica catalysts (5%Ni/SiO_2)

The 5%wt nickel on silica support was prepared by wet impregnation method. In the first step, 2.5000 g. of nickel nitrate hexahydrate ($Ni(NO_3)_2.6H_2O$) was dissolved in deionized water 41.00 mL. After that, 9.5000 g of SiO_2 was impregnated with this solution. The solid was dried in oven at 125 °C for 8 hours. Then, the dried catalyst was calcined in tube furnace at 500 °C for 3 hour with the heating rate of 5 °C/min.

3.3.4 Preparation of 5%wt Copper on silica catalysts (5%Cu/SiO_2)

The 5%wt copper supported silica was prepared by wet impregnation method using copper nitrate trihydrate ($Cu(NO_3)_2.3H_2O$) as a precursor. 1.9317 g. of copper nitrate trihydrate was dissolved in deionized water 7.9 mL. After that, 9.5550 g of SiO_2 was impregnated by the solution. Then, the solid was dried in oven at 70 °C for 24 hours. The dried catalyst was calcined in a horizontal tube furnace under a flow of air zero grade (60 mL/min) at 450 °C for 5 hours with the heating rate of 10 °C/min.

3.3.5 Preparation of 5%wt Chromium on silica catalysts (5%Cr/SiO_2)

The 5%wt chromium supported silica was prepared by wet impregnation method using chromium nitrate nonahydrate ($Cr(N_3O)_3.9H_2O$) as a precursor. First, 5.7835 g. of chromium nitrate nonahydrate was dissolved in deionized water 14.40 mL. After that, 14.35 g of SiO_2 was impregnated in this solution. Then, the solid was dried in oven at 70 °C for 24 hours. The dried catalyst was calcined in a horizontal tube furnace under a flow of air zero grad (60 mL/min) at 650 °C for 3 hours with the heating rate of 5 °C/min.

3.3.6 Preparation of 2%wt Cobalt on silica catalysts (2%Co/SiO_2)

The 2%wt cobalt on silica support was prepared by wet impregnation method. In the first step, 0.9993 g. of cobalt nitrate hexahydrate ($Co(NO_3)_2.6H_2O$) was dissolved in deionized water 34.00 mL. After that, 9.8863 g of SiO_2 was impregnated in this solution. The solid was dried in oven at 70 °C for 6 hours. Then, the dried catalyst was calcined in tube furnace under a flow of air zero grade (60 mL/min) at 600 °C for 1 hour with the heating rate at 5 °C/min.

3.3.7 Preparation of 10%wt Cobalt on silica catalysts (10%Co/SiO_2)

The 10%wt cobalt on silica support was prepared by wet impregnation method. In the first step, 4.9970 g. of cobalt nitrate hexahydrate ($Co(NO_3)_2.6H_2O$) was dissolved in deionized water 42.00 mL. After that, 9.1043 g of SiO_2 was impregnated in this solution. The solid was dried in oven at 70 °C for 6 hours. Then, the dried catalyst was calcined in tube furnace under a flow of air zero grade (60 mL/min) at 600 °C for 1 hour with the heating rate at 5 °C/min.

3.3.8 Preparation of 15%wt Cobalt on silica catalysts (15%Co/SiO_2)

The 15%wt cobalt on silica support was prepared by wet impregnation method. In the first step, 7.49390 g. of cobalt nitrate hexahydrate ($Co(NO_3)_2.6H_2O$) was dissolved in deionized water 64.00 mL. After that, 8.6056 g of SiO_2 was impregnated in this solution. The solid was dried in oven at 70 °C for 6 hours. Then, the dried catalyst was calcined in tube furnace under a flow of air zero (60 mL/min) at 600 °C for 1 hour with a heating rate 5 °C/min.

3.3.9 Preparation of 5%wt Cobalt bimetallic by co-impregnation method

3.3.9.1 5%wt Cobalt bimetallic with 0.5%wt Platinum on silica catalysts (5%Co+0.5%Pt/SiO_2)

The 5%wt cobalt - 0.5%wt platinum bimetallic on silica support was prepared by wet impregnation method. In the first step, 1.2350 g. of cobalt nitrate hexahydrate ($Co(NO_3)_2.6H_2O$) was dissolved in deionized water 11.00 mL and then 0.0496 g. of tetraammineplatinum(II) nitrate ($(Pt(NH_3)_4)(NO_3)_2$) was dissolved in deionized water 0.50 mL. The two precursors were mixed together. After that, 4.8191 g of SiO_2 was impregnated by this solution. The solid was dried in oven at 70 °C for 6 hours. Then, the dried catalyst was calcined in tube furnace under a flow of air zero grade (60 mL/min) at 600 °C for 1 hour with the heating rate of 5 °C/min.

3.3.9.2 5%wt Cobalt bimetallic with 0.5%wt Palladium on silica catalysts (5%Co+0.5%Pd/SiO_2)

The 5%wt cobalt - 0.5%wt palladium bimetallic on silica support was prepared by wet impregnation method. First, 1.2356 g. of cobalt nitrate hexahydrate ($Co(NO_3)_2 \cdot 6H_2O$) was dissolved in acetone 30.00 mL and then 0.0545 g of palladium acetate ($Pd(OCOCH_3)_2$) was dissolved in acetone 5.00 mL. The two precursors were mixed together. After that, 4.8278 g of SiO_2 was impregnated by this solution. The solid was dried in oven at 70 °C for 6 hours. Then, the dried catalyst was calcined in tube furnace under a flow of air zero grade (60 mL/min) 600 °C for 1 hour with the heating rate of 5 °C/min.

3.3.9.3 5%wt Cobalt bimetallic with 0.5%wt Ruthenium on silica catalysts (5%Co+0.5%Ru/SiO_2)

The 5%wt cobalt - 0.5%wt ruthenium bimetallic on silica support was prepared by wet impregnation method. In the first step, 1.2358 g. of cobalt nitrate hexahydrate ($Co(NO_3)_2 \cdot 6H_2O$) was dissolved in ethanol 20.00 mL and then 0.0757 g. of dichloro (p-cymene)ruthenium (II) dimer ($Ru(p\text{-}cymene)Cl_2)_2$) was dissolved in ethanol 15.00 mL. The two precursors were mixed together. After that, 4.8606 g of SiO_2 was impregnated by this solution. The solid was dried in oven at 70 °C for 6 hours. Then, the dried catalyst was calcined in tube furnace under a flow of air zero grade (60 mL/min) at 600 °C for 1 hour with the heating rate of 5 °C/min.

3.3.9.4 5%wt Cobalt bimetallic with 0.5%wt Gold on silica catalysts (5%Co+0.5%Au/SiO_2)

The 5%wt cobalt - 0.5%wt gold bimetallic on silica support was prepared by wet impregnation method. In the first step, 1.2350 g. of cobalt nitrate hexahydrate ($Co(NO_3)_2 \cdot 6H_2O$) was dissolved in deionized water 9.00 mL and then 0.0503 g. of gold (III) chloride trihydrate ($HAuCl_4$) was dissolved in deionized water 3.00 mL. The two precursors were mixed together. After that, 4.8335 g of SiO_2 was impregnated by this solution. The solid was dried in oven at 70 °C for 6 hours. Then, the dried catalyst was calcined in tube furnace under a flow of air zero grade (60 mL/min) at 600 °C for 1 hour with the heating rate of 5 °C/min.

3.3.9.5 5%wt Cobalt bimetallic with 0.25%wt Platinum on silica catalysts (5%Co+0.25%Pt/SiO_2)

The 5%wt cobalt - 0.25%wt platinum bimetallic on silica support was prepared by wet impregnation method. In the first step, 1.2369 g. of cobalt nitrate hexahydrate ($Co(NO_3)_2{\cdot}6H_2O$) was dissolved in deionized water 12.00 mL and then 0.0249 g. of tetraammineplatinum(II) nitrate ($(Pt(NH_3)_4)(NO_3)_2$) was dissolved in deionized water 1.00 mL. The two precursors were subsequently mixed together. After that, 4.8942 g of SiO_2 was impregnated by this solution. The solid was dried in oven at 70 °C for 6 hours. Then, the dried catalyst was calcined in tube furnace under the flow of air zero grade (60 mL/min) at 600 °C for 1 hour with the heating rate of 5 °C/min.

3.3.9.6 5%wt Cobalt bimetallic with 0.75%wt Platinum on silica catalysts (5%Co+0.75%Pt/SiO_2)

The 5%wt cobalt - 0.75%wt platinum bimetallic on silica support was prepared by wet impregnation method. In the first step, 1.2372 g. of cobalt nitrate hexahydrate ($Co(NO_3)_2{\cdot}6H_2O$) was dissolved in deionized water 11.00 mL and then 0.0745 g. of tetraammineplatinum(II) nitrate ($(Pt(NH_3)_4)(NO_3)_2$) was dissolved in deionized water 1.00 mL. The two precursors were subsequently mixed together. After that, 4.8079 g of SiO_2 was impregnated by this solution. The solid was dried in oven at 70 °C for 6 hours. Then, the dried catalyst was calcined in tube furnace under a flow of air zero grade (60 mL/min) at 600 °C for 1 hour with the heating rate of 5 °C/min.

3.3.10 Preparation of 5%wt Cobalt bimetallic by sequential impregnation method

3.3.10.1 5%wt Cobalt bimetallic with 0.5%wt Platinum on silica catalysts (5%Co+0.5%Pt/SiO_2 (SIP))

The 5%wt cobalt on silica support was prepared by wet impregnation method. In the first step, 2.5049 g. of cobalt nitrate hexahydrate ($Co(NO_3)_2{\cdot}6H_2O$) was dissolved in deionized water 21 mL. After that, 9.6019 g of SiO_2 was impregnated with this solution. The solid was dried in oven at 70 °C for 6 hours. Then, the dried catalyst was calcined in tube furnace by ramping to 600 °C for 1 hour with a heating rate 5 °C/min. Then the obtain 5%Co/SiO_2 was impregnated with a solution of 0.0497 g. tetraammineplatinum(II) nitrate ($(Pt(NH_3)_4)(NO_3)_2$) in water 10 mL. The solid was dried in oven at 70 °C for 6 hours. Then, the dried catalyst was calcined in tube furnace by ramping to 600 °C for 1 hour with the heating rate of 5 °C/min.

3.4 Catalysts characterization

3.4.1 Brunauer Emmett Teller technique (BET)

Specific surface area of a catalyst was measured by an Autosorb-1 (Quantachrome) instrument. Each sample (weighed approximately 0.1 g) was degassed at 300 °C for 12 hours prior to analysis. After that, nitrogen gas was adsorbed on the surfaces of the sample at -196 °C. The adsorbate pressure was fixed at 1 torr, the equilibration time of 3 min at each point, and the scaled tolerances were set at zero. The surface area was analyzed employing BET equation [48]. The BJH pore size distribution was also calculated [49].

3.4.2 X-ray Fluorescence (XRF)

The chemical composition of catalysts can be also determined by a wavelength-dispersive X-ray fluorescence spectrometry (WD-XRF). The sample is prepared by mixing 4.5 grams of boric acid and 0.5 grams of catalyst followed by manual grinding. The mixture is packed onto the sample holder and then compressed at 150 kN. The sample is placed in the sample chamber. CuK_{α} is employed as a source for the measurement with 50 kV, 60 mA.

3.4.3 Scanning Electron Microscopy with Energy Dispersive X-ray Analysis (SEM-EDX)

The chemical composition of catalysts can be also determined by a dispersive X-ray spectroscopy. The catalyst powder was dispersed on stub with carbon tape was pressed on those dispersed particles which have been previously deposited. The sample is placed in the sample chamber.

3.4.4 H_2-Temperature programmed reduction by hydrogen gas (H_2-TPR)

The reducibility property of metal contents can be determined by a temperature- programmed reduction by H_2 gas (H_2- TPR). The measurement was performed in a quartz tube connected with a thermal conductivity detector (VICI). Prior to an analysis, the sample (0.1 g approximately) was activated in air (flow rate of 30 mL min^{-1}) from room temperature to 600 °C at a heating rate 10 °C min^{-1}, followed by an isothermal treatment at 600 °C for 1 h. Subsequently, the system was naturally cooled down in the atmosphere of nitrogen gas (flow rate of 30 mL min^{-1}) to room temperature. Then, the temperature reduction profile was recorded using 10% H_2 in Ar at the heating rate 10 °C min^{-1}, from 35 to 900 °C. The TCD signal was calibrated employing a known mass of CuO as a standard, considering that CuO is reduced stoichiometrically and completely to Cu and H_2O. The reduction profile of CuO and

the calculation of the hydrogen consumption can be found in **Appendix B**. The amount of metal loading is expressed as mmol of H_2 consumed per mass of a catalyst (mmol H_2/g).

3.4.5 Transmission Electron Microscopy (TEM)

For transmission electron microscopic study (TEM), the sample was crushed in a mortar with few drops of acetone, and the suspended powder was dispersed on a carbon-coated copper TEM grid. Electron micrographs are acquired in the magnification range of 3,000-1,500,000×.

3.4.6 Thermogravimetric Analysis (TGA)

The thermal stability of a catalyst was measured by a thermogravimetric analyzer (Pyris). The sample was manually grinded in a mortar to homogeneous fine particles. Then, approximately 10 mg was put into a platinum pan. The measurement was conducted in 20 mL/min of nitrogen atmosphere, from 50 to 900 °C with the heating rate of 5 °C/min. The mass of the sample as the function of temperature was recorded by the instrument.

3.5 Catalysts activity

Deoxygenation of heptanoic acid was investigated at atmospheric pressure in a continuous fixed-bed reactor made with quartz tube (6.3 mm O.D.). Schematic of the catalytic testing rig is shown in **Figure 3.1**. The catalyst bed was packed in the middle of the reactor and topped with quartz wool and quartz beads. The reactor was then installed inside a temperature-controlled electrical furnace. The gas flows were controlled by the mass flow controllers and checked by bubble flow meter. Before the catalytic testing, the catalyst was activated by heating at 5°C/min to its calcination temperature (600 °C) and was hold at that temperature for 1 hour under the stream of air zero grade (100 mL/min). Then N_2 was flowed to eliminate the remaining air in the line. Finally, the gas stream was switched to a flow of H_2 gas for the reduction with a heating of 5 °C/min to 600 °C and hold for 3 hours. After that the reaction was run at 350 – 425 °C under the stream of H_2 100 mL/min for 6 hour. A solution of reactant, 10% wt/wt hepatnoic acid in octane, was fed to the reactor by a 10-mL syringe connected to a syringe-pump.

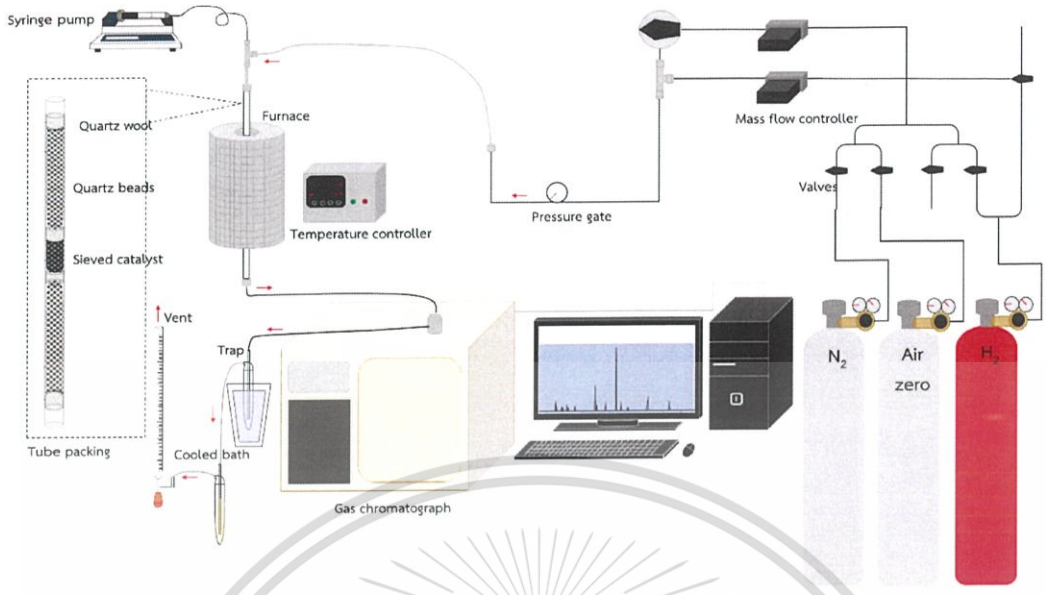

Figure 3.1 Schematic diagram of the catalytic testing rig

In each run, 10% wt/wt hepatnoic acid in octane was passed through the catalyst bed under a 100 mL/min flow of H_2. The catalytic testing was continued for at least 6 hours on stream. The reacted gaseous mixture was flowed out of the reactor and passed through a gas sampling loop. In order to prevent condensation of products, the line after reactor was heated by heating tapes. Description of the reactor set up and the reaction conditions are summarized in **Table 3.2**

Table 3.2 Description of the reactor set up and the reaction condition

Parameters	Value
Reactor outside diameter (mm)	6.3
Bed length (mm)	8-25
Total flow (mL/min)	100
Catalyst weight (g)	0.02 - 0.10
Contact time: W/F (g•h/mol)	12 – 34
Catalyst pallet size (μm)	250 - 425
Catalyst activation (before reaction)	Heating rate: 5 °C/min Calcination temperature: 600 °C Gas: air zero (100 ml/min)
Catalyst reduction (before reaction)	Heating rate: 5 °C/min Reduction temperature: 600 °C Gas: Hydrogen (100 mL/min)
Reaction temperature (°C)	350-425
Total reaction pressure	Atmospheric pressure (1 atm)

Online gas chromatograph was used for product's analysis. The gas sample was collected in gas sampling loop, then periodically injected into GC column (MXT-1, 60 m length, 0.25 mm internal diameter, 0.5 μm film thickness) connected to flame ionized detectors (FID). The following temperature program was used for the analysis: holding at 40 °C for 5 min, followed by the ramping to 280 °C at the rate of 15 °C/min holding for 4.04 min. N_2 gas was used as a carrier gas. Each component was separated as passed though the column with an inert carrier N_2 gas and their presence in the effluent were recorded as a chromatogram. Each peak area from the chromatogram was measured and calculated. Then each peak was identified by comparing with standard and the composition of each product was determined by calibration of standard.

CHAPTER 4

Result and Discussion

4.1 Catalyst Characterization

4.1.1 Elemental analysis and surface area

The metal loadings determined by XRF and surface area of the catalysts are summarized in **Table 4.1**.

Table 4.1 The amounts of metal loaded on SiO_2 and surface area of catalysts.

Catalysts	Elemental analysis (XRF)		S_{BET} (m^2/g)
	Primary metal (wt%)	Secondary metal (wt%)	
SiO_2	-	-	319
5%Cu/SiO_2	4.83	-	230
5%Cr/SiO_2	4.89	-	243
5%Ni/SiO_2	5.16	-	231
5%Co/SiO_2	4.81	-	277
2%Co/SiO_2	1.95	-	286
10%Co/SiO_2	9.20	-	236
15%Co/SiO_2	13.69	-	225
5%Co+0.5%Pd/SiO_2	4.43	0.55	252
5%Co+0.5%Au/SiO_2	4.67	0.45[a]	254
5%Co+0.5%Ru/SiO_2	4.52	0.65[a]	251
5%Co+0.5%Pt/SiO_2 (CIP)	4.38	0.50	253
5%Co+0.5%Pt/SiO_2 (SIP)	4.86	0.51	227
5%Co+0.25%Pt/SiO_2	4.58	0.22	249
5%Co+0.75%Pt/SiO_2	4.55	0.67	226

[a] *SEM-EDX*

The observed metal loadings are in agreement with the desired catalyst preparation. The N_2 adsorption-desorption isotherm of SiO_2 and all the catalysts show type-IV isotherms, indicating typical characteristics of materials with mesoporous

structure (**Appendix A**). Silica support shows a high surface area of 319 m^2/g. After impregnation the surface area is decreased because the support's surface/pore was partially covered/blocked by the loaded metal species. When the cobalt loading was increased from 2 to 15 wt% Co/SiO_2, the surface area is decreased proportionally.

4.1.2 Temperature program reduction

The H_2-TPR profiles of 5 wt% monometallic catalysts including, Cu, Cr, Ni, and Co supported on SiO_2 catalysts are shown in **Figure 4.1**. The y-axis indicates the signal from the TCD detector normalized by the sample mass. The reducibility of a catalyst can be deduced from the reduction temperature and peak area.

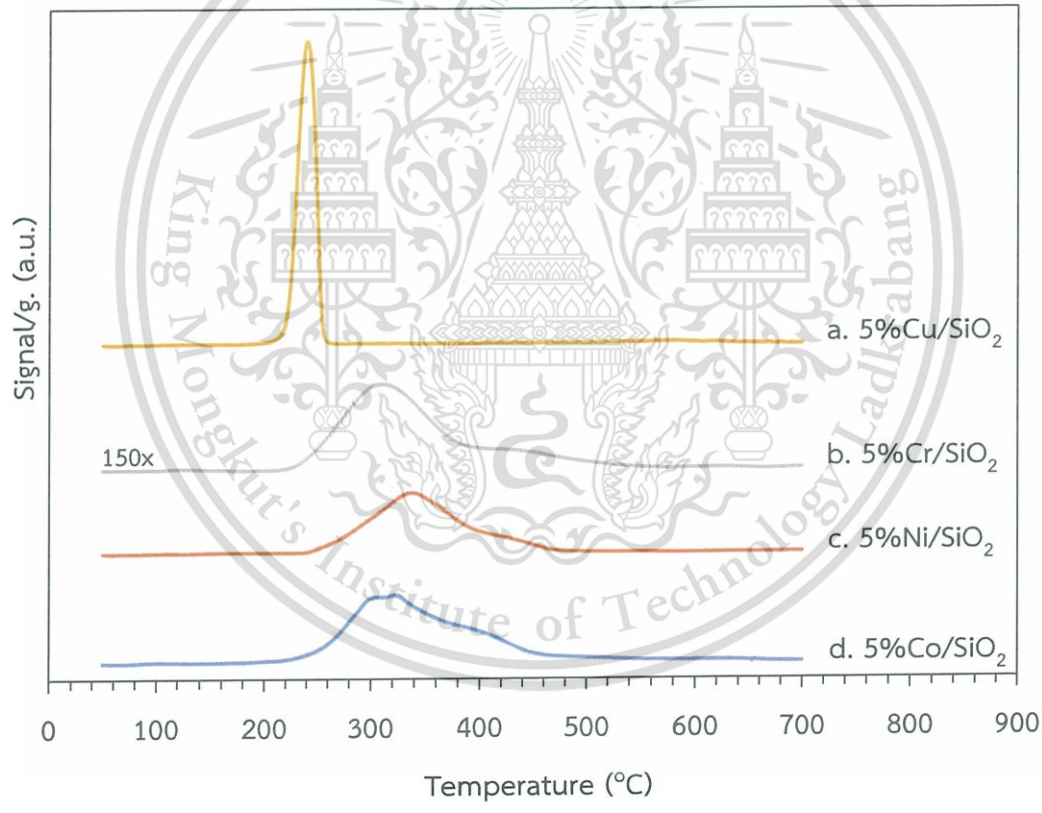

Figure 4.1 Temperature programmed reduction profiles of each catalyst.

It can be seen that only $5\%Cu/SiO_2$ shows a sharp reduction peak at 250 °C corresponding to the reduction of CuO to metallic Cu [50]. However, the others exhibit two humps of reduction temperature higher than that of the Cu/SiO_2. $5\%Cr/SiO_2$ catalyst is reduced around 200 - 550 °C representing the reduction of CrO_3 to Cr_2O_3

[51]. The reduction of NiO to metallic Ni also takes place at 200 - 500 °C [52]. For the cobalt impregnated catalyst, two peaks at around 300 °C and 320 - 400 °C are attributed to the reduction of Co_3O_4 to CoO species and CoO to metallic Co, respectively [53]. The amount of H_2 consumption is corresponded to metal loading as shown in **Table 4.2**, except for 5%Cr/SiO_2. The low H_2 consumption for Cr/SiO_2 is presumably due to the fact that there are two species of chromium oxide on silica surface, including the reducible CrO_3 (Cr^{6+}) and non-reducible Cr_2O_3 (Cr^{3+}) [54]. The result indicates that 5%Cr/SiO_2 is originally composed of Cr_2O_3 (Cr^{3+}) that cannot be reduced. Therefore, Cr content calculated from H_2 consumption is much less than that obtained from the XRF results (**Table 4.1**).

Table 4.2 Hydrogen consumption of each catalysts.

Catalysts	T_{onset} (°C)	T_{offset} (°C)	H_2 consumption mmol/g	*Metal content (wt%)
SiO_2	-	-	-	-
5%Cu/SiO_2	209	271	0.87	5.54
5%Cr/SiO_2	216	552	0.01	0.01
5%Ni/SiO_2	223	491	0.90	5.30
5%Co/SiO_2	193	543	1.25	5.52
2%Co/SiO_2	191	557	0.53	2.35
10%Co/SiO_2	229	465	2.22	9.82
15%Co/SiO_2	206	451	3.18	14.06
5%Co+0.5%Pt/SiO_2	94	311	1.26	-
5%Co+0.5%Pd/SiO_2	55	364	1.07	-
5%Co+0.5%Au/SiO_2	186	407	1.26	-
5%Co+0.5%Ru/SiO_2	76	295	1.36	-

** Calculated from H_2 consumption*

When cobalt loading was increased from 2% to 15wt%, the H_2 consumption was increased proportionally (**Table 4.2**) and in line with the Co loading determined by XRF (**Figure 4.2**).

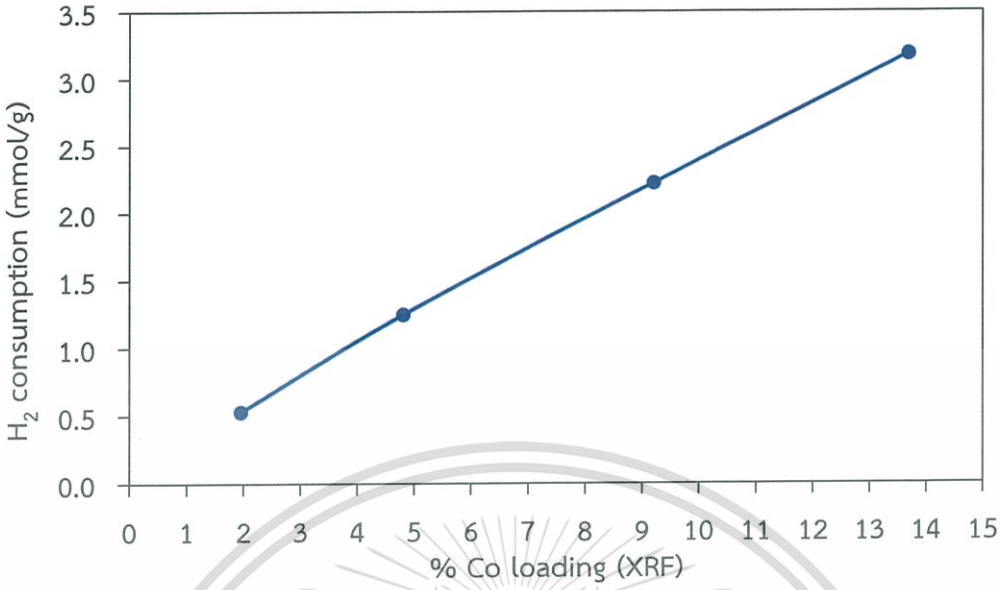

Figure 4.2 Cobalt loading versus H_2 consumption.

For 2% and 5 wt% Co/SiO_2, they show low reduction temperature approximately 300 - 320 °C; while, 10% and 15 wt% Co/SiO_2 show higher reduction temperature approximately 320 – 340 °C (**Figure 4.3**). It is suggested that the catalysts with high cobalt loading contain large cobalt particle as confirmed by TEM result (**Figure 4.4**). Hence, a higher lactice energy of CoO and Co_2O_3 can be expected and the reduction temperature is increased [55].

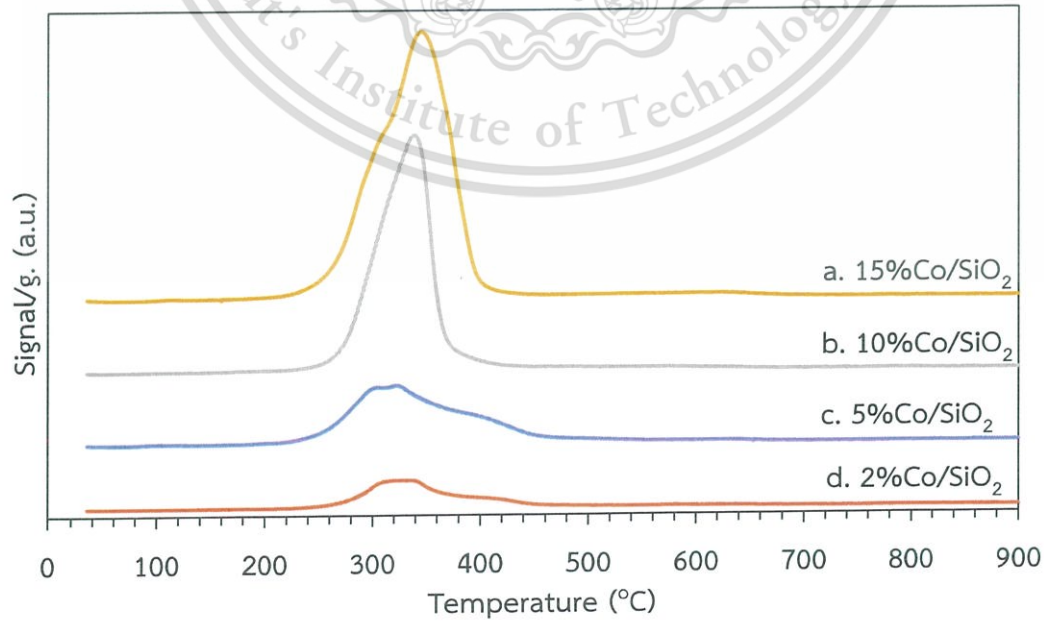

Figure 4.3 Temperature programmed reduction profiles of various cobalt loadings.

Furthermore, **Figure 4.4** the Co particles are dispersed on the SiO_2 support. TEM Images showed that the distribution of the metal particles on the silica support is uniform with a spherical particle shape. The particle size distribution histograms, which include analysis of several different regions, also quantitatively reflect the uniform size distribution of Co particles on the catalysts. The average particle size for the prepared Co catalysts is increased with the cobalt loading content on silica (2 wt% to 15 wt%) from 18 nm to 52 nm, respectively. This indicates a weak interaction between cobalt and support since SiO_2 is considered as an inert support. In consistent with H_2-TPR result, the agglomeration of Co particles at higher metal loading; thus, makes its lower dispersed and leads to higher reduction temperature (300 °C to 320 °C) [56].

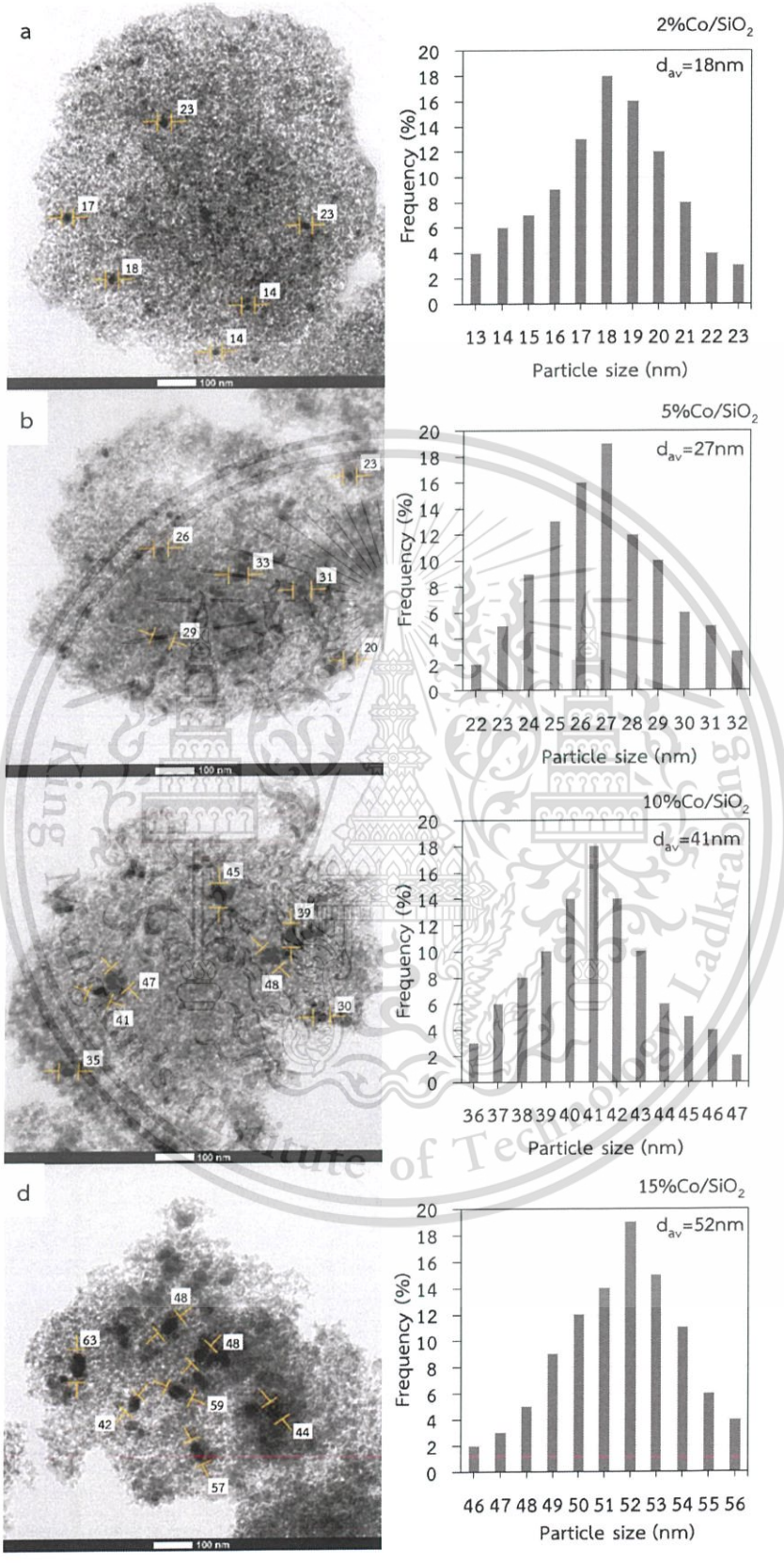

Figure 4.4 TEM images and particle size distribution histograms of reduced catalysts: a) 2%Co/SiO_2, b) 5%Co/SiO_2, c) 10%Co/SiO_2, d) 15%Co/SiO_2.

In a different manner, the H_2-TPR profiles of cobalt/metal bimetallic catalysts are shown in **Figure 4.5**.

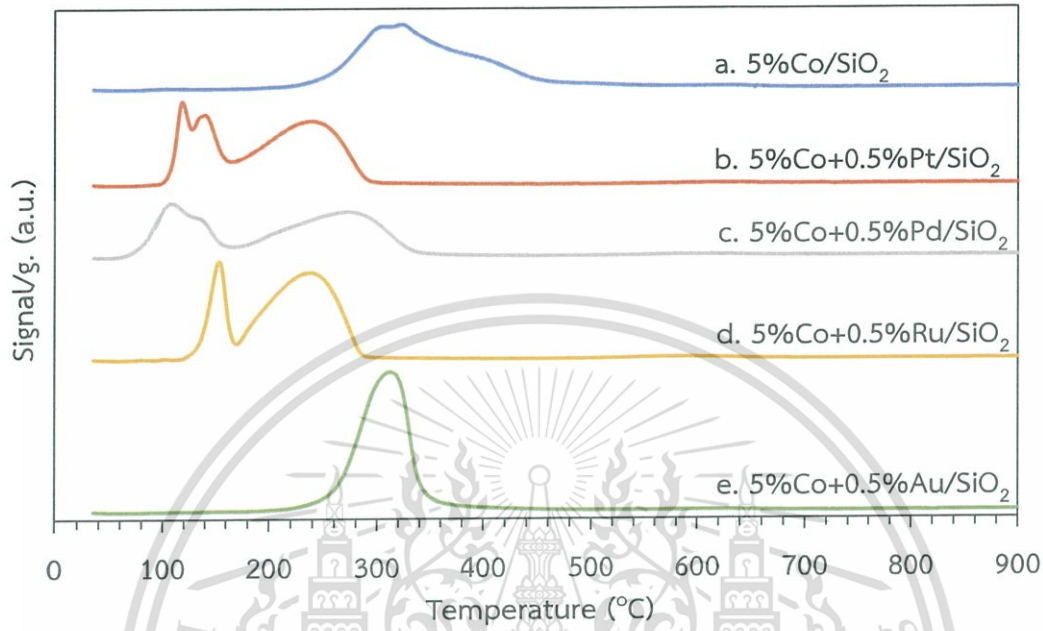

Figure 4.5 Temperature programmed reduction profiles of each cobalt metal bimetallic catalyst.

It can be seen that the reduction peak of Co bimetallic catalysts shifts to a lower temperature, as compared with monometallic cobalt catalyst; while, H_2 consumption are similar (**Table 4.2**). This suggests that the presence of the secondary metal enhanced the reducibility of cobalt oxide because the secondary metal could be easily reduced and become adsorption sites for H_2 that could spill over to facilitate the reduction of nearby cobalt oxide particles [57,58]. Therefore, the incorporated secondary metal decreased the reduction temperature of cobalt oxide.

Considering 5%Co+0.5%Pt/SiO_2, it shows three main reduction peaks. The first peak at 120 °C is assigned to the reduction of Co-Pt mixed oxide to bimetallic Co-Pt. While, the second and third peaks (130 and 240 °C) suggest the reduction of Co^{3+} to Co^{2+} and Co^{2+} to Co^0, respectively [59].

In case of 5%Co+0.5%Pd/SiO_2, three reduction peaks at 115, 135, 280 °C are also observed. The peak at 115 °C is referred to the reduction of Co-Pd mixed oxide to bimetallic Co-Pd, in a similar manner to 5%Co+0.5%Pt/SiO_2. The reduction temperature at 135, 280 °C are referred to the reduction of Co^{3+} to Co^{2+} and Co^{2+} to

Co^0, respectively [60]. Unlike 5%Co+0.5%Pt/SiO_2 and 5%Co+0.5%Pd/SiO_2, 5%Co+0.5%Ru/SiO_2 shows two reduction peaks at 155 and 245 °C that are the reduction of Co-Ru mixed oxide to bimetallic Co-Ru and remaining Co^{2+} to Co^0, respectively [61]. On the other hand, 5%Co+0.5%Au/SiO_2 shows the single reduction peak at 300 °C. It is suggested that Au facilitates reduction of Co^{3+} to metallic Co in a single step. This is presumably because when Au is added to Co/SiO_2 catalyst, a small particle of cobalt oxide is generated and the interaction of Au with Co_2O_3 facilitate the reduction of cobalt oxide, especially Co^{2+} to Co^0.

Considering the H_2 consumption of the bimetallic Co catalysts from **Table 4.2**, in which they are 1.07 – 1.30 mmol/g, is similar to that of monometallic Co (approximately 1.25 mmol/g). This is because only small amount of secondary metal is incorporated (0.5 wt%). Though, the reducibility property of cobalt is changed.

4.2 Catalysts Activity

4.2.1 Effect of types of metal

In this study Cu, Cr, Ni, and Co supported on silica (SiO_2) were screened as a catalyst for the production of α–olefin from fatty acid. The preparation of these catalysts are discussed in chapter 3. In this section, the comparative study on the catalytic activity are reported. The conversions of heptanoic acid over various catalysts were investigated under the atmospheric of H_2 at 350 °C as shown in **Table 4.3**.

Table 4.3 Catalytic performance on deoxygenation of heptanoic acid using various metals over silica catalysts.

Catalysts	Conversion (%)	Yield (%)								Hexene/Hexane ratio
		C_1-C_5	Hexene	Hexane	Iso C_6	Heptene	Heptanal	Heptanol	7-tridecanone	
5%Co/SiO_2	22.5	4.5	8.8	0.5	0.0	1.1	6.7	0.0	0.9	17.6
5%Ni/SiO_2	8.1	1.0	3.5	0.4	0.2	0.2	2.3	0.2	0.5	8.8
5%Cu/SiO_2	3.6	0.1	0.1	0.2	0.0	0.0	1.8	0.0	1.5	0.5
5%Cr/SiO_2	2.8	0.1	0.1	0.1	0.0	0.0	1.6	0.0	1.0	1.0

Condition: 10 wt% heptanoic acid in octane, contact time 20 g·h/mol, reaction temperature 350 °C, activation temperature 550 °C and reduction temperature 500 °C, 1 atm, and 100 mL/min of H_2. The activity is at 30 min on stream.

The conversion and product yields shown in **Table 4.2** are taken at 30 min on stream. It can be seen that 5%Co/SiO_2 gives higher activity (22.5% conversion), as compared to Ni (8.1%), Cu (3.6%), and Cr (2.8%), respectively. Over 5%Co/SiO_2, hexene can be produced as a main product presumably via decarbonylation of heptanal that can be produced from the reduction of heptanoic acid as shown **Scheme 4.1**

Scheme 4.1 The decarbonylation of heptanoic acid.

7-tridecanone was observed as a minor product over cobalt catalyst. It is clear that 7-tridecanone was produced from ketonization of heptanoic acid [64] as presented in **Scheme 4.2**.

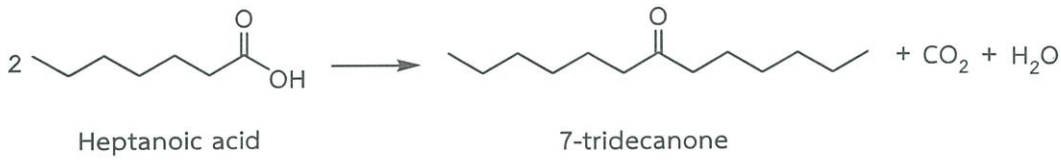

Heptanoic acid 7-tridecanone

Scheme 4.2 Ketonization of heptanoic acid.

Light hydrocarbon products (C1 – C5) were also observed as a result of hexane and hexene hydrogenolysis [62] and 7-tridecanone cracking [25]. This is due to Lewis acid character of cobalt.

Unlike noble metal, hexane selectivity is relatively low over Co catalysts. This suggests that cobalt cannot readily promote the decarboxylation of heptanoic acid to hexane. Nevertheless, the hydrogenation of hexene is also suppressed in the reaction using a cobalt catalyst. Hence, alkene or unsaturated products can be mainly obtained over cobalt catalyst.

5%Ni/SiO_2 catalyst gives lower activity as compared to 5%Co/SiO_2 catalyst. Since Ni is less oxophilic metal compared with Co, Ni would possess weaker adsorption with the feed (heptanoic acid) than Co. Although, the product distribution over Ni catalyst is similar to that over Co catalyst. The lower unsaturated/saturated ratio is observed for Ni catalyst due to a higher decarboxylation and hydrogenation ability of Ni catalyst.

Considering 5%Cu/SiO_2, the relatively low activity is observed with heptanal and 7-tridecanone as main products. Cu is favorable for the reduction of heptanoic acid to heptanal and ketonization of heptanoic acid to 7-tridecanone. It is suggested that Cu is not active towards the decarbonylation of heptanal to hexene [63]. Moreover, Yifei Chen *et al.*, (2017) reported that aldehyde adsorption on Cu surface is not stable [64], leading to the high yield of heptanal over Cu catalyst.

5%Cr/SiO_2 also shows low activity and gives heptanal and 7-tridecanone as main products. This is because Cr is in oxide form, as suggested by H_2-TPR result. The chromium oxide facilitates the reduction of heptanoic acid to heptanal [65] and ketonization of heptanoic acid to 7-tridecanone. In other words, Cr_2O_3 is not appropriated for olefin production via decarbonylation reaction.

4.2.2 Effect of temperature

Since Co catalysts give high activity and alkene selectivity, the effect of reaction temperature for deoxygenation of heptanoic acid over Co/SiO_2 was studied from 350 to 425 °C. The results are presented in **Figure 4.6**.

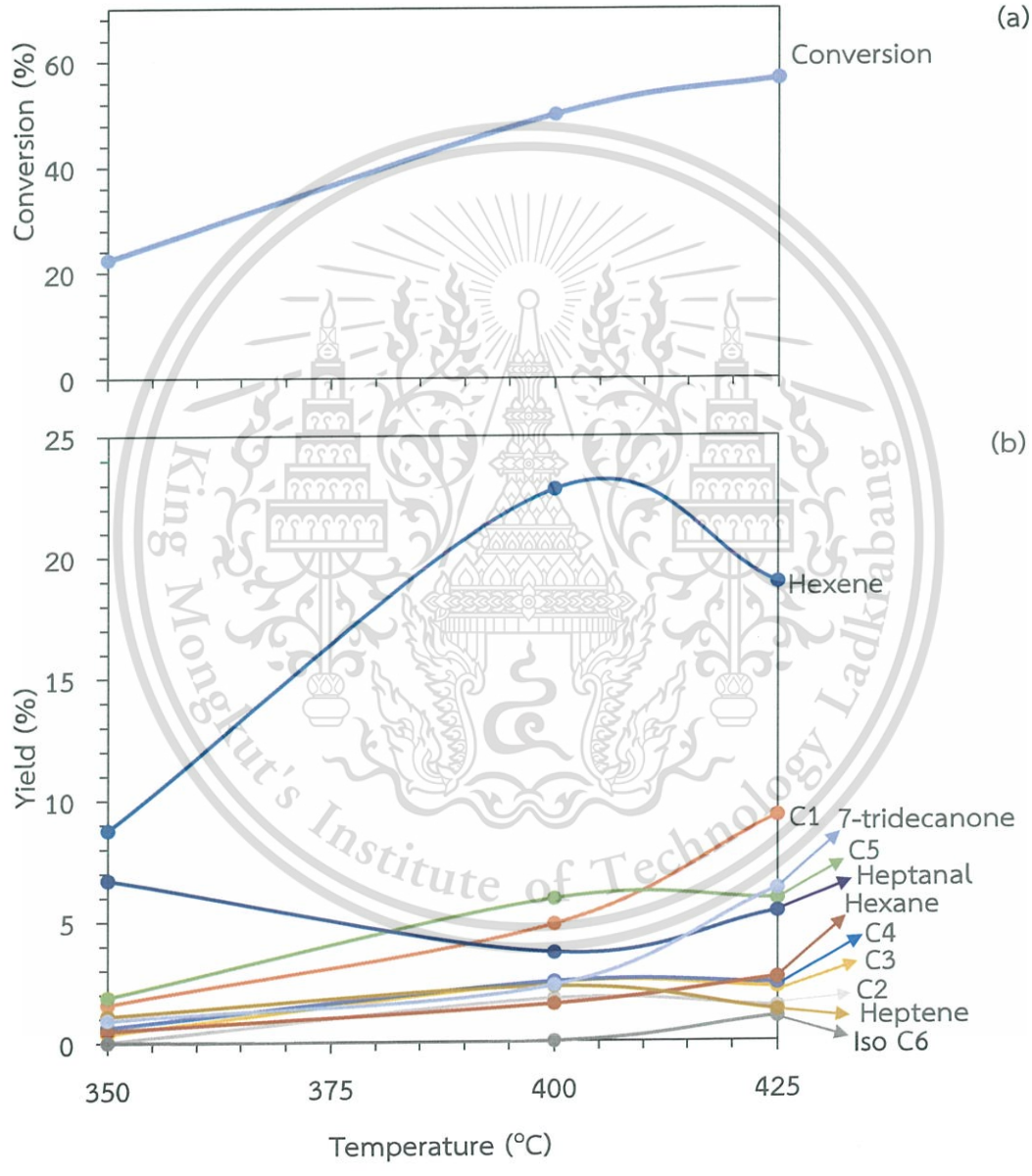

Figure 4.6 The effect of the reaction temperature on the (a) conversion of heptanoic acid and (b) yield of products from the deoxygenation of heptanoic acid over 5%Co/SiO_2. *Reaction conditions: 10 wt% heptanoic acid in octane, contact time 20 g·h/mol, activation temperature 550 °C and reduction temperature 500 °C, reaction*

temperature 350 - 425 °C, , 1 atm, and 100 mL/min of H_2. The activity is at 30 min on stream.

As expected, the conversion is enhanced (22% to 56%) upon increasing the reaction temperature from 350 °C to 425 °C. Yields of all products are also increased with temperature, except for heptanal. This is because heptanal can be converted to hexene via decarbonylation at high temperature. The major product, hexene is also increased with temperature because the decarbonylation activity is thermodynamically favorable as temperature is raised [52]. However, hexene was decreased at 425 °C since hydrogenation of hexene to hexane is enhanced. Moreover, higher hydrocarbons, such as, hexene and hexane can be hydrogenolysed to light hydrocarbon products. In line with this view, yield of CH_4 is significantly pronounced; while, yield of C2 - C5 are also decreased at 425 °C. In addition, CH_4 is formed by the hydrogenation of CO/CO_2 [62, 66] produced by decarbonylation and decarboxylation of heptanoic acid, respectively. In the case of 7-tridecanone, the yield is also increased with temperature as the ketonization is preferred at high temperature [25].

From these observations, the reaction temperature of 400 °C was selected for further studies on the cobalt loading catalysts since it especially gives high hexene yield.

4.2.3 Effect of cobalt loading

The effect of cobalt loading (2%, 5%, 10%, and 15 wt%) upon heptanoic acid decarbonylation activity and selectivity toward hexene was determined. The experiment data is collected over the catalysts with the same number of Co active site as shown in **Table 4.4**.

Table 4.4 Product distribution of 2%, 5%, 10%, and 15 wt% Co catalysts

Catalysts	Contact time (g.h/mol)		Conversion (%)	Yield (%)							Hexene/Hexane ratio
	by Co weight	by catalyst weight		C_1-C_5	Hexene	Hexane	Iso C_6	Heptene	Heptanal	7-tridecanone	
2%Co/SiO_2	1.64	82	57.2	13.3	29.4	1.3	0.0	2.4	4.2	6.5	22.6
5%Co/SiO_2	1.62	33	84.7	19.1	46.4	2.2	2.2	3.6	3.5	7.7	21.1
10%Co/SiO_2	1.65	17	78.6	9.5	53.7	1.4	4.8	3.5	0.6	5.0	38.4
15%Co/SiO_2	1.63	11	49.0	6.1	26.5	0.5	0.6	1.9	2.6	10.8	53.0

Condition: 10 wt% heptanoic acid in octane, contact time 1.6 g·h/mol, basis on cobalt, reaction temperature 400 °C, activation temperature 600 °C and reduction temperature 600 °C, 1 atm, and 100 mL/min of H_2. The activity is at 1 h on stream.

It can be seen that with the same contact time based on Co weight, the conversion is decreased when cobalt loading is increased from 5% to 15%. This is because cobalt particles are agglomerated as confirmed by TEM image in **Figure 4.4.** Hence, the cobalt surface is reduced leading to a lower conversion (from 84.7% to 49.0%). However, hexene/hexane ratio is increased due to decarboxylation is suppressed. Despite that 2%Co/SiO_2 shows high dispersion than 5%Co/SiO_2, the 2%Co/SiO_2 gives low conversion. This is because the severe deactivation of this catalysts as shown in **Figure 4.7**.

All cobalt catalysts give hexene as a main product from the reduction/decarbonylation of the heptanoic acid (**Scheme 4.1**). However, over 15%Co/SiO_2, yield of 7-tridecanone is higher than other catalysts. This is because non-reduced cobalt oxide strongly interacted with SiO_2 may well be presented particularly at high Co loading as confirmed by TPR profile. Fom **Figure 4.3**, the reduction of cobalt oxide strong interacted with SiO_2 requires a higher temperature (above 600 °C) [67]. Such non-reduced cobalt oxide species presenting in the catalyst with high Co loading, can readily promote the ketonization of heptanoic acid to 7-tridecanone, as observed [68].

In fact a 100% conversion was initially obtained for all Co loadings suggesting the excess of catalysts. However, over the time, the deactivation was particularly observed as shown in **Figure 4.7**.

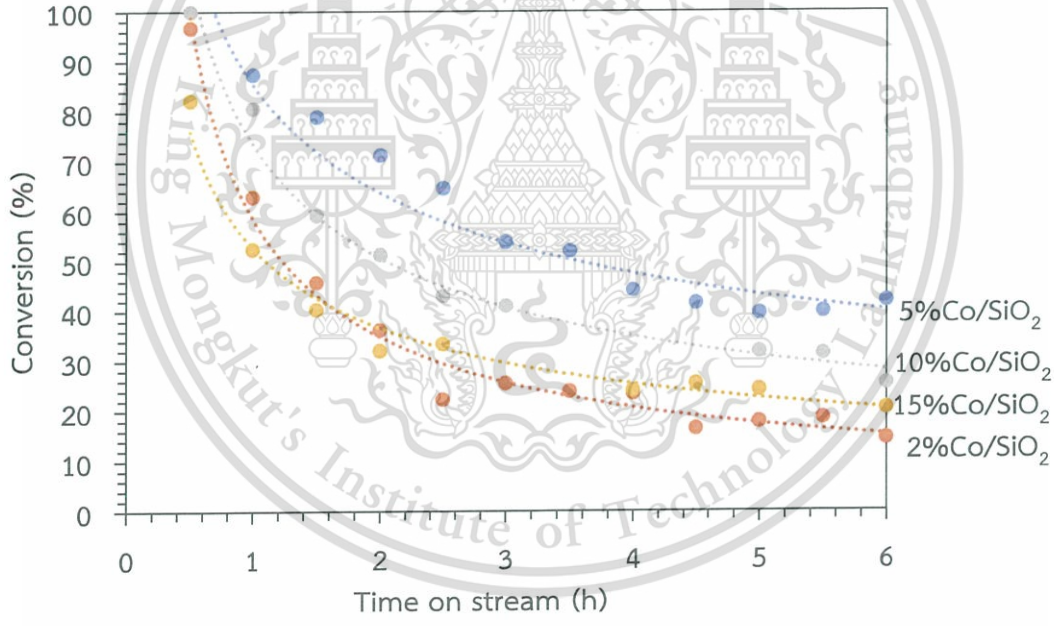

Figure 4.7 Deoxygenation catalytic performance of various cobalt loadings over silica catalysts. Reaction *condition: 10 wt% heptanoic acid in octane, contact time 1.6 g·h/mol, basis on cobalt, reaction temperature 400 °C, activation temperature 600 °C and reduction temperature 600 °C, 1 atm, and 100 mL/min of H_2.*

Obviously, the product yields are decreased, except for 7-tridecanone (**Figure 4.8**). It is suggesting that cobalt surface is deactivated resulting in the decrease in hydrocarbons and heptanal. While 7-tridecacone, which is produced via ketonization

of heptanoic acid, is continually observed since the ketonization takes place over the non-reduced cobalt oxide species, as discussed previously.

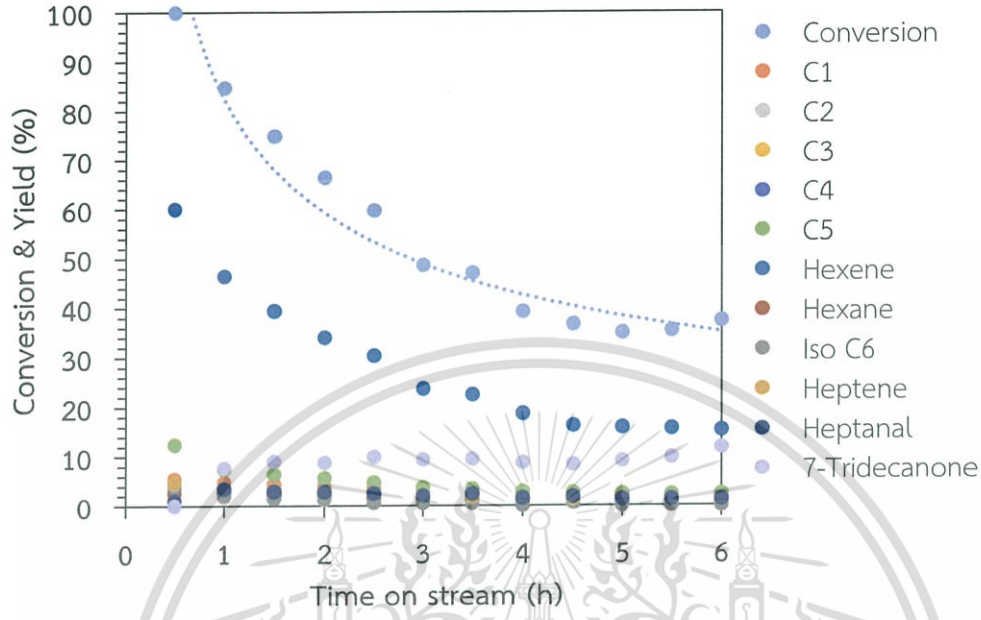

Figure 4.8 Conversion of heptanoic acid and yield of products from the deoxygenation of heptanoic acid over 5 wt% Co/SiO_2. *Reaction conditions: 10 wt% heptanoic acid in octane, contact time 33 g·h/mol, activation temperature 600 °C and reduction temperature 600 °C, reaction temperature 400 °C, 1 atm, and 100 mL/min of H_2.*

The cause of catalyst deactivation could be the results of (i) strongly adsorbed heptanoic acid or (ii) coke formation on Co surface. To verify a nature of adsorbed species, TGA was performed over the used catalysts and the major weight loss at 330 °C was shown in **Figure 4.9**.

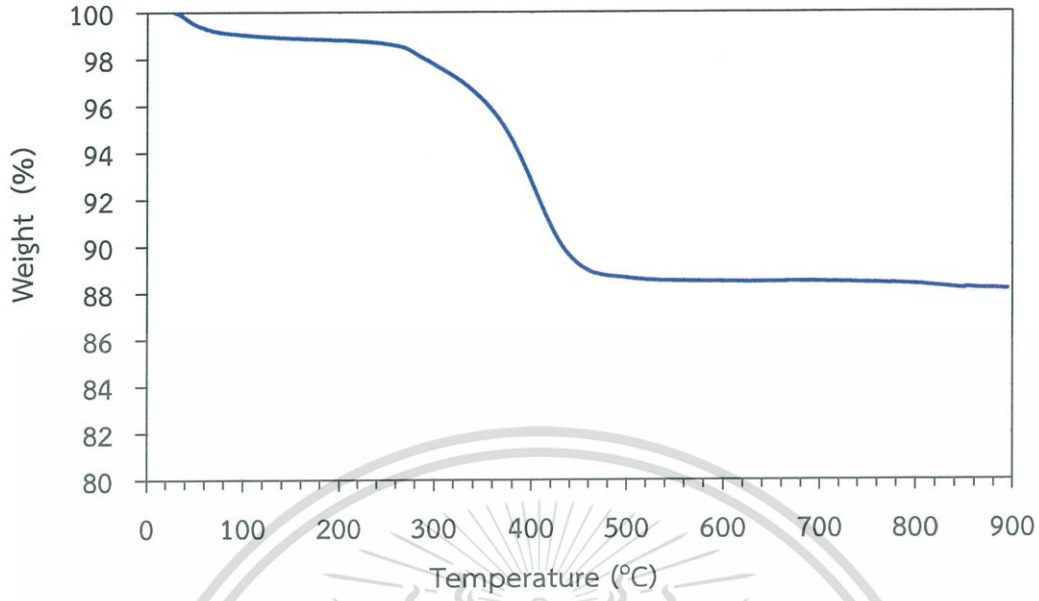

Figure 4.9 TGA profile of spent 5%Co/SiO_2 catalyst.

In addition to small weight loss at 50 °C (moisture on the surface), the 10% weight loss at 330 °C is assumed to be the main cause of the deactivation. Since the weight loss was observed at low temperature, this weight loss may be due to decomposition of adsorbed heptanoic acid on cobalt surface rather than the coke deposition. To validate this assumption feeding of heptanoic acid was paused after 6 h., then the catalysts were flushed with steam at the reaction temperature (400 °C). After that, the heptanoic acid was re-introduced at the same reaction condition and the result is shown in **Figure 4.10**.

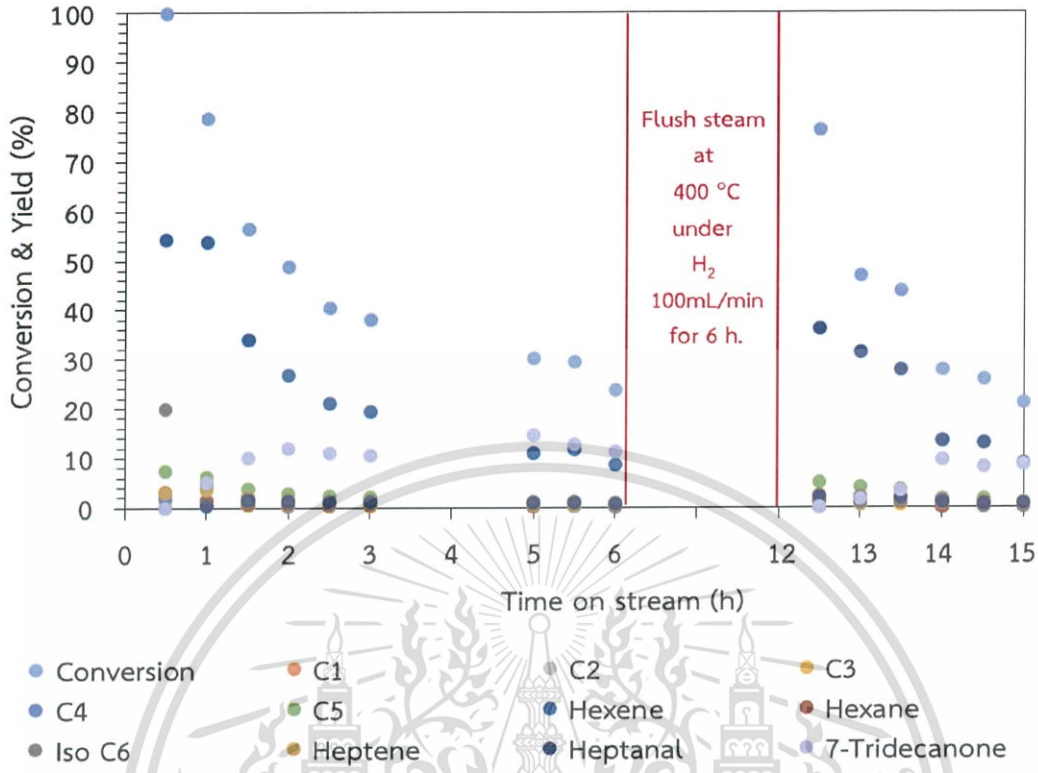

Figure 4.10 Conversion of heptanoic acid and yield of products from the deoxygenation of heptanoic acid over 10 wt% Co/SiO_2. *Reaction conditions: 10 wt% heptanoic acid in octane, contact time 17 g·h/mol, activation temperature 600 °C and reduction temperature 600 °C, reaction temperature 400 °C, 1 atm, and 100 mL/min of H_2.*

It can be seen that after steaming, the activity is recovered with the similar product distribution where hexene is still a major product. It is clear from this experiment that steaming can displace the feed that is adsorbed on the surface of catalysts. If the coke deposit is the cause of catalyst's deactivation, the activity shall not regain after steaming. Hence, it is suggested that heptanoic acid adsorption on the cobalt surface is the cause of catalyst's deactivation.

The deactivation by feed indicates that heptanoic acid can be strongly adsorbed on the cobalt surface. To verify this, adsorption acetic acid on $5\%Co/SiO_2$ and SiO_2 at 140 °C was tested as a model compound. In a manner similar to heptanoic acid, acetic acid, a smaller probe, can readily adsorb and then desorb under inert atmosphere (helium) as shown in **Figure 4.11**.

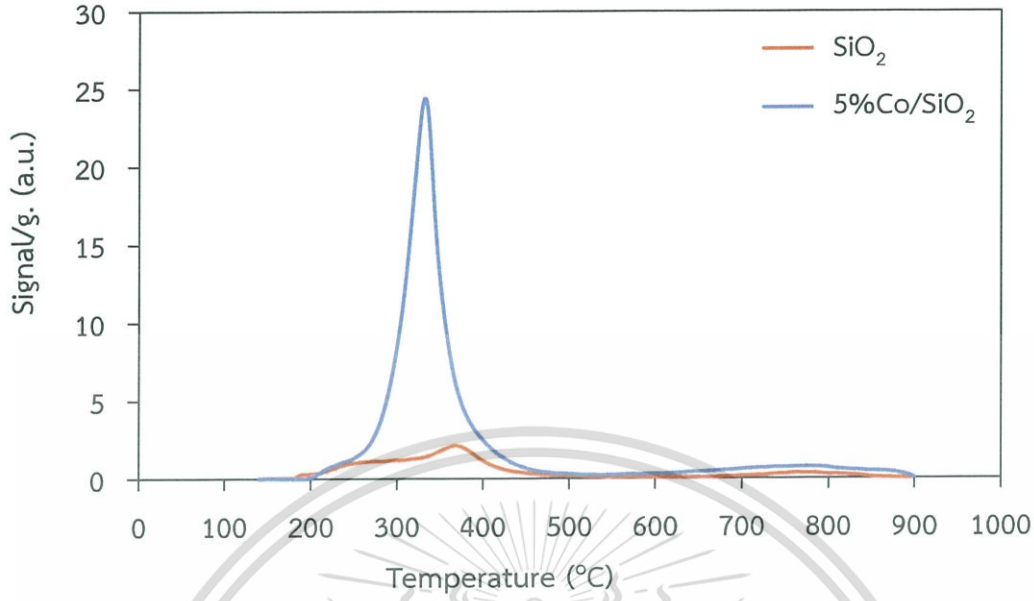

Figure 4.11 Acetic acid decomposition of SiO_2 and 5%Co/SiO_2. The y axis is the signal from TCD normalized by the mass of the sample.

It can be seen that the thermal desorption is found at 320 °C and the amount of acetic acid covered on the surface can be estimated by the peak area. 5%Co/SiO_2 shows a significantly high amount of acetic acid as compared to the inert SiO_2 support despite SiO_2 showing surface area higher than 5%Co/SiO_2 (**Table 4.1**). This indicates the strong interaction between carboxylic acid and cobalt surface. It is noted that acetic acid is adsorbed on the surface and undergone ketonization to acetone upon the desorption. Therefore, the observed desorption peak is referred to acetone that is formed via ketonization of adsorbed acetic acid [69].

From the result in **Figure 4.7**, the deactivation of 2 wt% Co/SiO_2 is more severe, as compared to that of 5%, 10%, and 15 wt% Co/SiO_2. These results point the importance of a particle size of cobalt, which could influence the heptanoic acid adsorption. The smaller the cobalt particle size (2 wt%), the higher the surface energy of Co. Accordingly, the active surface are fully covered by heptanoic acid and no vacant site is available for the feed or dissociated H_2. Thus, catalysts with small particle size show faster deactivation. In contrast, over the large particle size (5%Co loading), the interaction between feed and metal surface are weakened resulting in the relatively slower deactivation rate.

While the catalysts with loading higher than 5 wt% Co/SiO_2, also show faster deactivation as cobalt loading is increased (10 and 15 wt%). This is because the catalyst with high cobalt loading possesses a low Co dispersion providing low metal surface area, as discussed previously in **section 4.1.2**. Hence, the catalysts deactivation in this case is the reason of low dispersion providing the higher deactivation rate for 15%, as compared to 10% Co/SiO_2 and 5%Co/SiO_2. Consequently, 5% Co/SiO_2 will be used for further investigation.

4.2.4 Effect of a secondary metal incorporated to Co catalysts

It is well known that the modification of a monometallic catalyst by the addition of a secondary metal yielding a bimetallic catalyst, can lead to the improvement of an activity, selectivity, and particularly stability. In this section we investigated the effect of various secondary metals, including, Pt, Au, Pd, and Ru incorporated to Co catalysts for deoxygenation of heptanoic acid. The results are summarized in **Figure 4.12**.

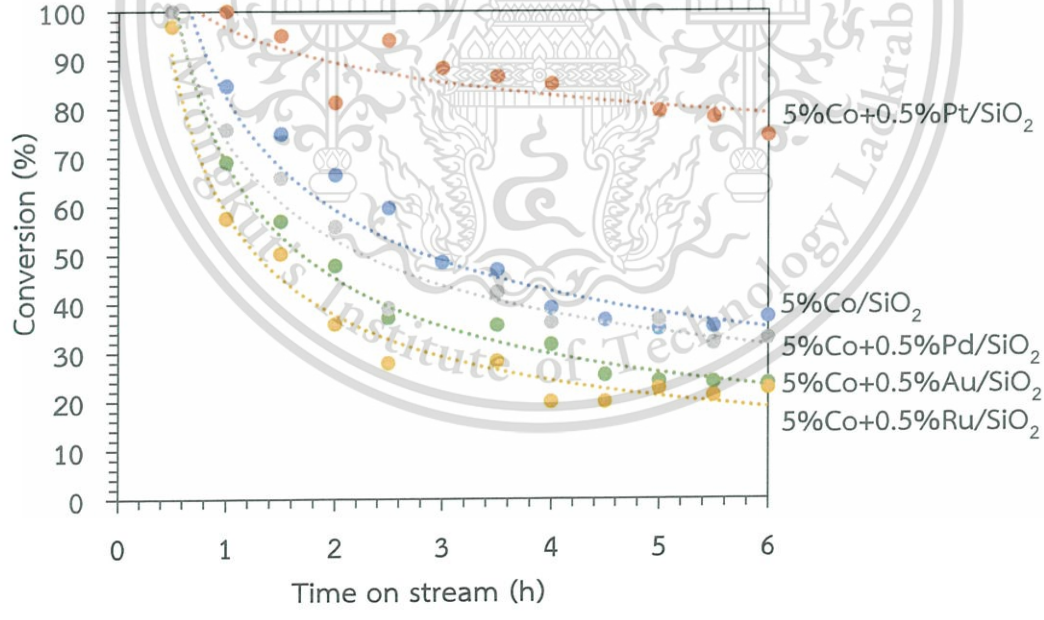

Figure 4.12 Catalytic performance on deoxygenation of various cobalt/metal bimetallic supported on silica catalysts. *Condition: 10 wt% heptanoic acid in octane, contact time 34 g·h/mol, reaction temperature 400 °C, activation temperature 600 °C and reduction temperature 600 °C, 1 atm, and 100 mL/min of H_2.*

Amongst the catalysts investigated, Co-Pt/SiO_2 provided the highest stability with 100% conversion and seem to reach a steady state at 74%. This suggests that Co-Pt/SiO_2 is more stable than Co/SiO_2 because the incorporation of Pt improves the H_2 spillover on the surface. As Pt increased the electron density on Co, a higher efficiency of H_2 adsorption and dissociation can be expected. In line with TPR result, the reduction peak shifts to the low temperature (**Figure 4.5**). Thus, the H_2 spillover at the perimeter of Pt can improve the desorption of heptanoic acid over bimetallic surface. The result can be validated by an experiment of acetic acid decomposition over cobalt and bimetallic cobalt catalysts as shown in **Figure 4.13**.

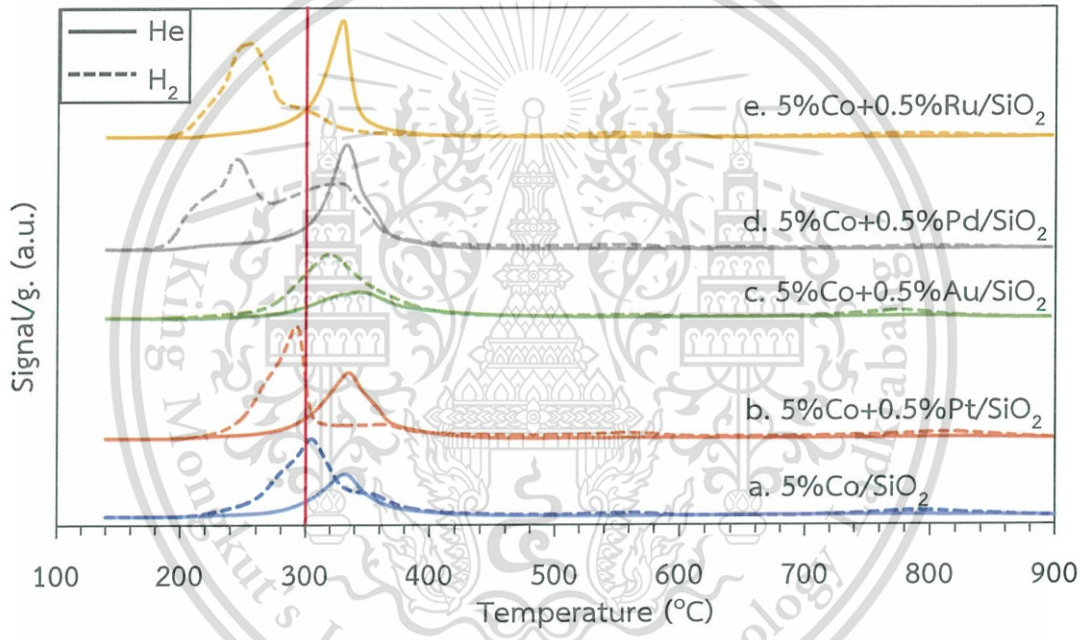

Figure 4.13 Acetic acid decomposition of 5%Co/SiO_2 and 5%Co/metal bimetallic catalysts: helium atmosphere (solid lines) and hydrogen atmosphere (square dot).

According to **Figure 4.13**, when H_2 is used as a carrier gas (square dot), acetic acid decomposition over Co/SiO_2 is shifted to lower temperature (310 °C), suggesting that H_2 can assist the desorption of carboxylic acid over a metal surface. Moreover, the incorporated Pt can improve H_2 spillover to Co. Hence, the acetic acid desorption peak of Co-Pt/SiO_2 is shifted to at even lower temperature (295 °C). This could also be the case for the reaction with heptanoic acid. Hence, the stability of Co-Pt/SiO_2 is higher than that of Co/SiO_2.

The activity and production distribution of metal incorporated Co catalysts are shown in **Table 4.5**.

Table 4.5 Conversion and yield of various cobalt/metal bimetallic over silica catalysts.

Catalysts	Conversion (%)	Selectivity (%)							Hexene/Hexane ratio
		C_1-C_5	Hexene	Hexane	Iso C_6	Heptene	Heptanal	7-tridecanone	
5%Co/SiO_2	84.7	22.6	54.8	2.6	2.5	4.3	4.2	9.0	21.1
5%Co+0.5%Pt/SiO_2	100.0	11.2	54.4	17.9	14.3	2.2	0.0	0.0	3.0
5%Co+0.5%Au/SiO_2	69.1	19.1	56.6	2.2	2.7	4.1	4.5	10.9	25.7
5%Co+0.5%Pd/SiO_2	75.7	12.0	48.4	4.4	2.0	3.0	20.2	10.0	11.0
5%Co+0.5%Ru/SiO_2	57.5	15.2	64.7	1.8	2.1	3.6	5.2	7.4	35.9

Condition: 10 wt% heptanoic acid in octane, contact time 34 g·h/mol, reaction temperature 400 °C, activation temperature 600 °C and reduction temperature 600 °C, 1 atm, and 100 mL/min of H_2, The activity is at 1 h on stream.

According to **Table 4.5**, Co-Pt/SiO_2 gives activity higher than Co/SiO_2; while, Co-Pd/SiO_2, Co-Au/SiO_2, Co-Ru/SiO_2 give lower activity. All of catalysts give hexene as a major product. The catalyst's activity and hexene selectivity are still high when the secondary metal is added suggesting the Co surface remained in the active metallic phase.

For Co-Pt/SiO_2, hexane and iso-C6 are particularly increased. This is because the hydrogenation of hexene to hexane, decarboxylation of heptanoic acid to hexane, and isomerization of hexane to iso-C6 are promoted over Pt particle. However, the reduction peak of monometallic Pt is not observed in TPR profile because the Pt loading is relatively small to be detected by TPR. (**Figure 4.5**).

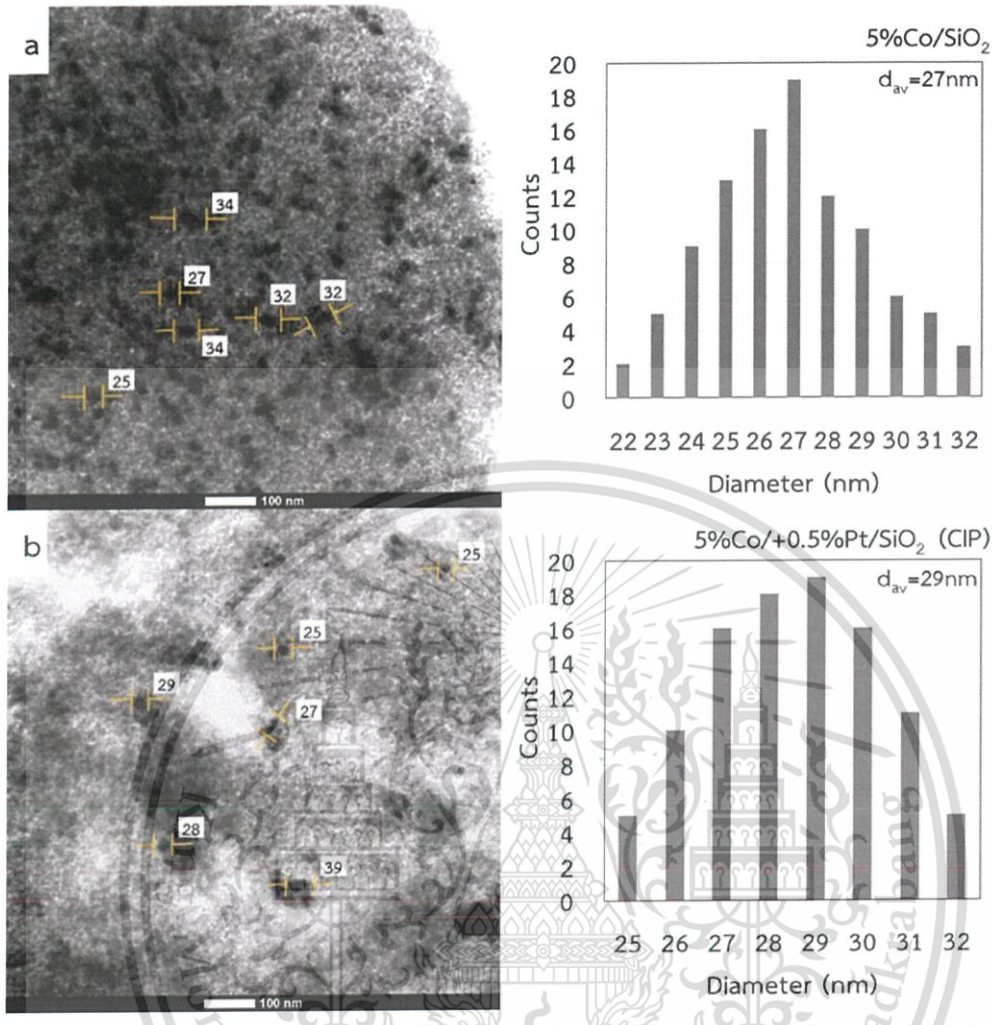

Figure 4.14 TEM images and particle size distribution histograms of reduce catalysts: a) 5%Co/SiO_2, b) 5%Co+0.5%Pt/SiO_2.

In line with above suggestion, TEM shows that monometallic Co and bimetallic Co-Pt are dispersed on SiO_2 matrix with the mean size 27 and 29 nm, respectively (**Figure 4.14**). The size distribution of these two catalysts is monomodal and not significantly different. This could attribute to the Pt may well be interacted with parent Co particles. Due to increased electron density of bimetallic Co-Pt, the selectivity of C1-C5 are decreased. This is because the cracking and hydrogenolysis activity are minimized. Furthermore, the ketonization of heptanoic acid is suppressed.

Once incorporated Au to cobalt catalyst, it gives product distribution similar to Co/SiO_2. However, Co-Au/SiO_2 shows lower initial activity (69.1%, **Table 4.5**) and stability (**Figure 4.12**), as compared to Co/SiO_2. This is presumably because Au is less effective for H_2 dissociation and hence H_2 spillover. This is confirmed by TPR profile as

shown in **Figure 4.5** that the reduction temperature of Co-Au is relatively high compared with other bimetallic catalysts. In line with this view, acetic acid decomposed under H_2 at higher temperature (**Figure 4.13**), as compared to that of Co/SiO_2. It is suggested that carboxylic acid can be strongly adsorb on Co-Au surface leading to faster deactivation rate.

For $Co\text{-}Pd/SiO_2$, low activity and stability was also obtained, as compared to Co/SiO_2 despite that H_2 spillover is enhanced as evidenced by the lower reduction temperature (**Figure 4.5**). This suggests that the observed deactivation of Co-Pd is due to the strong adsorption of heptanoic acid over Co-Pd surface as seen by acetic acid decomposition in **Figure 4.13**. $Co\text{-}Pd/SiO_2$ shows two decomposition peak under H_2 atmosphere. The second peak at higher temperature indicates that carboxylic acid possesses strong interaction with Co-Pd surface resulting in the low catalyst's stability. In a different manner, $Co\text{-}Pd/SiO_2$ shows the high selectivity to heptanal (**Table 4.5**), suggesting that Co-Pd promotes the reduction of heptanoic acid to heptanal but suppresses the decarbonylation.

In case of $Co\text{-}Ru/SiO_2$, the highest selectivity of hexene was obtained. However, the lowest activity and stability, as compared to the other catalysts, were evidenced. It is possible that Ru is deactivated by CO (that is produced from the decarbonylation of heptanal). CO poisoning could be responsible for the decrease in activity and stability of $Co\text{-}Ru/SiO_2$ catalyst, as suggested by Bo Carrillo (2014) [70,71].

From above results, $5\%Co{+}0.5\%Pt/SiO_2$ provides the relatively high activity and stability for deoxygenation of heptanoic acid to hexene in which it will be further investigated the effect of catalyst's preparation.

4.2.5 Effect of the preparation method for bimetallic Co-Pt catalysts

In this section, the catalytic performances of bimetallic 5%Co+0.5%Pt/SiO_2 prepared by co-impregnation (CIP) and sequential impregnation (SIP) for the production of α–olefin from fatty acid using heptanoic acid as a model were investigated under H_2 100 mL/min at 400 °C. The results are shown in **Figure 4.15**.

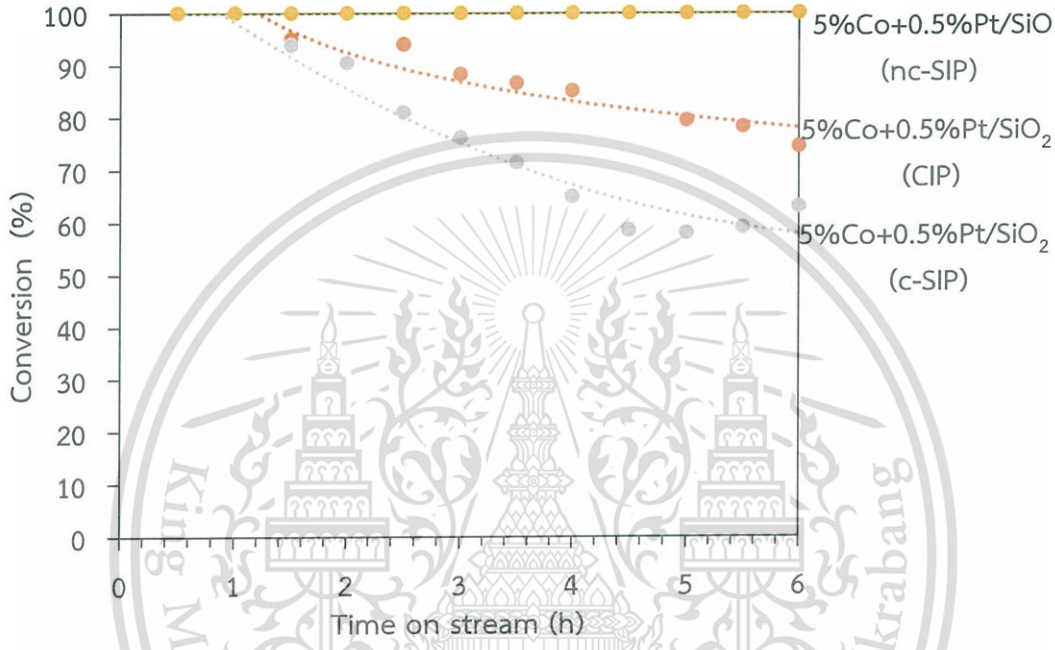

Figure 4.15 Catalytic performance of deoxygenation of heptanoic acid using various preparation methods for Co-Pt bimetallic catalysts. *Condition: 10 wt% heptanoic acid in octane, contact time 34 g·h/mol, reaction temperature 400 °C, activation temperature 600 °C and reduction temperature 600 °C. 1 atm, and 100 mL/min of H_2, (5%Co+0.5%Pt/SiO_2 (nc-SIP) is not insitu-calcined).*

Considering the catalyst prepared by a sequential impregnation (SIP), it can be seen that the Co-Pt/SiO_2 (nc-SIP) gives stability higher than the calcined Co-Pt/SiO_2 (c-SIP) as shown in **Figure 4.15**. However, the Co-Pt/SiO_2 (nc-SIP) gives undesired hexane as a main product (**Table 4.6**).

Table 4.6 Conversion and selectivity of various preparation method of bimetallic Co-Pt over silica catalysts.

Catalysts	Conversion (%)	Yield (%)							Hexene/Hexane ratio
		C_1-C_5	Hexene	Hexane	Iso C_6	Heptene	Heptanal	7-tridecanone	
5%Co+0.5%Pt/SiO_2 (nc-SIP)	100.0	3.0	1.0	70.6	21.5	0.0	3.9	0.0	0.0
5%Co+0.5%Pt/SiO_2 (c-SIP)	94.0	14.5	49.7	12.7	8.8	2.2	3.9	2.2	3.9
5%Co+0.5%Pt/SiO_2 (CIP)	95.3	10.4	49.1	15.7	10.7	2.0	4.1	3.3	3.1

Condition: 10 wt% heptanoic acid in octane, contact time 34 g·h/mol, reaction temperature 400 °C, activation temperature 600 °C and reduction temperature 600 °C, 1 atm, and 100 mL/min of H_2. The activity is at 1.5 h on stream. (5%Co+0.5%Pt/SiO_2 (nc-SIP) is not insitu-calcined).

Considering Co-Pt/SiO_2 (nc-SIP) from **Table 4.6**, the decarboxylation of heptanoic acid and hydrogenation of hexene are promoted over active Pt phase. This is because in this catalyst, isolated Pt particle is present, as confirmed by TPR profile in **Figure 4.16**. The Co-Pt/SiO_2 (nc-SIP) catalyst shows a small peak at 128 °C that indicated a reduction of platinum (II) nitrate. This leads to a suggestion that the isolated Pt species is separated from Co particle from the sequential impregnation without the calcination. Large peaks at 178 and 314 °C can be referred to the reduction peaks of Co^{3+} to Co^{2+} and Co^{2+} to Co^0. Since, the isolated Pt successively promote the decarboxylation yielding hexane over Co-Pt/SiO_2 (nc-SIP), the decarbonylation of heptanal to hexene and hydrogenolysis of hexane to C1 – C5 over Co-Pt/SiO_2 (nc-SIP) are decreased. Thus, Co-Pt/SiO_2 (nc-SIP) is not suitable for the production of α–olefin from fatty acid.

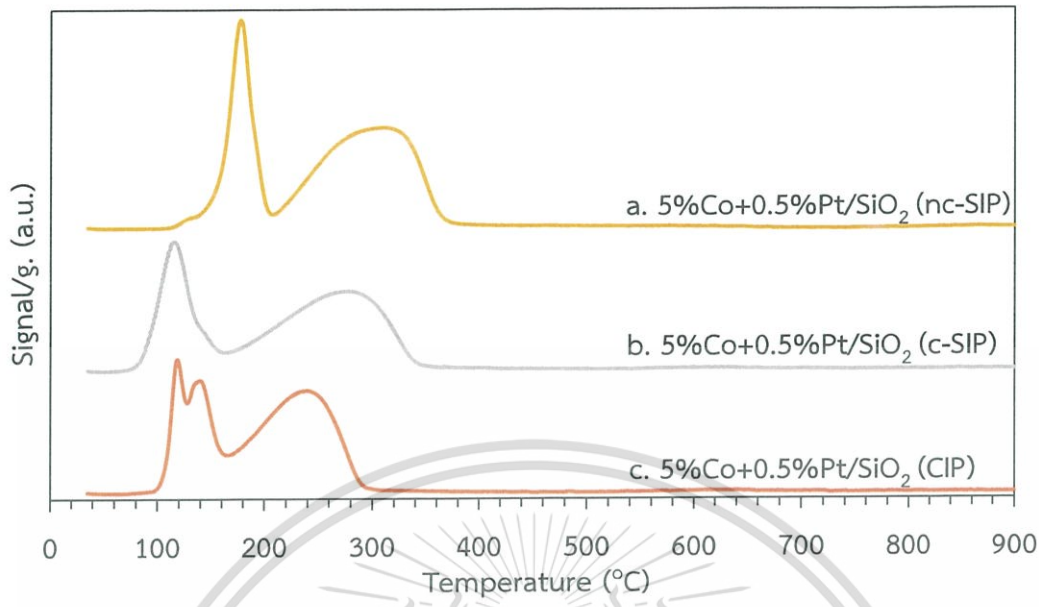

Figure 4.16 Temperature programmed reduction profiles of 5%Co+0.5%Pt/SiO_2 with various preparation methods.

In sharp contrast, Co-Pt/SiO_2 (c-SIP) gives hexene as a major product, in a manner similar to the Co-Pt/SiO_2 catalyst prepared by co-impregnation (Co-Pt/SiO_2 (CIP)). It is suggested that, over these catalysts, Co acts as an active phase for the decarbonylation. This is because, when the catalysts prepared by sequential impregnation (SIP) and co-impregnation (CIP) are calcined, Co-Pt mixed oxide can be formed and re-dispersed on the silica support. After the reduction, bimetallic Co-Pt is formed and no separate phase of Pt is detected from TPR profile (**Figure 4.16**). Moreover, for both catalysts, the reduction temperature shift to lower temperature, as compared with 5%Co/SiO_2 (**Figure 4.5**) and the reduction of Co-Pt mixed oxide is observed. The TPR profile of Co-Pt/SiO_2 (c-SIP) shows two large peaks at 118 and 284 °C. The first peak is the reduction of Co-Pt mixed oxide to bimetallic Co-Pt combined with the reduction peak of Co^{3+} to Co^{2+} and the second peak is referred to Co^{2+} to Co^0. In line with this view, Co-Pt/SiO_2 (CIP) shows the reduction peak of Co-Pt mixed oxide to bimetallic Co-Pt and Co^{3+} to Co^{2+} at 120 - 145 °C. While, the reduction of Co^{2+} to Co^0 is at 246 °C with similar H_2 consumption (**Table 4.7**).

Table 4.7 Hydrogen consumption of each catalyst.

Catalysts	T_1 (°C)	T_2 (°C)	T_3 (°C)	H_2 consumption mmol/g
5%Co+0.5%Pt/SiO_2(nc-SIP)	128	178	314	1.56
5%Co+0.5%Pt/SiO_2(c-SIP)	118	-	284	1.32
5%Co+0.5%Pt/SiO_2(CIP)	120	145	246	1.26

nc-SIP is non calcined sequential impregnation

c-SIP is calcined sequential impregnation

CIP is calcined co-impregnation

Accordingly, both calcined catalysts (Co-Pt/SiO_2 (CIP) and Co-Pt/SiO_2 (c-SIP)) can promote mainly decarbonylation since the incorporated Pt well interacts with the Co. Therefore, heptanoic acid decarboxylation and hexene hydrogenation are suppressed by these catalysts.

However, Co-Pt/SiO_2 (CIP) gives higher stability, than Co-Pt/SiO_2 (c-SIP). In similar support manner, the reduction temperature (Co^{2+} to Co^0) of Co-Pt/SiO_2 (CIP) is significantly lower than Co-Pt/SiO_2 (c-SIP) since the metal precursor is well-mixed prior to co-impregnation. The Pt and Co precursors are homogeneously dispersed over the support facilitating the strong interaction between Co-Pt during the reduction. Accordingly, the catalyst was prepared by co-impregnation (CIP) provides the greater fraction of bimetallic Co-Pt, as compared to sequential impregnation method (SIP). The bimetallic Co-Pt can improve the H_2 spillover and facilitate the desorption of feed. Overall, co-impregnation catalysts (CIP) provides higher stability, than sequential catalysts (c-SIP).

4.2.6 Effect of platinum loading on Co/SiO_2 catalysts

To further investigate the role of Pt incorporated on Co catalysts, the different Pt loading (0.25 wt%, 0.5 wt%, and 0.75 wt%) catalysts were prepared by the co-impregnation method and tested for deoxygenation of heptanoic acid under H_2 atmosphere at 400 °C. The results are demonstrated in **Table 4.8**.

Table 4.8 Conversion and yield of various % load Pt over Co-Pt catalysts.

Catalysts	Conversion (%)	Yield (%)							Hexene/Hexane ratio
		C_1-C_5	Hexene	Hexane	Iso C_6	Heptene	Heptanal	7-tridecanone	
5%Co+0.25%Pt/SiO_2	85.1	12.8	46.5	9.5	7.2	2.3	3.8	3.0	4.9
5%Co+0.5%Pt/SiO_2	95.2	10.4	49.1	15.7	10.6	2.0	4.1	3.3	3.1
5%Co+0.75%Pt/SiO_2	94.1	10.8	48.5	15.5	12.1	1.9	3.8	1.5	3.1

Condition: 10 wt% heptanoic acid in octane, contact time 34 g·h/mol, reaction temperature 400 °C, activation temperature 600 °C and reduction temperature 600 °C, 1 atm, and 100 mL/min of H_2. The activity is at 1.5 h on stream.

From **Table 4.8**, the activity of bimetallic Co-Pt catalysts is increased with the platinum loading. All catalysts give high selectivity of hexene. However, hexane and iso-C6 yield are slightly increased with the Pt loading. This result suggests that Pt can promote **(i)** the decarboxylation of heptanoic acid to hexane, **(ii)** the hydrogenation of hexene to hexane, and **(iii)** the isomerization of hexane to iso-C6. Considering the hexene/hexane ratio, the results suggest that, at Pt loading lower than 1 wt%, the catalyst performs well for selective conversion of fatty acid to α–olefin. In addition, Pt does not only increase activity but also the stability as shown in **Figure 4.17**.

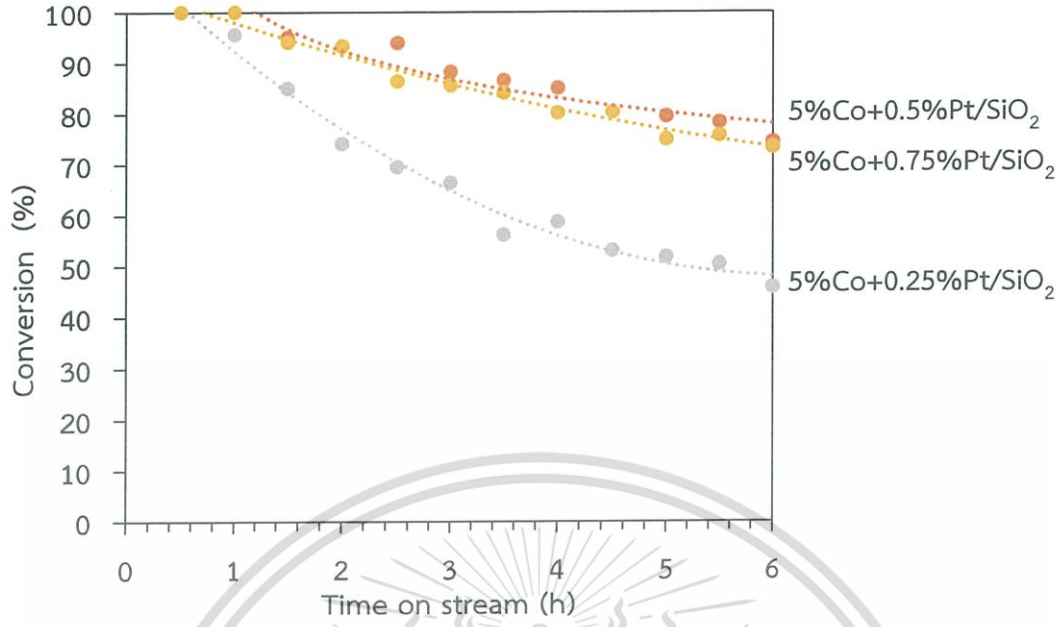

Figure 4.17 Catalytic performance on deoxygenation of various % load Pt over Co-Pt catalysts. *Condition: 10 wt% heptanoic acid in octane, contact time 34 g·h/mol, reaction temperature 400 °C, activation temperature 600 °C and reduction temperature 600 °C, 1 atm and 100 mL/min of H_2.*

Upon the reaction up to 6 h, the stability of Co-Pt catalysts is increased with the Pt loading. This is because the increased Pt content in the bimetallic Co-Pt surface would increase the adsorption of H_2. Therefore, H_2 dissociation and H_2 spillover would also be increased. This assists the desorption of heptanoic acid over the bimetallic surface as discussed earlier. Moreover, the improved reducibility of the catalysts with high Pt loading can be confirmed by TPR profile as shown in **Figure 4.18**.

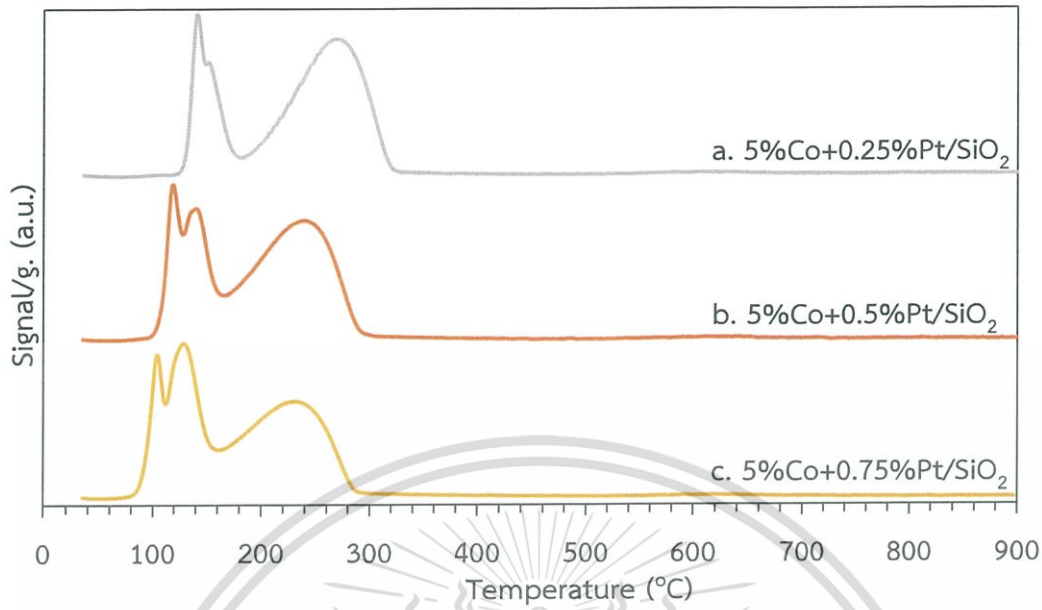

Figure 4.18 Temperature programmed reduction profiles of various platinum loading on bimetallic Co-Pt catalysts.

According to **Figure 4.18**, when Pt loading is increased the reduction peak shift to lower temperature [72] and the H_2 consumption is increased as shown in **Table 4.9**. This indicates that H_2 spillover and hence stability is increased with Pt loading. However, with Pt loading higher than 0.5 wt%, the stability is not significantly improved because the catalysts was already tested at the high conversion.

Table 4.9 Hydrogen consumption of each catalyst.

Catalysts	T_1 (°C)	T_2 (°C)	T_3 (°C)	H_2 consumption mmol/g
5%Co+0.25%Pt/SiO_2	139	149	276	1.20
5%Co+0.5%Pt/SiO_2	121	142	246	1.26
5%Co+0.75%Pt/SiO_2	102	127	232	1.30

From these observations, 5%Co+0.5%Pt/SiO_2 was selected for further investigation on the effect of a contact time.

4.2.7 Effect of contact time

To verify the reaction pathway, the conversion of heptanoic acid are investigated as a function of the contact time (12 – 34 g·h/mol). The experiments were performed over 5%Co+0.5%Pt/SiO_2 (CIP) with the reduction at 600 °C in H_2, and the reaction was tested at 400 °C under H_2 atmosphere. The results are shown in **Figure 4.19**.

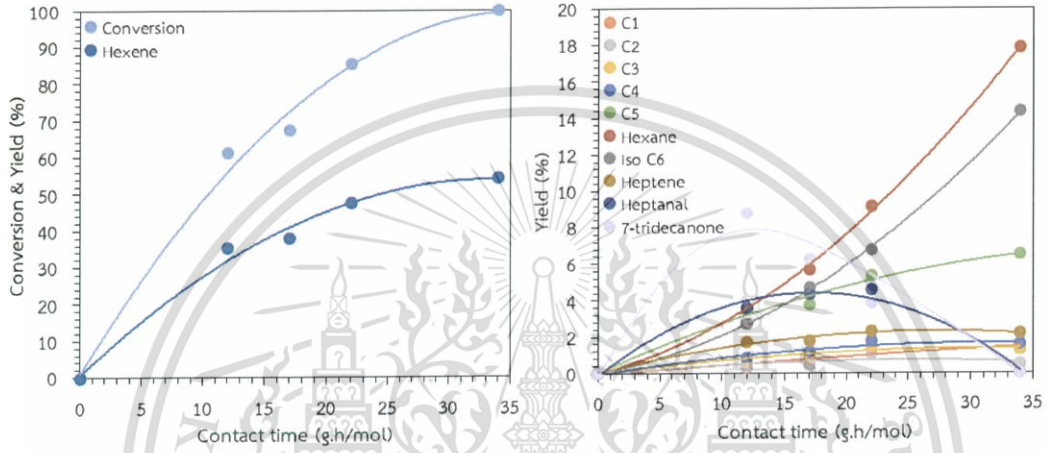

Figure 4.19 Contact time using 5%Co+0.5%Pt/SiO_2 as a catalyst for the heptanoic acid conversion. *Condition: 10 wt% heptanoic acid in octane, reaction temperature 400 °C, activation temperature 600 °C and reduction temperature 600 °C, 1 atm, and 100 mL/min of H_2.*

It can be seen that the conversion of heptanoic acid is increased with contact time (W/F) up to 100% at 34 g·h/mol. This suggests that the activity of catalysts toward the deoxygenation depends on the number of metal site. Hexene, heptanal, and 7-tridecanone are observed initially (≤12 g·h/mol) with hexene as a main product. While, hexane and iso-C6 are predominately observed at high contact time. Heptanal and 7-tridecanone was particularly pronounced at low contact time. It is suggested that heptanal can be preliminary produced via the reduction of heptanoic acid as shown below.

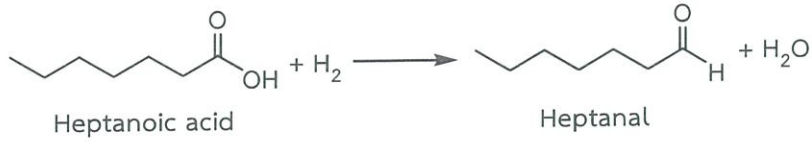

Heptanoic acid Heptanal

While, 7-tridecanone can be produced via ketonization of heptanoic acid as shown below.

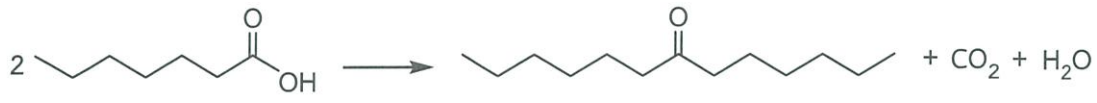

Heptanoic acid 7-tridecanone

Although, yields of all products are increased with the contact time, except heptanal and 7-tridecanone are diminished when the contact time is increased. This indicates that heptanal and 7-tridecanone are an intermediate in the reaction. The major product, hexene, can be produced via the decarbonylation of heptanal in which it is formed initially. The heptanal can be adsorbed in acyl form ((η^1(c)-acylo) on Co surface and decarbonylation to hexene as shown below [52, 73].

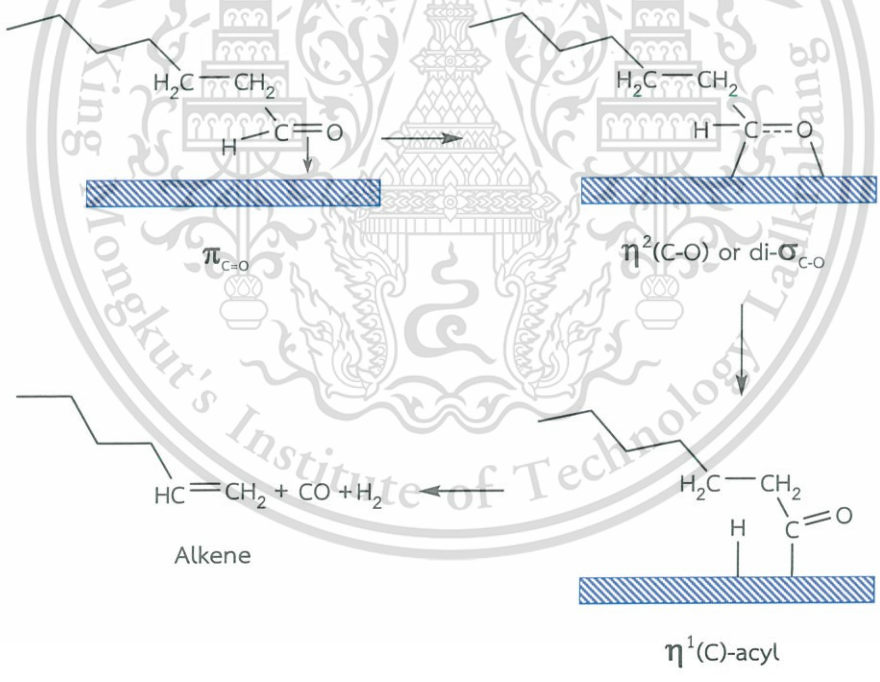

Scheme 4.3 Decarbonylation of heptanal

The minor product hexane can be produced from **(i)** decarboxylation of heptanoic acid or **(ii)** hydrogenation of hexene. Iso-C6 can be produced via isomerization of hexane **(iii)**.

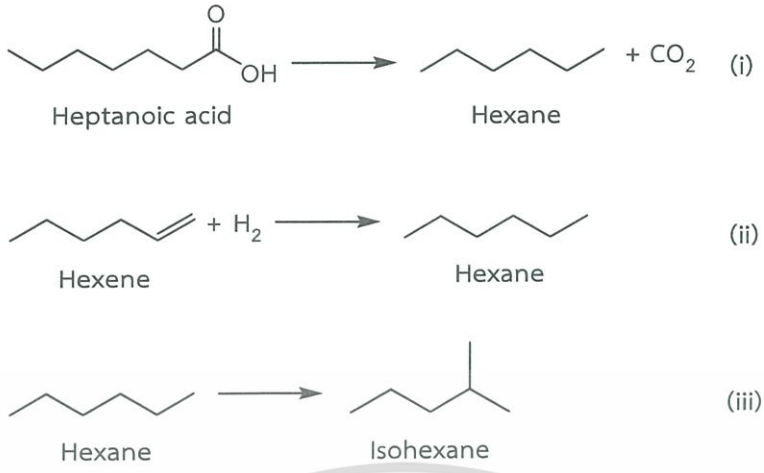

C5 can be produced particularly from cracking of 7-tridecanone **(iv)**. Cracking at the α-carbon of 7-tridecanone produces pentene and octanone in which octanone can further crack to another pentene and acetone. The acetone cannot be observed because it can be hydrogenated, dehydrated, followed by hydrogenation to propane. In line with this view, C5 is particularly observed; while, 7-tridecanone is decreased.

Furthermore, C5 can also be produced by hydrogenolysis of hexane **(v)** or deacetylation of heptanoic acid **(vi)**. Acetic acid produced from heptanoic acid deacetylation, was not observed because the acetic acid can be converted to acetone via ketonization. Acetone is then hydrogenated, dehydrated, and followed by hydrogenation to propane.

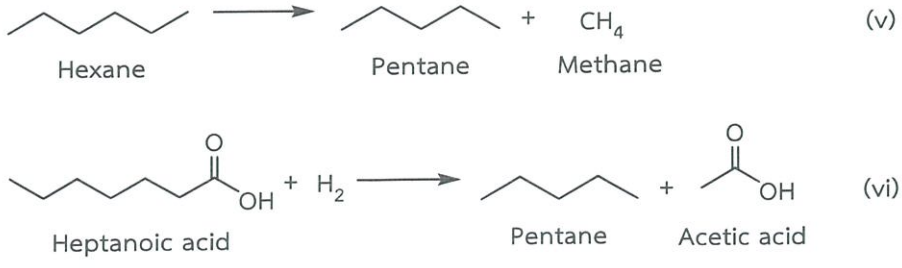

While, heptene can be produced via hydrogenation of heptanal followed by dehydration forming heptane **(vii)**.

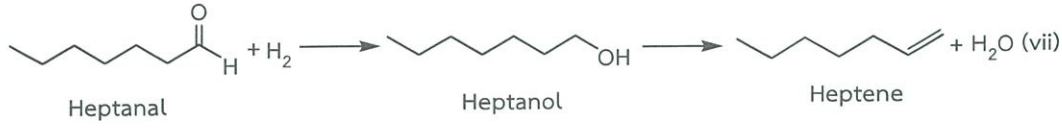

From the above observation, the overall reaction path way for the deoxygenation of heptanoic acid over 5%Co+0.5%Pt/SiO_2 catalyst can be proposed, as demonstrated in **Scheme 4.4**.

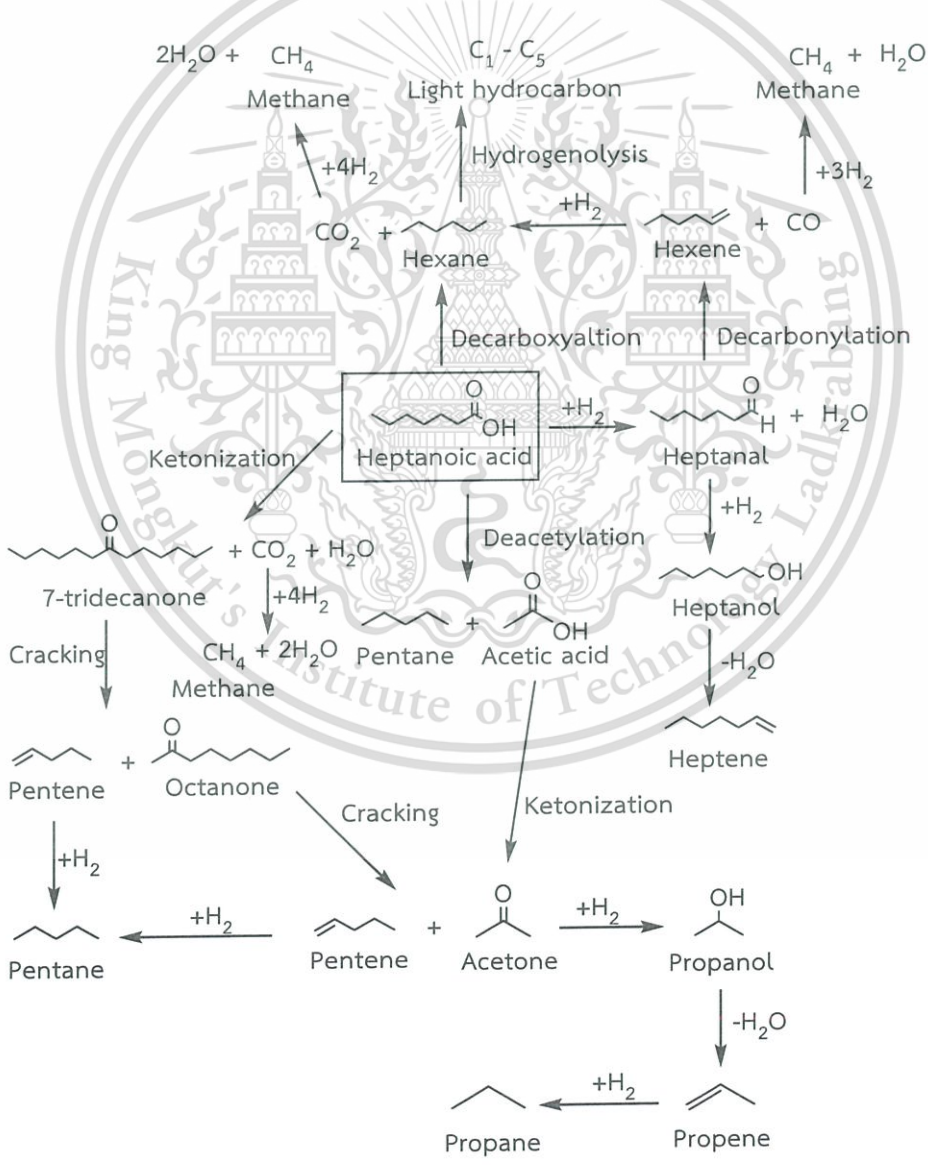

Scheme 4.4 Reaction path way of heptanoic acid over 5%Co+0.5%Pt/SiO_2

CHAPTER 5
Conclusion and Suggestion

5.1 Conclusion

The deoxygenation of heptanoic acid to hexene over cobalt supported silica catalysts were investigated as a model reaction for the conversion of fatty acid to α–olefins. All catalysts shows high surface area (225 – 319 m^2/g) and that area is decreased proportionally when Co loading is increased. XRF results and SEM-EDX show expected metal loading about 2 wt% - 15 wt% of monometallic catalysts (Co, Cu, Ni, Cr) and approximately 5.25 wt% - 5.75 wt% for bimetallic catalysts (Co-Pt, Co-Au, Co-Pd, Co-Ru). H_2-TPR of all monometallic catalysts shows the reduction temperature around 200 – 500 °C with H_2 consumption corresponding to the metal content. However, the H_2 consumption of 5%Cr/SiO_2 is relatively less than its loading since this catalyst contains predominantly non-reducible Cr_2O_3 (Cr^{3+}). Co bimetallic catalysts show a lower reduction temperature, as compared to the monometallic Co catalyst. This suggests that bimetallic Co clusters are formed and the secondary incorporated metal can improve H_2 spillover facilitating the reduction of Co oxide. The metallic Co particle size is increased (18 nm to 52 nm) with Co loading (2 wt% – 15 wt%) as confirmed by TEM images.

Deoxygenation of heptanoic acid to hexene over 5%Co/SiO_2 gives high yield of hexene via reduction/decarbonylation of heptanoic acid; while, 5%Ni/SiO_2 gives similar product distribution but activity lower than the cobalt catalysts. 5%Cu/SiO_2 and 5%Cr/SiO_2 give heptanal and 7-tridecanone as major products via reduction and ketonization, respectively. When the reaction temperature is increased (from 350 to 425 °C), the catalysts show an improved activity. However, at higher temperature (425 °C), the yield of 7-tridecanone is significantly increased because the ketonization of heptanoic acid is particularly promoted at high temperature.

When Co loading is increased from 5wt% to 15wt%, the activity is decreased. This is because the Co surface is decreased since metallic Co particles are agglomerated. All catalysts can promoted hexene as a main product. However, the deactivation is observed for all catalysts due to the strong adsorption of the feed, particularly over 2%Co/SiO_2.

To improve catalyst's stability, Pt, Au, Pd, and Ru are incorporated in to Co catalysts. Co-Pt/SiO_2 gives stability higher than monometallic Co/SiO_2 since Pt facilitates H_2 dissociation and adsorption of heptanoic acid. However, the yield of hexane is slightly increased because Pt can also promote hydrogenation of hexene to hexane and decarboxylation of heptanoic acid to hexane. For Co-Au/SiO_2, Au does not affect H_2 dissociation on Co surface; hence, the stability cannot be improved. Although, Co-Pd/SiO_2 shows a low reduction temperature due to H_2 spillover from Pd to Co surface, the stability is not modified. This is because Co-Pd/SiO_2 provides the strong interaction with carboxylic acid as deduced from the high decomposition temperature of adsorbed acetic acid. In case of Co-Ru/SiO_2 high selectivity of hexene is obtained. However, the catalyst is rapidly deactivated due to the adsorption of CO that is produced from decarbonylation of heptanoic acid/heptanal.

The non-calcined catalysts prepared by sequential impregnation (5%Co+0.5%Pt/SiO_2 (nc-SIP)) shows high activity and stability. However, 5%Co+0.5%Pt/SiO_2 (nc-SIP) gives undesired hexane as a major product since the separated phase of Pt is present. 5%Co+0.5%Pt/SiO_2 (CIP) and 5%Co+0.5%Pt/SiO_2 (c-SIP) gives similar product distribution with hexene as a main product. Since strong interaction between Co and Pt is obtained when Co and Pt precursors are well mixed before impregnation, 5%Co+0.5%Pt/SiO_2 (CIP) shows stability higher than that of 5%Co+0.5%Pt/SiO_2 (c-SIP).

The activity and stability are increased with Pt content (0.25 wt% - 0.75 wt%) because H_2 dissociation and adsorption are increased. The feed desorption is also improved leading to low catalyst deactivation. However, the yield of hexane and iso-C6 is slightly increased with Pt loading since hydrogenation of hexene to hexane and isomerization of hexane to iso-C6 are increased.

The overall results suggested that the 5%Co+0.5%Pt/SiO_2 (CIP) is effective for deoxygenation of heptanoic acid to hexene. The reaction pathway for heptanoic acid conversion to hexene proceeds via the reduction of heptanoic acid to heptanal that is an intermediate for decarbonylation to hexene. However, parallel reactions, including ketonization of heptanoic acid to 7-tridecanone, decarboxylation of heptanoic acid to hexane, and deacetylation of heptanoic acid to pentane can also be promoted. In addition, 7-tridecanone that is primarily produced can be cracked to light hydrocarbons at a high contact time.

5.2 Suggestion

5.2.1 The deactivation can be suppressed when incorporate alkaline metal on bimetallic Co-Ru catalysts due to the increase of surface electron density.

5.2.2 Al_2O_3 can be used as a support for increase in the interaction between active site and thus gaining well-dispersed active site.

5.2.3 Hexane yield (undesired product) can be dispelled by reduce H_2 partial pressure.

5.2.4 Natural fatty acid or high molecular weight fatty acids can be used for industrial-scale.

Reference

[1] Linde-engineering. "Linear alpha olefins (LAOs)" [Online]. Available: http://www.lindeengineering.com/en/process_plants/chemical_and_petrochemical_plants/linear_alpha_olefins/index.html

[2] Arthur, Abraham; Madden, William; Percy, Ryan; and Soliman, Eiman, 2013. "Ethylene to Linear, Alpha Olefins (1-Hexene & 1-Octene)" *Senior Design Reports (CBE).* Paper 52.

[3] A. N. Imane Hachemi,a Klara Jeništová,a,b Päivi Mäki-Arvela,a Narendra Kumar,a Kari Eränen,a Jarl Hemmingc and Dmitry Yu. Murzin, 2016. "Comparative study of sulfur-free nickel and palladium catalysts in hydrodeoxygenation of different fatty acids feedstock for production of biofuels" *CataJ. Sci. Tech.*, 00, 1-3.

[4] Osamu Nagashima, Satoshi Sato, Ryoji Takahashi, Toshiaki Sodesawa, 2005. "Ketonization of carboxylic acids over CeO_2-based composite oxides" Journal of Molecular Catalysis A: Chemical, 227, 231–239.

[5] Lopez-Ruiz, J., 2014. "Decarbonylation of Carboxylic Acids over Supported Metal Catalysts" Retrieved from http://libra.virginia.edu/catalog/libra-oa:7979.

[6] Eduardo Santillan-Jimenez and Mark Crocker, 2012. "Catalytic deoxygenation of fatty acids and their derivatives to hydrocarbon fuels via decarboxylation/decarbonylation" Published online in Wiley Online Library: 26 March 2012.

[7] Jeong-Geol Na, Bo Eun Yi, Ju Nam Kim, Kwang Bok Yi, Sung-Youl Park, Jong-Ho Park, Jong-Nam Kim, Chang Hyun Ko, 2010. "Hydrocarbon production from decarboxylation of fatty acid without hydrogen" Catalysis Today, 156, 44–48.

[8] Juan A. Lopez-Ruiz and Robert J. Davis, 2014. "Decarbonylation of heptanoic acid over carbon-supported platinum nanoparticles", Green Chem., 16, 683.

[9] Elvan Sari a, Manhoe Kimb,c, Steven O. Salleya,b, K.Y. Simon Nga, 2013. "A highly active nanocomposite silica-carbon supported palladium catalyst for decarboxylation of free fatty acids for green diesel production: Correlation of activity and catalyst properties" Applied Catalysis A: General, 467, 261–269.

[10] Mathias Snåre, Iva Kubičková, Päivi Mäki-Arvela, Kari Eränen, and Dmitry Yu. Murzin, 2006. "Heterogeneous Catalytic Deoxygenation of Stearic Acid for Production of Biodiesel" *Ind. Eng. Chem. Res., 45,* 5708-5715.

[11] Maria, R.J. Carmen, F.M. Abraham, C. Lourdes R. and Angel, P. 2009. "Influence of fatty acid composition of raw materials on biodiesel properties." *Bioresource Technology.*, 100, 261-268, 86.

[12] Elmhurst college. "Fatty Acids." [Online]. Available: http://www.elmhurst.edu/~chm/vchembook/551fattyacida.html.

[13] Baca, A. "Animal fat as fuel alternative." [Online]. Available : http://www.polimerieuropa.com/200page.lasso.html.2001

[14] Tamime, A. Y. 2009. "Dairy Fats and Relateed Products." Blackwell Publishing.

[15] Jerry, L. 2004. "Fats and Fatty Acids" The Gale Group, Inc.

[16] Siedlecka, E.M., Kumirska, J., Ossowski, T., Glamowski, P., Gotebiowski, M., Gajdus, J., Kaczynski, Z. and Stepnowski, P. 2008. "Determination of volatile fatty acids in environmental aqueous samples." Journal of Environmental Studies., 17(3): 351-356.

[17] Aparadh, V.T. and Karadge, B.A. 2010. "Fatty acid composition of seed oil from some *Cleome* species." Pharmacognosy Journal, 324-327.

[18] Shahidi, F. 2005. Baily's Industrial Oil and Fat Products. John Wiley & Sons: German.

[19] Świzdor, A., Panek, A., Milecka-Tronina, N. and Kołek, T., 2012. "Biotrans-formations ytilizing β-oxidation cycle reactions in the synthesis of natural compounds and medicines." International Journal of Molecular Sciences, 13(12): 16514-16543.

[20] Chemical21. "Enanthoic acid" [Online]. Available: http://www.chemicalland21.com/industrialchem/organic/ENANTHOIC%20ACID.htm

[21] Lappin, G.R. and Sauer, J.D. 1989. Alpha Olefins Applications Handbook. USA: Marcel Dekker.

[22] Wikipedia. "Deoxygenation" [Online]. Available: http://en.wikipedia.org/wiki/Deoxygenation.

[23] Santillan-Jimenez, E., Morgan, T., Shoup, J., Harman-Ware, A.E. and Crocker, M., 2014. "Catalytic deoxygenation of triglycerides and fatty acids to hydrocarbons over Ni–Al layered double hydroxide." Catalysis Today, 237, 136-144.

[24] Yang, C., Nie, R., Fu, J., Hou, Z. and Lu, X. 2013. "Production of aviation fuel via catalytic hydrothermal decarboxylation of fatty acids in microalgae oil." Bioresource Technology., 146: 569–573.

[25] Promchana, P. 2016. "Mechanistic study on the conversion of fatty acid to long chain olefins over titanate-based catalysts." Faculty of science. King Mongkut's Institute Technology of Ladkrabang.

[26] M. Fleisher, V. Stonkus, T. Liepina, K. Edolfa, D. Jansone, L. Leite, E. Lukevics, 2009. "Theoretical study of the ketonization reaction mechanism of acetic acid over SiO_2" 13rd International Electronic Conference on Synthetic Organic Chemistry (ECSO-13), 1-30 November 2009.

[27] Chiappero, M., Do, P.T.M., Crossley, S., Lobban, L.L. and Resasco, D.E., 2011. "Direct conversion of triglycerides to olefins and paraffins over noble metal supported catalysts." Fuel, 90(3): 1155-1165.

[28] Cao, L. and Zhang, S., 2015. "Production and characterization of biodiesel derived from Hodgsonia macrocarpa seed oil." Applied Energy, 146, 135-140.

[29] Clark, J., 2002, "The mechanism for the esterification reaction". [Online]. Available: http://www.chemguide.co.uk/physical/catalysis/esterify.html

[30] L.G. Wade, Jr. 2013. "Organic chemistry." USA: Pearson education.

[31] Manríquez-Ramírez, M., Gómez, R., Hernández-Cortezc, J.G., Zúniga-Moreno, A., Reza-San Germána, C. M. and Flores- Valle, S. O., 2013. "Advances in the trans-esterification of triglycerides to biodiesel using MgO–NaOH, MgO–KOH and MgO–CeO_2 as solid basic catalysts." Catalysis Today, 212(1): 23-30.

[32] Fu , J., Chen, L., Lv, P., Yang, L. and Yuan, Z. 2015. "Free fatty acids esterification for biodiesel production using self-synthesized macroporous cation exchange resin as solid acid catalyst." Fuel, 154(15): 1-8.

[33] Alsobaai, A.M., Shaibani, A.M.A., Moustafa, T. and Derhem, A., 2012. "Effect of hydrogenation temperature on the palm mid-fraction fatty acids composition and conversion." Journal of King Saud University-Engineering Sciences., 24(1): 45-51.

[34] Saeb, M.R., Mohammadi, Y., Ahmadi, M., Khorasani, M.M. and Stadler, F.J., 2015. "A Monte Carlo-based feeding policy for tailoring microstructure of copolymer chains: Reconsidering the conventional metallocene catalyzed polymerization of α-olefins." Chemical Engineering Journal, 274, 1385-8947.

[35] Curtis, N., Kang, S.C., Choi, S., Oh, S.H. and Park, Y.K., 2015. "A Catalytic Cracking Process for Ethylene and Propylene from Parafin streams: The Advanced Cataltic Olefins (OXO) Process." Prepared for Presentation at the 2007 Spring National Meeting – Houston. Texas KBR Internal Reference Paper.

[36] Kurokawa, H., Miura, K., Yamamoto, K., Sakuragi, T., Sugiyama, T., Ohshima, M. and Miura, H., 2013. "Oligomerization of Ethylene to Produce Linear α-Olefins Using Heterogeneous Catalyst Prepared by Immobilization of α-Diiminenickel(II) Complex into Fluorotetrasilicic Mica Interlayer." Catalysts, 3(1): 125-136.

[37] Arthur, Abraham; Madden, William; Percy, Ryan; and Soliman, Eiman, 2013. "Ethylene to Linear, Alpha Olefins (1-Hexene & 1-Octene)." Senior Design Reports (CBE). Paper 52.

[38] Mathias Snåre, Iva Kubičková, Päivi Mäki-Arvela, Kari Eränen, and Dmitry Yu. Murzin, 2006. "Heterogeneous Catalytic Deoxygenation of Stearic Acid for Production of Biodiesel." Ind. Eng. Chem. Res., 45, 5708-5715.

[39] Mathias Snåre, Iva Kubičková, Päivi Mäki-Arvela, Kari Eränen, and Dmitry Yu. Murzin, 2008. "Catalytic deoxygenation of unsaturated renewable feedstocks for production of diesel fuel hydrocarbons" Fuel, 87, 933–945.

[40] Irina Simakova, Olga Simakova, Päivi Mäki-Arvela, Andrey Simakov, Miguel Estrada, Dmitry Yu. Murzin, 2009. "Deoxygenation of palmitic and stearic acid over supported Pd catalysts: Effect of metal dispersion." Applied Catalysis A: General, 355, 100–108.

[41] P. Mäki-Arvela, M. Snåre, K. Eränen, J. Myllyoja, D.Yu. Murzin, 2008. "Continuous decarboxylation of lauric acid over Pd/C catalyst." Fuel, 87, 3543–3549.

[42] Siswati Lestari, Pa¨ivi Ma¨ki-Arvela, Heidi Bernas, Olga Simakova, Rainer Sjo¨holm, Jorge Beltramini, G. Q. Max Lu, Jukka Myllyoja, Irina Simakova, and Dmitry Yu. Murzin, 2009. "Catalytic Deoxygenation of Stearic Acid in a Continuous Reactor over a Mesoporous Carbon-Supported Pd Catalyst." Energy & Fuels, 23, 3842–3845.

[43] Juan A. Lopez-Ruiz and Robert J. Davis, 2014. "Decarbonylation of heptanoic acid over carbon-supported platinum nanoparticles" Green Chem., 16, 683

[44] Michael Dennis and P. E. Kolattukudy, 1992. "A cobalt-porphyrin enzyme converts a fatty aldehyde to a hydrocarbon and CO." Proc. Natl. Acad. Sci. USA 89.

[45] Shuo Yuan, Hongjian Sun, Shumiao Zhang, Xiaoyan Li, 2016. "Synthesis of fluorophenyl carbonyl cobalt (I) complexes and decarbonylation of 2,4,5-trifluorobenzaldehyde catalyzed by $CoMe(PMe_3)_4$." Inorganica Chimica Acta, 439, 100–105.

[46] G. Leendert Bezemer, Johannes H. Bitter, Herman P. C. E. Kuipers, Heiko Oosterbeek, Johannes E. Holewijn, Xiaoding Xu, Freek Kapteijn, A. Jos van Dillen, and Krijn P. de Jong, 2006. "Cobalt Particle Size Effects in the Fischer-Tropsch Reaction Studied with Carbon Nanofiber Supported Catalysts" J. AM. CHEM. SOC., 128, 3956.

[47] Tatsumi Ishihara, Koichieguchi and Hiromichi Arai, 1998. "Supported Iron-Cobalt-Nickel Ternary Alloy Catalysts for the Hydrogenation of Carbon Monoxide." Applied Catalysis, 40, 87-100.

[48] de Lange, M.W. 2000. Selective deoxygenation of carboxylic acid. Innovation Oriented reseach Programme on Catalysis.

[49] Liu, H., Ma, H.T., Li, X.Z., Li, W.Z., Wu, M. and Bao, X.H. 2003. "The enhancement of TiO_2 photocatalytic activity by hydrogen thermal treatment." Chemosphere, 50, 39-46.

[50] Shuo Zhao, Hairong Yue, Yujun Zhao, Bo Wang, Yaochen Geng, Jing Lv, Shengping Wang, Jinlong Gong, Xinbin Ma, 2013. "Chemoselective synthesis of ethanol via hydrogenation of dimethyl oxalate on Cu/SiO_2: Enhanced stability with boron dopant" Catalysis, 291, 142-150.

[51] Li Huiyun, Yue Yinghong, Miao Changxi, Xie Zaiku, Hua Weiming, Gao Zi, 2006. "Preparation of Highly Active Cr_2O_3-SiO_2 Catalyst by Sol-Gel Method for Ethylbenzene Dehydrogenation in the Presence of CO_2" Chin J Catal, 27(1), 4–6.

[52] Surapas Sitthisa, Daniel E. Resasco, 2011. "Hydrodeoxygenation of Furfural Over Supported Metal Catalysts: A Comparative Study of Cu, Pd and Ni" Catal Lett, 141, 784–791.

[53] Evandro B. Pereira, Narcís Homsa, Salvador Martí, J.L.G. Fierro, Pilar Ramírez de la Piscina, 2008. "Oxidative steam-reforming of ethanol over Co/SiO_2, Co–Rh/SiO_2 and Co–Ru/SiO_2 catalysts: Catalytic behavior and deactivation/regeneration processes" Journal of Catalysis 257, 206–214.

[54] A. Zecchina, E. Groppo, A. Damin, C. Prestipino, 2005. "Anatomy of Catalytic Centers in Phillips Ethylene Polymerization Catalyst" Top. Organomet. Chem, 16, 1-35.

[55] C. Medina, R. García, P. Reyes, J.L.G. Fierro, N. Escalona, 2010. "Fischer Tropsch synthesis from a simulated biosyngas feed over $Co(x)/SiO_2$ catalysts: Effect of Co-loading" Applied Catalysis A: General, 373, 71-75.

[56] F. Maillard, S. Schreier, M. Hanzlik, E. R. Savinova, S. Weinkauf and U. Stimming, 2005. "Influence of particle agglomeration on the catalytic activity of carbon-supported Pt nanoparticles in CO monolayer oxidation" Phys. Chem. Chem. P h y s., 7, 385-393

[57] F. Diehl and A.Y. Khodakov, 2009. "Promotion of Cobalt Fischer-Tropsch Catalysts with Noble Metals: a Review" Oil & Gas Science and Technology – Rev. IFP, 64, 11-24.

[58] M. de Beer, A. Kunene, D. Nabaho, M. Claeys, and E. van Steen, 2014. "Technical and economic aspects of promotion of cobalt-based Fischer-Tropsch catalysts by noble metals–a review" The Journal of The Southern African Institute of Mining and Metallurgy, 114, 157-165.

[59] D. Schanke, S. Vada, E. A. Blekkan, A.M. Hilmen, A. Hoff, and Holmen, 1995. "Study of Pt-Promoted Cobalt CO Hydrogenation Catalysts" Journal of catalysis, 156, 85-95.

[60] Nitin Kumar, Miranda L. Smith, J.J. Spivey, 2012. "Characterization and testing of silica supported cobalt–palladium catalysts for conversion of syngas to oxygenates" Journal of Catalysis, 289, 218–226.

[61] Bin Wang, Jian-Feng Chen and Yi Zhang, 2015. "Synthesis of highly dispersed cobalt catalyst for hydroformylation of 1-hexene" RSC Adv., 5, 22300–22304.

[62] Atthapon Srifa, Nawin Viriya-empikul, Suttichai Assabumrungrat and Kajornsak Faungnawakij, 2015. "Catalytic behaviors of Ni/γ-Al_2O_3 and Co/γ-Al_2O_3 during the hydrodeoxygenation of palm oil" Catal. Sci. Technol., 5, 3693.

[63] Mshari A. Alotaibi, Elena F. Kozhevnikova, Ivan V. Kozhevnikov, 2012. "Deoxygenation of propionic acid on heteropoly acid and bifunctional metal-loaded heteropoly acid catalysts: Reaction pathways and turnover rates" Applied Catalysis A: General, 447–448, 32– 40.

[64] Minhua Zhang, Rui Yao,ab Haoxi Jiang, Guiming Li and Yifei Chen, 2017. "Catalytic activity of transition metal doped Cu (111) surfaces for ethanol synthesis from acetic acid hydrogenation: a DFT study" RSC Adv., 7, 1443.

[65] Naoko Yamagata, Naoko Fujita, Toshiharu Yokoyama and Takao Maki, 1998. "Direct Hydrogenation of Aliphatic Carboxylic Acids to Corresponding Aldehydes with Cr_2O_3 Catalyst" Science and Technology in Catalysis, 441-444.

[66] I. Fernandez-Morales, A. Guerrero-Ruiz, F.J. Lopez-Garzon, I. Rodriguez-Ramos and C. Moreno-Castilla, 1984. "Hydrogenolysis of n-Butane and Hydrogenation of carbon monoxide on Ni and Co Catalysts Supported on Saran Carbons" Applied Catalysis, 14, 159-172

[67] Eric van Steen, Gary S. Sewell, Rafene A. Makhothe, Craig Micklethwaite, Heiko Manstein, Martijn de Lange, and Cyril T. O'Connor, 1996. "TPR Study on the Preparation of Impregnated Co/SiO_2 Catalysts" JOURNAL OF CATALYSIS, 162, 220–229.

[68] M. Glinski, J. Kijenski, A. Jakubowski, 1995. "Ketones from monocarboxylic acids Catalytic ketonization over oxide systems" Applied Catalysis A: General, 128, 209-217.

[69] M. Glinski, J. Kijenski, A. Jakubowski, 1995. "Ketones from monocarboxylic acids: Catalytic ketonization over oxide systems" Applied Catalysis A: General, 128, 209-217.

[70] Bo Carrillo, 2014. "Deoxygenation properties of Ru-based phosphide catalysts" Western Washington University.

[71] M. Reinikainena, M.K. NiemelaÈ, N. Kakuta, S. Suhonen, 1998. "Characterisation and activity evaluation of silica supported cobalt and ruthenium catalysts" Applied Catalysis A: General, 174, 61-75.

[72] C. Pirola, M. Scavini, F. Galli, S. Vitali, A. Comazzi, F. Manenti, P. Ghigna, 2014. "Fischer–Tropsch synthesis: EXAFS study of Ru and Pt bimetallic Co based Catalysts" Fuel, 132, 62–70.

[73] Patcharee Jutalikitwong, 2017. "Catalytic deoxygenation of heptanoic acid to α-olefins over supported Pt catalysts" Faculty of science. King Mongkut's Institute Technology of Ladkrabang.

[74] Shuai Wang, Enrique Iglesia, 2017. "Experimental and theoretical assessment of the mechanism and site requirements for ketonization of carboxylic acids on oxides" Journal of Catalysis, 345, 183–206.

[75] Sivanandi Rajadurai, 1994. "Pathways for Carboxylic Acid Decomposition on Transition Metal Oxides" Catal. Rev.-Sci.Eng., 36(3), 385-403.

APPENDICES

APPENDIX A

ADSORPTION-DESORPTION ISOTHERM

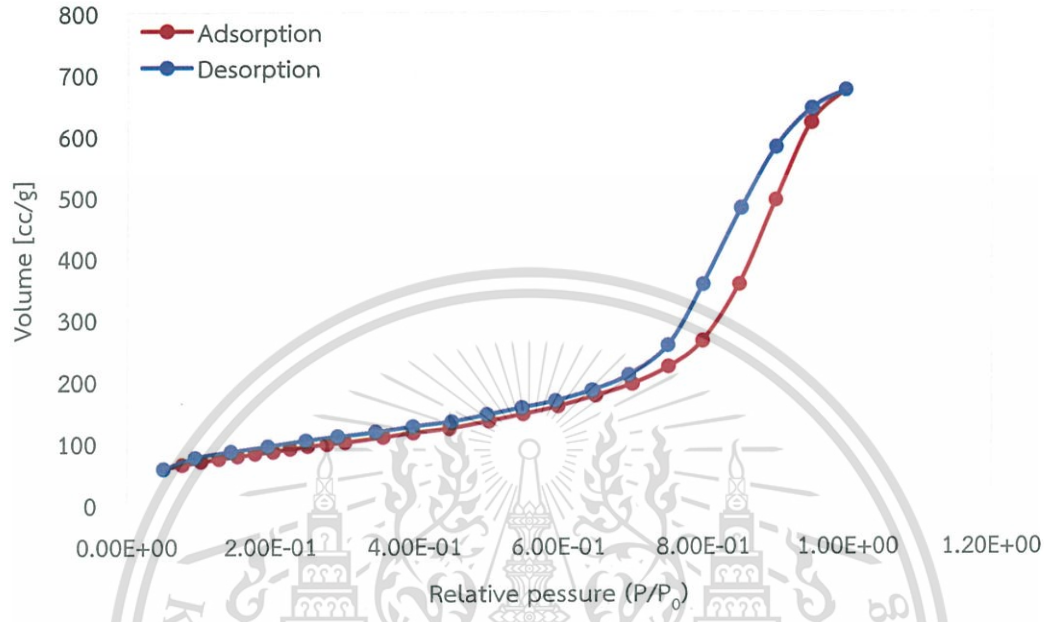

Figure A1 Adsorption-desorption isotherm of SiO_2

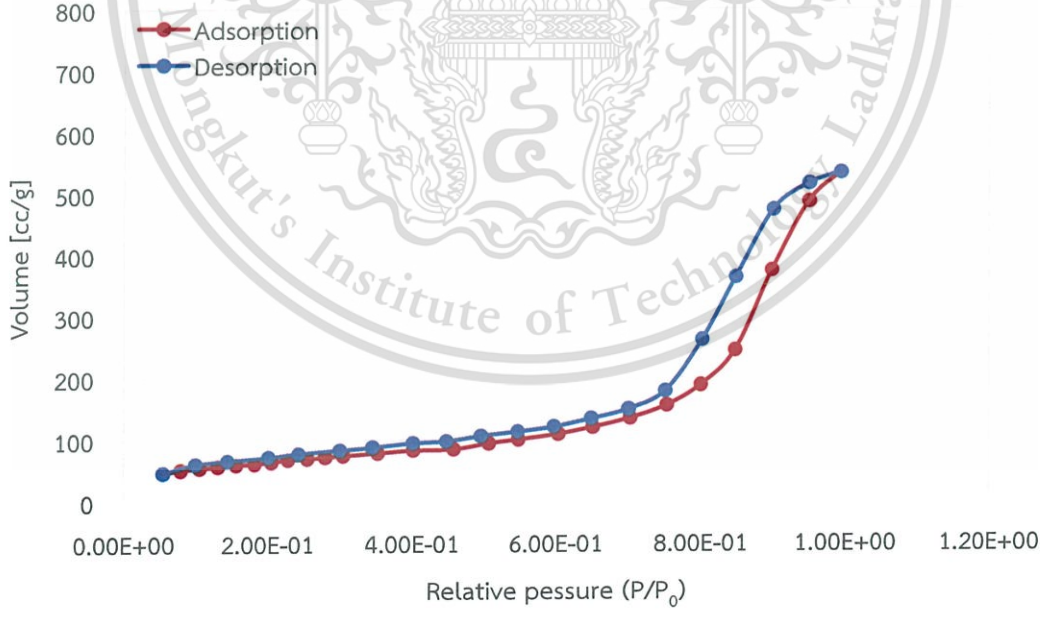

Figure A2 Adsorption-desorption isotherm of 5%Cu/SiO_2

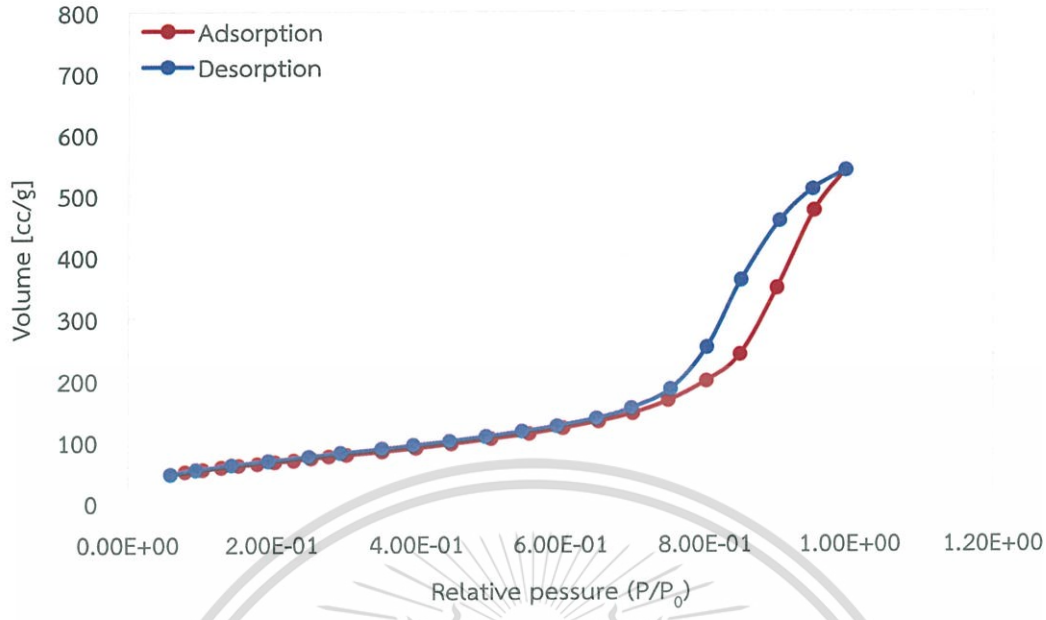

Figure A3 Adsorption-desorption isotherm of 5%Cr/SiO_2

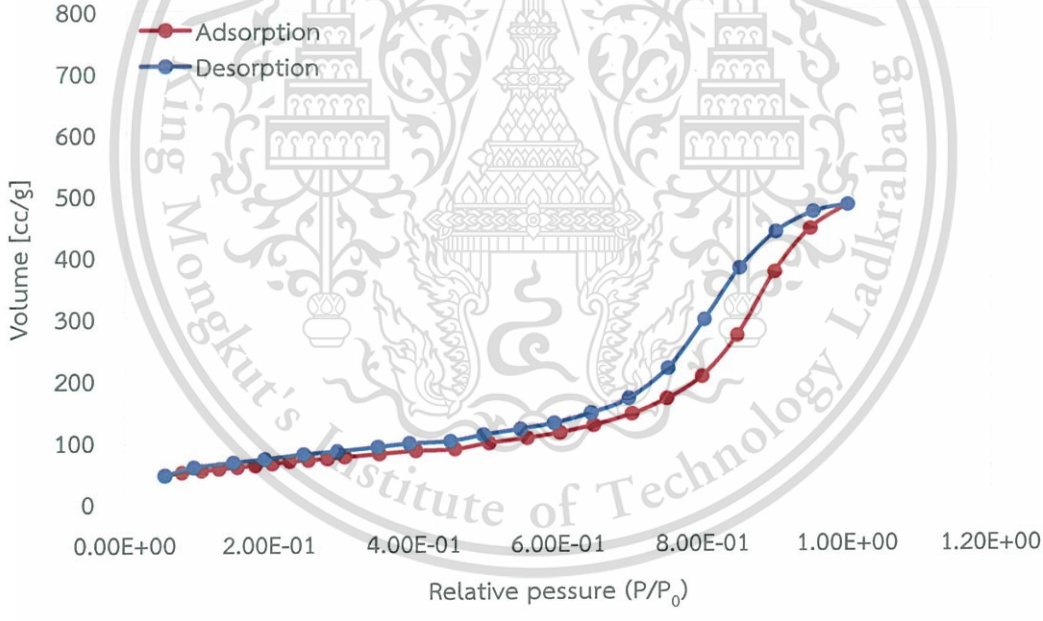

Figure A4 Adsorption-desorption isotherm of 5%Ni/SiO_2

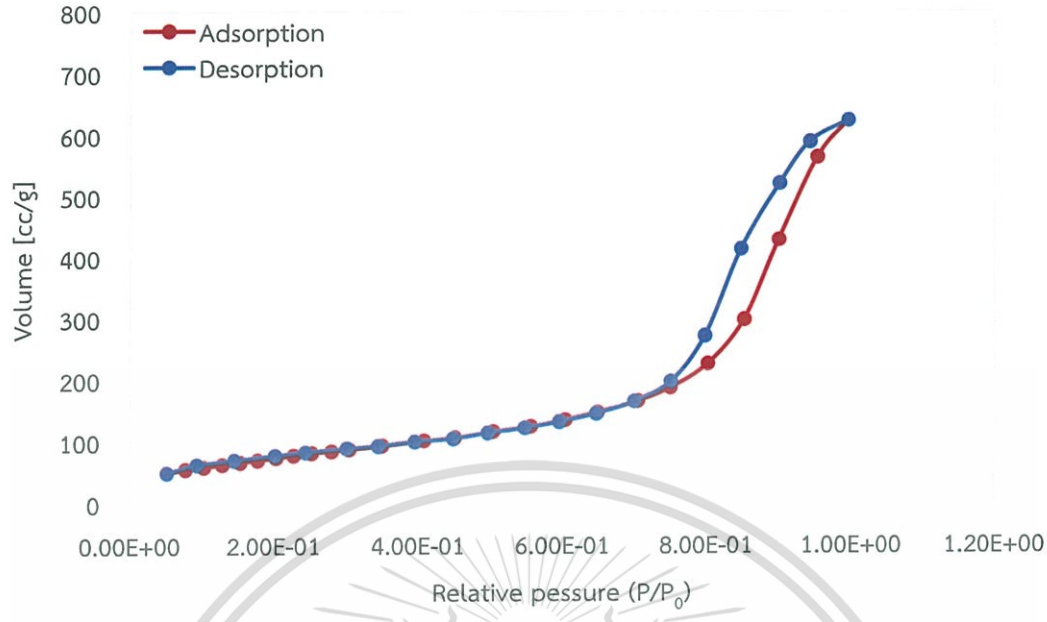

Figure A5 Adsorption-desorption isotherm of 5%Co/SiO_2

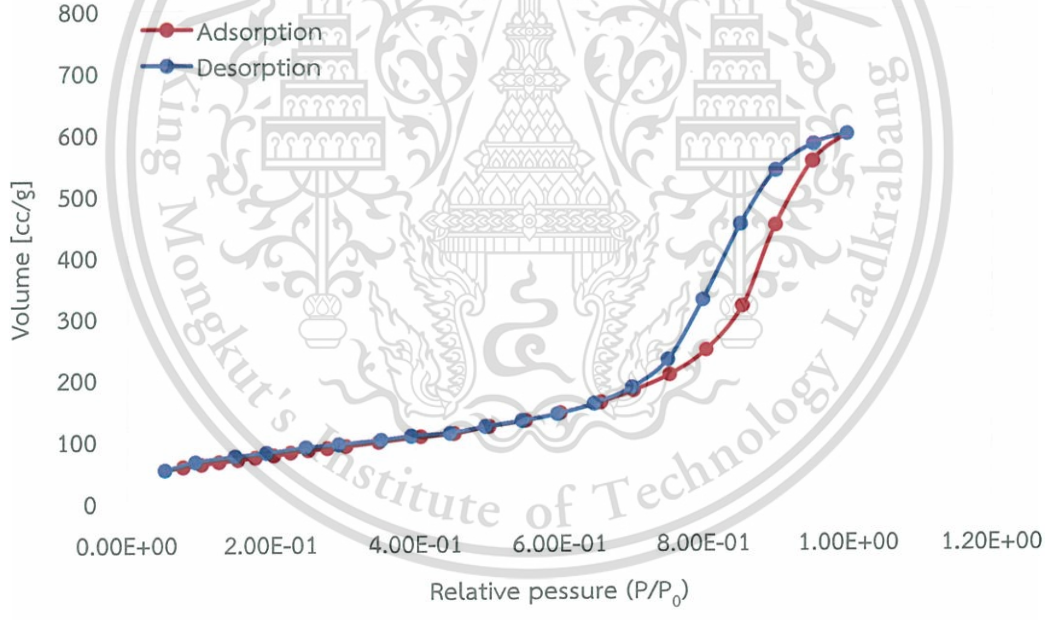

Figure A6 Adsorption-desorption isotherm of 2%Co/SiO_2

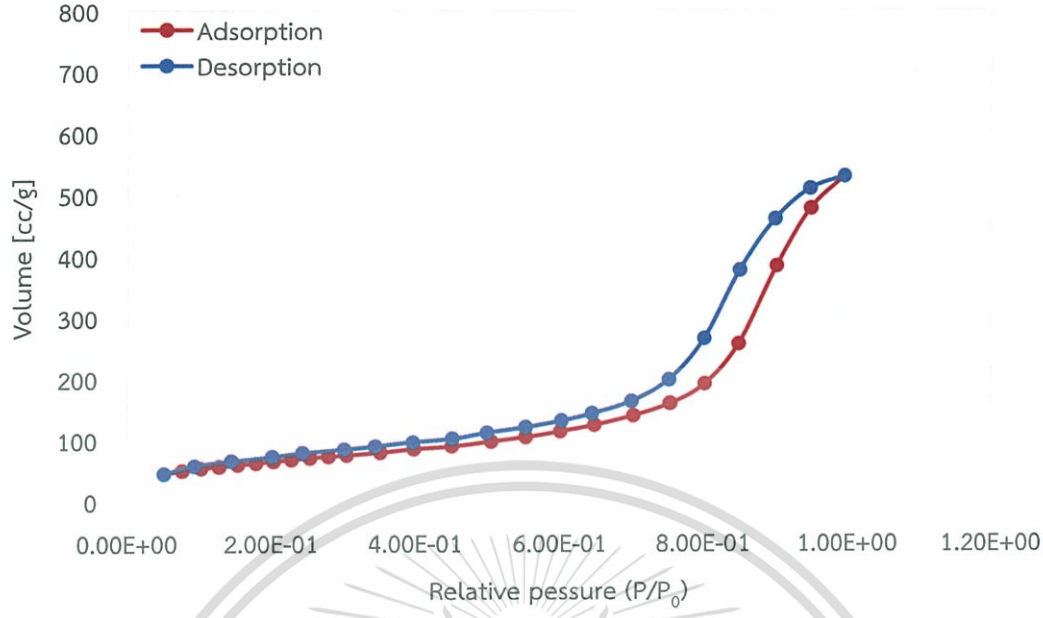

Figure A7 Adsorption-desorption isotherm of 10%Co/SiO_2

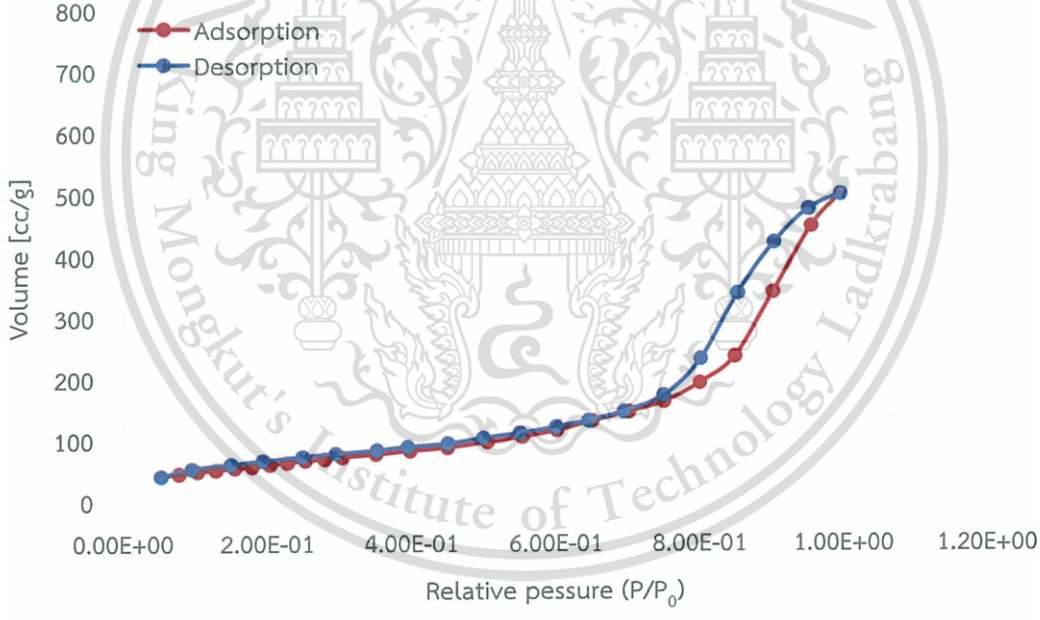

Figure A8 Adsorption-desorption isotherm of 15%Co/SiO_2

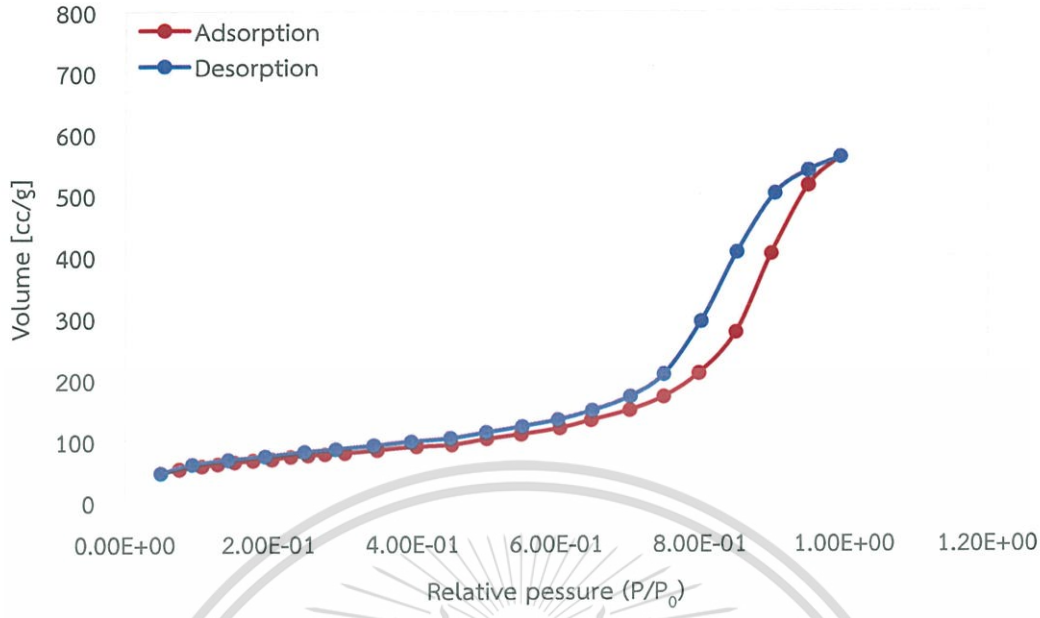

Figure A9 Adsorption-desorption isotherm of 5%Co+0.5%Pd/SiO_2

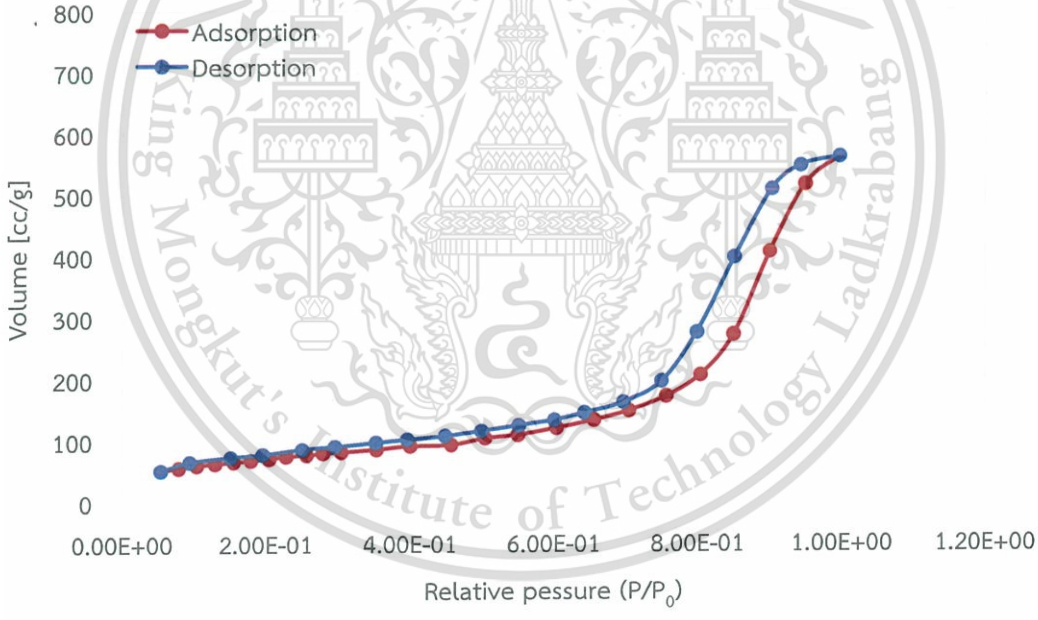

Figure A10 Adsorption-desorption isotherm of 5%Co+0.5%Au/SiO_2

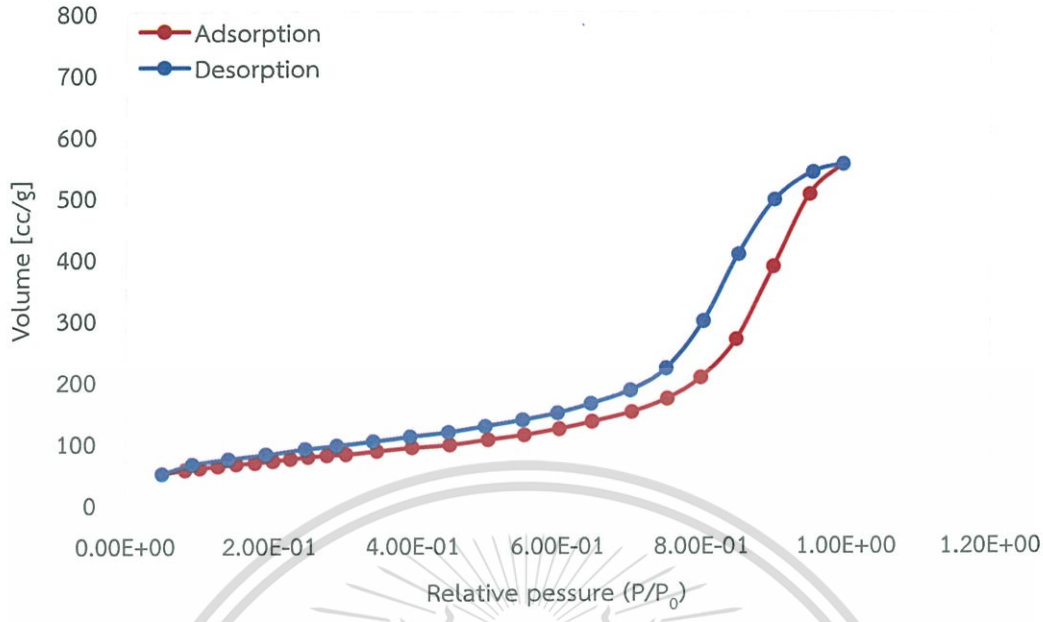

Figure A11 Adsorption-desorption isotherm of 5%Co+0.5%Ru/SiO_2

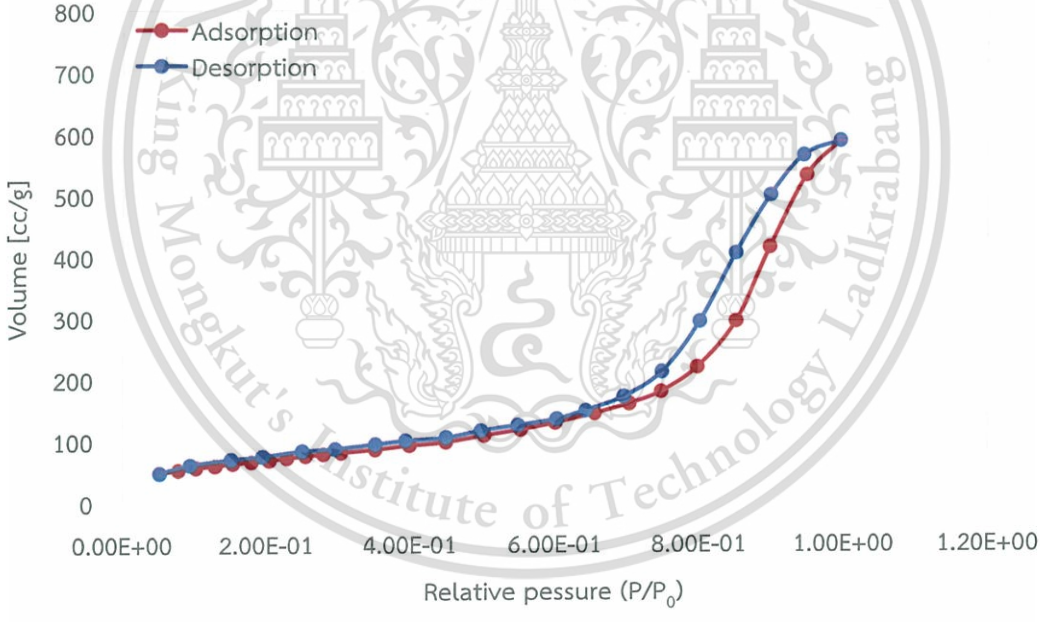

Figure A12 Adsorption-desorption isotherm of 5%Co+0.5%Pt/SiO_2 (CIP)

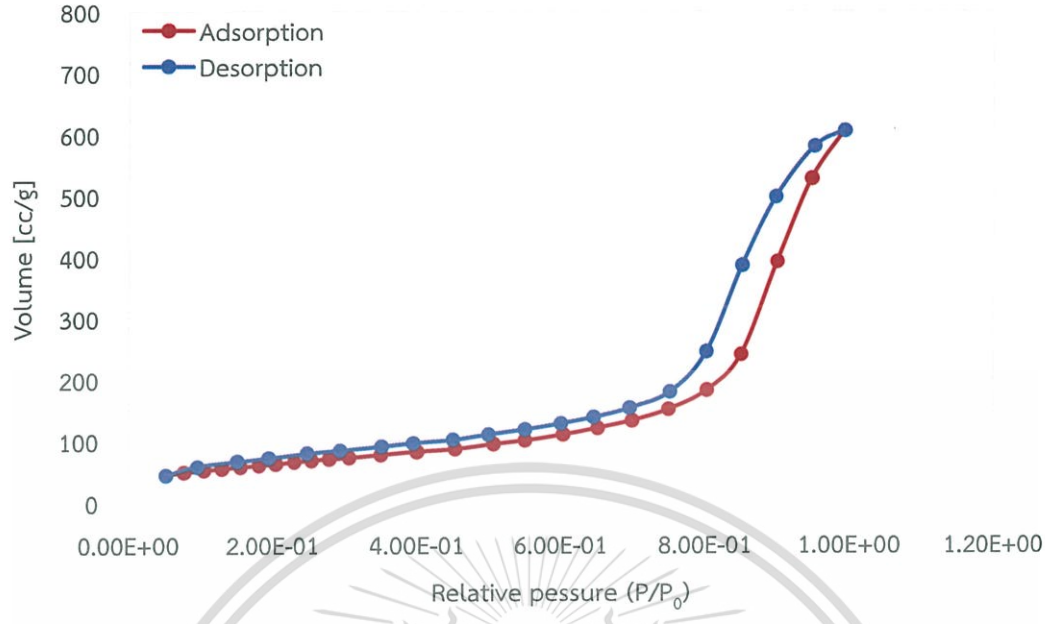

Figure A13 Adsorption-desorption isotherm of 5%Co+0.5%Pt/SiO_2 (SIP)

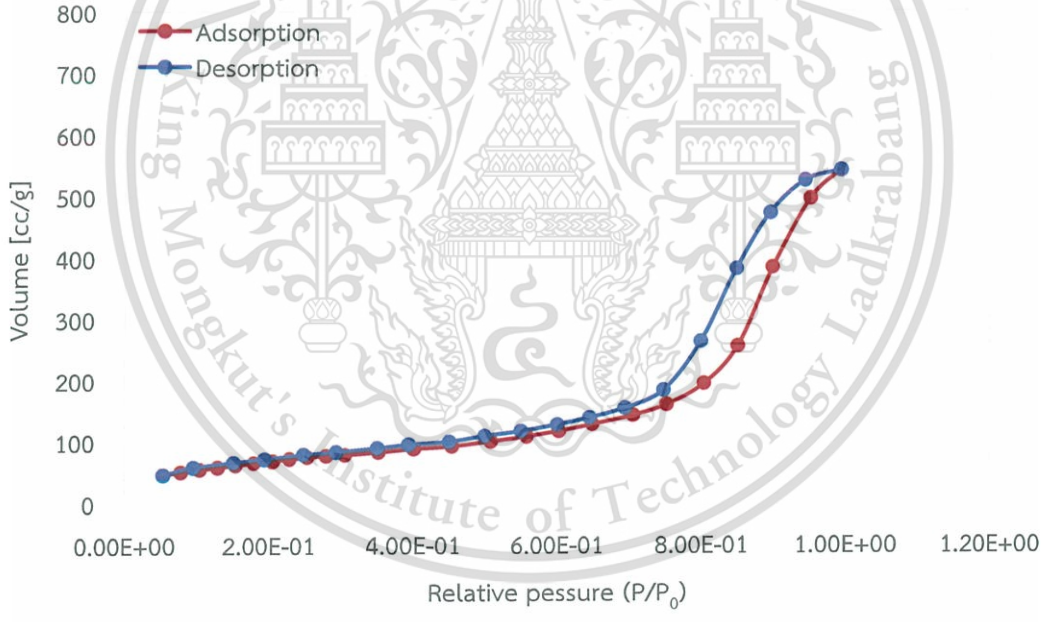

Figure A14 Adsorption-desorption isotherm of 5%Co+0.25%Pt/SiO_2

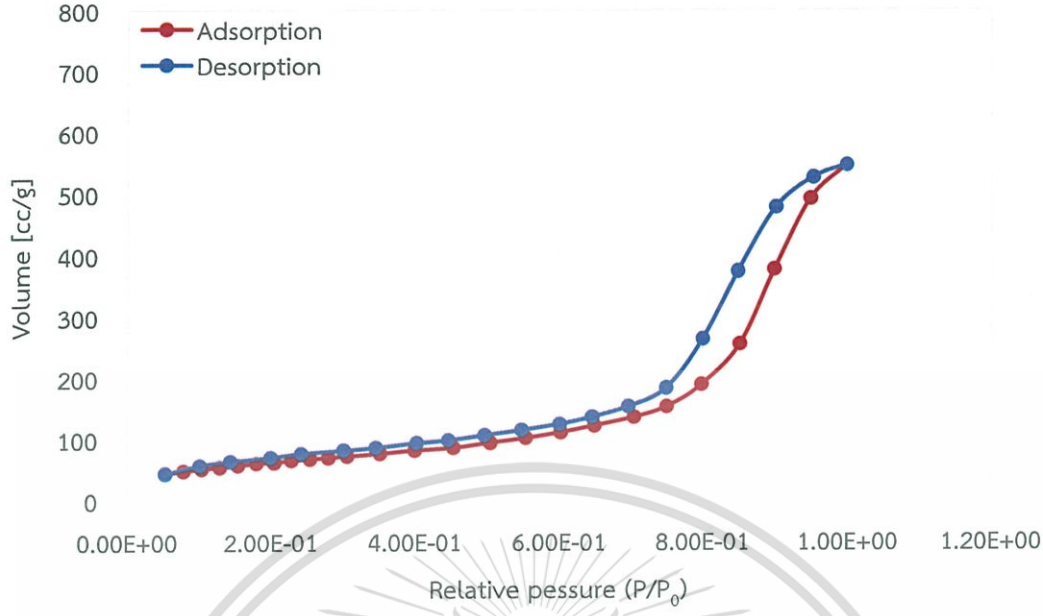

Figure A15 Adsorption-desorption isotherm of 5%Co+0.75%Pt/SiO_2

APPENDIX B

TPR SIGNAL EVALUATION

Calculations of reducibility

Here, CuO is used to metal oxide standard because it is a highly-reducible metal with clean and well-known reduction giving Cu metallic as a final product. The electronic signal from the TCD detector during TPR analysis is represents the H_2-consumption that converted to mmol H_2, CuO reduction following the equation;

$$CuO\ (s) + H_2\ (g) \longrightarrow Cu\ (s) + H_2O\ (g)$$

An example of TPR profile of CuO is shown in **Figure B1**.

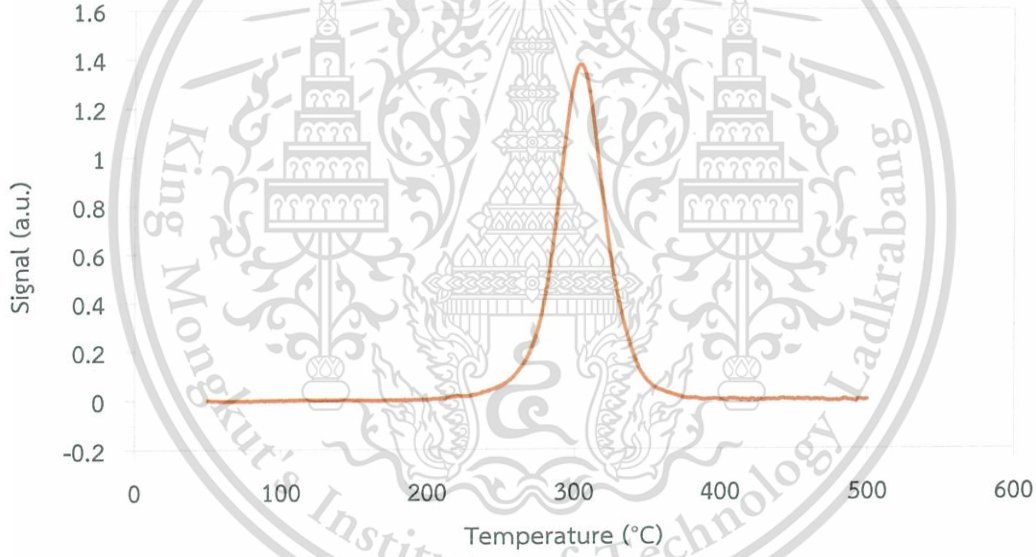

Figure B1 TPR profile of CuO standard

A few runs were performed by variation of the mass of CuO. Then, the peak area (integrated with **Origin Pro 8.0**) in the range T = 50-500 °C is plotted against the mole of CuO. The resulting plot (**Figure B2**) serves as a calibration curve where the mmol H_2 of any sample could be calculated from the peak area as shown below.

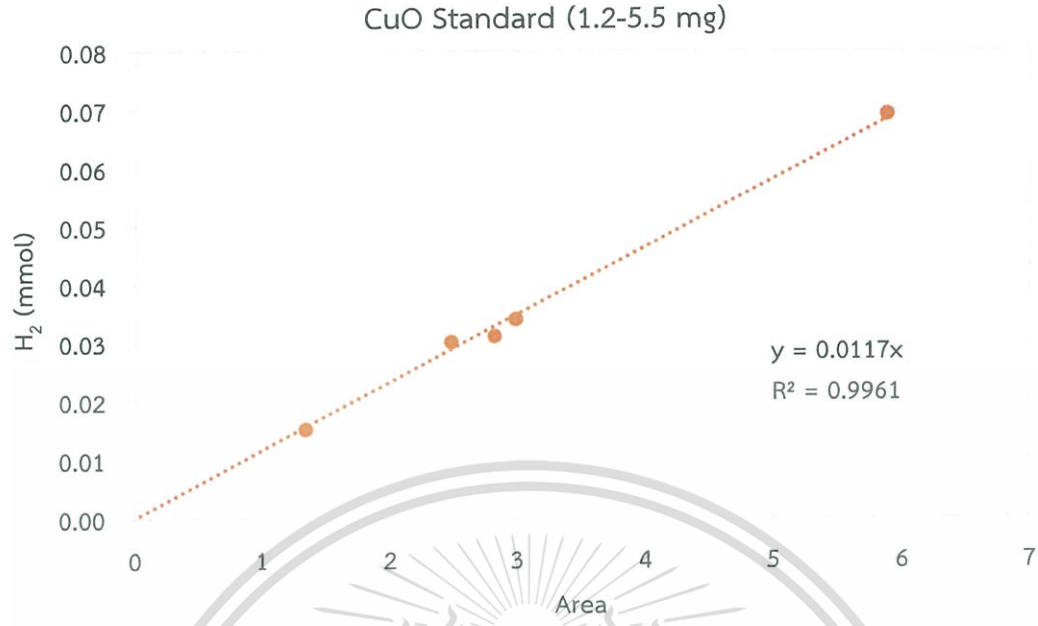

Figure B2 Standard curve of CuO; peak area vs the mole number of CuO

For example, TPR results of 5%Co/SiO_2 (0.1374 g.) catalyst gives the peak area of 106.8072 /g_{cat}. Substituting this number into the equation in **Figure B2** gives;

$$y = 0.0117x$$
$$y = 0.0117\ (106.8072)$$
$$y = 1.2496 \text{ mmol}$$

As the mole ratio of CoO to H_2 is 3:4, the number of mmol of H_2 consumed by 5%Co/SiO_2 equals 0.9372 mmol/g_{cat} as well. So, the reducibility of 5%Co/SiO_2 is;

$$\text{Co} = 0.9372 \text{ mmol/g}_{cat} \times 58.93 \text{ g/mol}$$
$$= 55.2312 \text{ mg/g}_{cat}$$
$$= 0.0552 \text{ g/g}_{cat}$$
$$= 5.5231 \text{ \%wt.}$$

APPENDIX C

TRANSMISSION ELECTRON MICROSCOPE IMAGE

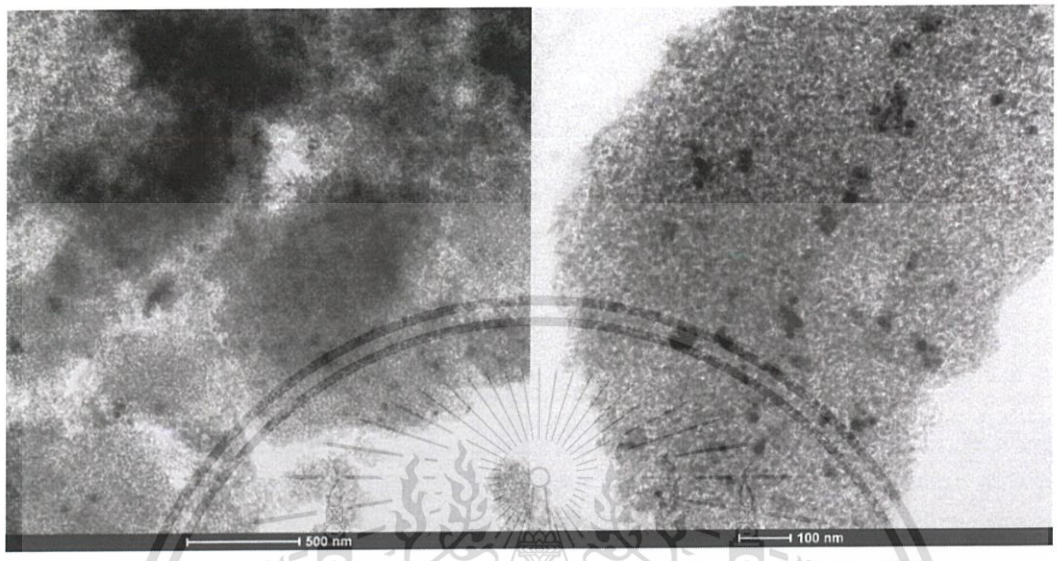

Figure C1 Transmission electron microscope image of 2%Co/SiO_2

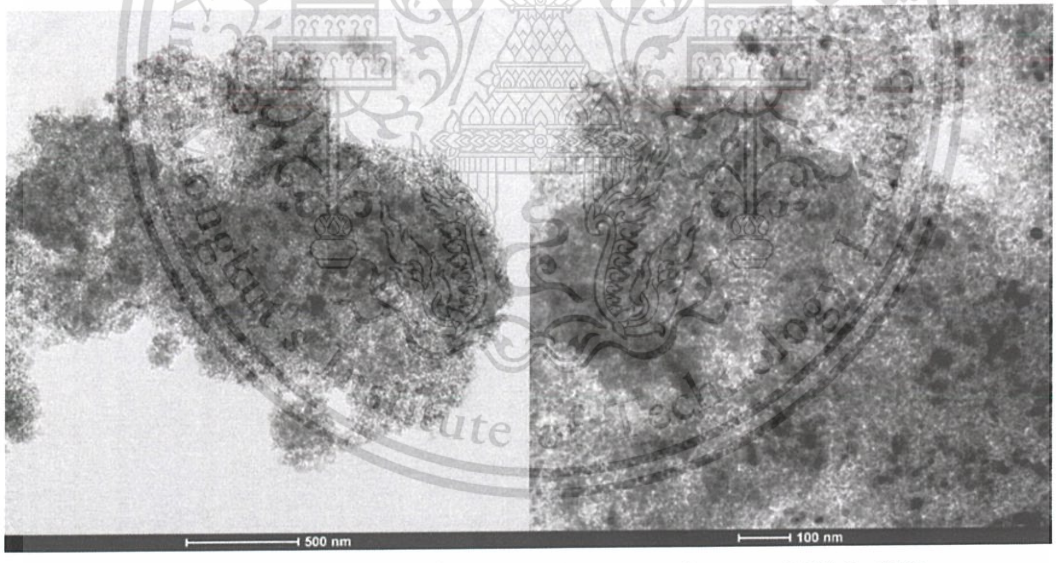

Figure C2 Transmission electron microscope image of 5%Co/SiO_2

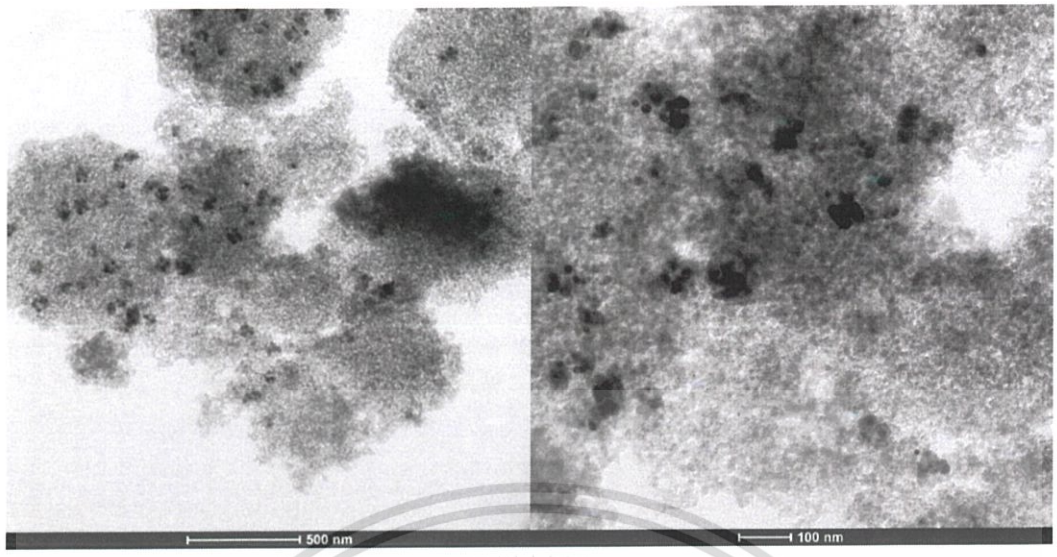

Figure C3 Transmission electron microscope image of 10%Co/SiO_2

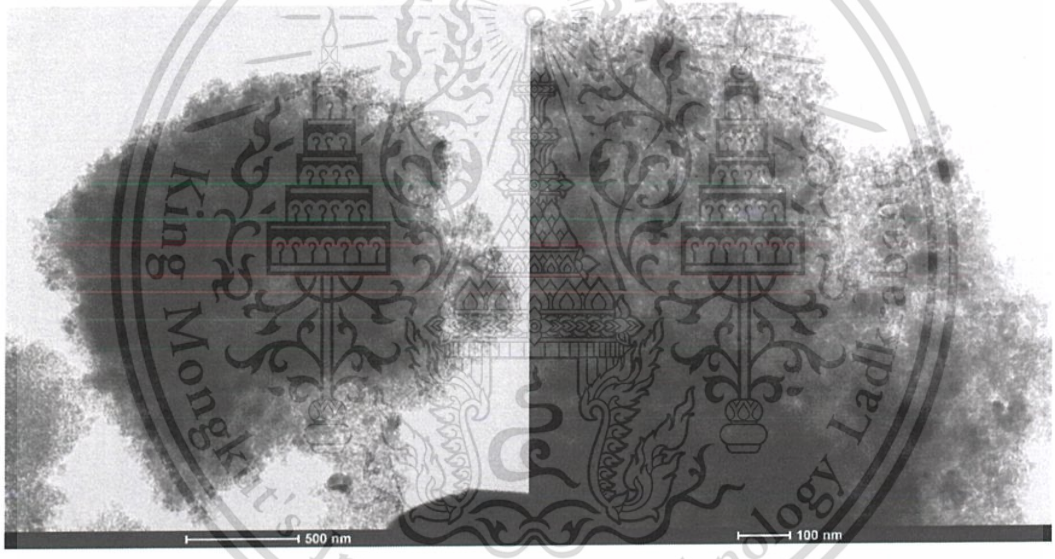

Figure C4 Transmission electron microscope image of 15%Co/SiO_2

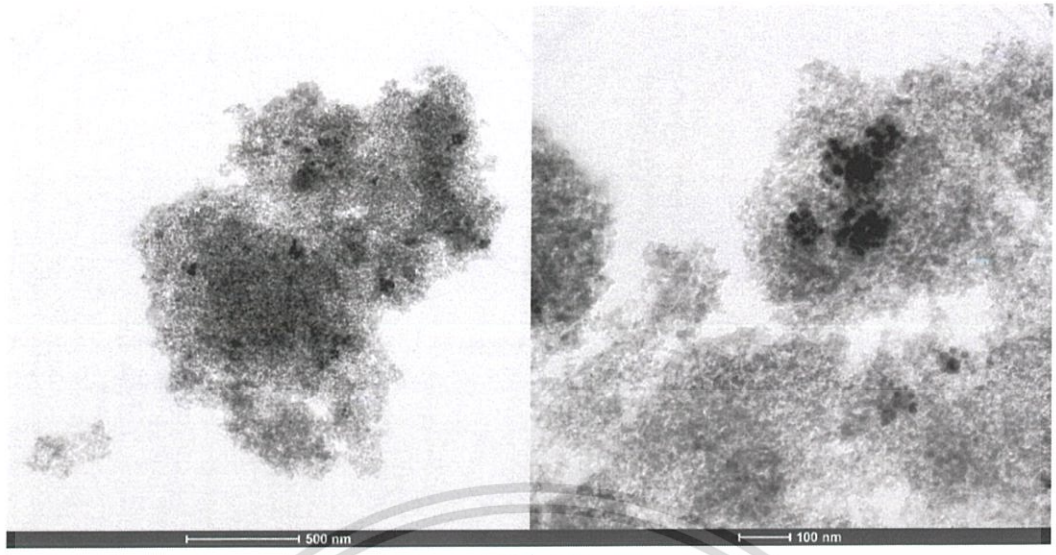

Figure C5 Transmission electron microscope image of 5%Co+0.5%Pt/SiO_2

APPENDIX D
GC-CONDITION

Conditions

The products from deoxygenation of heptanoic acid were identified by GC-MS (Gas chromatography equipped with Mass Spectrometer detector). Then, quantitative analysis was carried out with GC- FID (Gas chromatography equipped with Flame Ionization Detector). The analytical conditions of products from the deoxygenation of heptanoic acid is shown in **Table D1**.

Table D1 GC conditions for product analysis

Column	MTX-1, 60 m x 0.25 mm i.d., 5 μm
Temperature program	40 °C for 5 min to 280 °C rate 15 °C /min for 4.04 min
Carrier gas	Nitrogen gas 91.3 mL/min (21.2 cm/sec)
Injector temperature	250 °C (split ratio 50:1)
Injection volume	250 microliter (gas sampling loop)
Detector temperature	FID (280 °C)

The products from heptanoic acid were identified by comparing the retention time as listed in **Table D2**.

Table D2 Retention time of the products from heptanoic acid

Chemical	Retention time (min)
C_1	6.162
C_2	6.229
C_3	6.378
C_4	6.598 - 6.945
C_5	7.531 - 7.941
Hexene	9.047
n-hexane	9.258
Iso C6	8.962
Heptene	11.039
Heptanal	14.521
Heptanoic acid	16.756
7-Tridecanone	20.604

APPENDIX E
CALCULATION

1. Contact time, W/F

$$W/F = \frac{\text{Weight of catalyst (g)}}{\text{Reactant feed rate (mol/h)}}$$

In the reaction using 0.000671 mol/h of *n*-heptanoic acid in feed and using 0.0224 grams of catalyst, the *W/F* is calculated as follow:

$$W/F = \frac{0.0224\ (g)}{0.000671(mol/h)}$$
$$= 33.38\ g{\cdot}h/mol$$

In a similar manner; *W/F* of catalysts with different catalyst weight and different feed rate are calculated.

2. % Yield

From the chromatogram, the peaks of hydrocarbon samples were identified using of reference standard for comparison. The peak area of hydrocarbon (or oxygenated compounds) which possesses the equal number of carbon was summarized. The example of the peak area obtained from chromatogram of a mixture reactor outlet is shown in **Table E1.**

Table E1 The example of the peak area for reactor outlet.

Chemicals	Peak area	Corrected peak area	RF
C1	287	131	2.19
C2	107	49	2.19
C3	143	65	2.19
C4	174	79	2.19
C5	457	209	2.19
Hexene	2979	1295	2.30
n-Hexane	135	61	2.19
Iso C6	132	60	2.19
Heptene	239	101	2.36
Heptanal	158	98	1.60
Heptanoic acid	426	426	1.00
7-Tridecanone	342	211	1.62
Total	5579	2785	-

$$\text{Corrected peak area in each product} = \frac{\text{Peak area of sample}}{\text{RF}}$$

Where RF is the response factor of the analyzed sample showing in **Table E1**.

For example;

$$\text{Corrected peak area of hexene} = \frac{2979}{2.30}$$

$$= 1295$$

In the normalization method, the areas of all eluted peak were compute after correcting these areas for differences in the detector response (RF) to different compound types. After correcting areas, the concentration of the analyzed was found from the ratio of its area to the total area of all peaks.

Calculate the percent yield of each component in sample as follows:

$$\%\text{Yield in each product} = \frac{\text{Corrected peak area of sample} \times 100}{\text{Total corrected area}}$$

For example;

$$\%\text{Yield of hexene} = \frac{1295 \times 100}{2785}$$

$$= 46.50$$

The percent yield of each sample which is obtained from above calculation is shown in **Table E2**.

Table E2 % yield derived by normalization method.

Chemicals	%Yield of sample
C1	4.70
C2	1.76
C3	2.33
C4	2.84
C5	7.50
Hexene	46.50
n-Hexane	2.19
Iso C6	2.15
Heptene	3.63
Heptanal	3.52
Heptanoic acid	15.30
7-Tridecanone	7.58
Total	100.0

3. Conversion

%Conversion can be calculated from the following equation.

$$\%\text{Conversion} = 100 - (\%\text{Yield of heptanoic acid left in product})$$

For example;

$$\%\text{Conversion} = 100 - 15.30$$
$$= 84.70$$

4. Selectivity

%Selectivity can be obtained from the following equation.

$$\%\text{Selectivity in each product} = \frac{\%\text{ Yield in each product}}{\%\text{ Conversion}} \times 100$$

For example;

$$\%\text{Selectivity of hexene} = \frac{46.50}{84.70} \times 100$$
$$= 54.90$$

APPENDIX F

REACTION DATA

1. Effect of metal

Table F1 The heptanoic acid conversion and yield of products over 5%Ni/SiO_2

	Time on stream (min)					
	30	60	90	120	150	180
Conversion	8.11	4.52	3.00	2.62	2.32	1.80
Yield (%)						
C1	0.40	0.24	0.16	0.14	0.12	0.08
C2	0.00	0.00	0.00	0.00	0.00	0.00
C3	0.07	0.04	0.03	0.04	0.03	0.03
C4	0.11	0.09	0.05	0.04	0.04	0.03
C5	0.40	0.22	0.13	0.11	0.09	0.08
Hexene	3.46	1.60	0.84	0.62	0.48	0.36
Hexane	0.39	0.21	0.04	0.10	0.00	0.00
Iso C6	0.19	0.06	0.01	0.02	0.02	0.01
Heptene	0.15	0.09	0.05	0.04	0.03	0.02
Heptanal	2.26	1.36	0.77	0.59	0.45	0.36
7-Tridecanone	0.53	0.51	0.88	0.90	1.00	0.77

Reaction condition: W/F 20 g·h/mol, $T_{reaction}$ 350 °C, $T_{activate}$ 550 °C, T_{reduce} 500 °C, Flow H_2 100 ml/min, atmospheric pressure.

Table F2 The heptanoic acid conversion and yield of products over 5%Co/SiO_2

	Time on stream (min)					
	30	60	90	120	150	180
Conversion	22.50	3.84	3.81	3.65	3.65	3.45
Yield (%)						
C1	1.56	0.21	0.23	0.22	0.22	0.23
C2	0.03	0.02	0.02	0.02	0.02	0.02
C3	0.37	0.06	0.06	0.06	0.06	0.05
C4	0.64	0.09	0.07	0.06	0.06	0.06
C5	1.89	0.25	0.23	0.22	0.22	0.21
Hexene	8.78	1.17	1.16	1.08	1.08	1.09
Hexane	0.49	0.08	0.08	0.07	0.07	0.07
Iso C6	0.00	0.00	0.00	0.00	0.00	0.00
Heptene	1.10	0.14	0.12	0.11	0.11	0.12
Heptanal	6.73	0.93	0.87	0.80	0.80	0.74
7-Tridecanone	0.93	0.89	0.97	1.00	1.00	0.86

Reaction condition: W/F 20 g·h/mol, $T_{reaction}$ 350 °C, $T_{activate}$ 550 °C, T_{reduce} 500 °C, Flow H_2 100 ml/min, atmospheric pressure.

Table F3 The heptanoic acid conversion and yield of products over 5%Cr/SiO_2

	Time on stream (min)					
	30	60	90	120	150	180
Conversion	2.83	1.38	1.42	1.27	0.00	1.36
Yield (%)						
C1	0.00	0.00	0.00	0.00	0.00	0.00
C2	0.00	0.00	0.00	0.00	0.00	0.00
C3	0.00	0.00	0.00	0.00	0.00	0.00
C4	0.00	0.00	0.00	0.00	0.00	0.00
C5	0.11	0.03	0.03	0.03	0.00	0.03
Hexene	0.13	0.04	0.06	0.05	0.00	0.05
Hexane	0.00	0.00	0.00	0.00	0.00	0.00
Iso C6	0.00	0.00	0.00	0.00	0.00	0.00
Heptene	0.00	0.00	0.00	0.00	0.00	0.00
Heptanal	1.62	0.32	0.28	0.27	0.00	0.18
7-Tridecanone	0.96	1.00	1.05	0.93	0.00	1.11

Reaction condition: W/F 20 g·h/mol, $T_{reaction}$ 350 °C, $T_{activate}$ 550 °C, T_{reduce} 500 °C, Flow H_2 100 ml/min, atmospheric pressure.

Table F4 The heptanoic acid conversion and yield of products over 5%Cu/SiO_2

	Time on stream (min)					
	30	60	90	120	150	180
Conversion	3.61	2.88	2.34	2.36	2.71	1.93
Yield (%)						
C1	0.08	0.00	0.00	0.00	0.00	0.00
C2	0.00	0.00	0.00	0.00	0.00	0.00
C3	0.00	0.00	0.00	0.00	0.00	0.00
C4	0.00	0.00	0.00	0.00	0.00	0.00
C5	0.00	0.00	0.00	0.00	0.00	0.00
Hexene	0.22	0.27	0.13	0.13	0.09	0.08
Hexane	0.00	0.00	0.00	0.00	0.00	0.00
Iso C6	0.00	0.00	0.00	0.00	0.00	0.00
Heptene	0.00	0.00	0.00	0.00	0.00	0.00
Heptanal	1.75	0.80	0.49	0.46	0.29	0.36
7-Tridecanone	1.55	1.81	1.72	1.76	2.33	1.49

Reaction condition: W/F 20 g·h/mol, $T_{reaction}$ 350 °C, $T_{activate}$ 550 °C, T_{reduce} 500 °C, Flow H_2 100 ml/min, atmospheric pressure.

2. Effect of temperature

Table F5 The heptanoic acid conversion and yield of products over 5%Co/SiO_2 at 350°C

	Time on stream (min)					
	30	60	90	120	150	180
Conversion	22.50	3.84	3.81	3.65	3.65	3.45
Yield (%)						
C1	1.56	0.21	0.23	0.22	0.22	0.23
C2	0.03	0.02	0.02	0.02	0.02	0.02
C3	0.37	0.06	0.06	0.06	0.06	0.05
C4	0.64	0.09	0.07	0.06	0.06	0.06
C5	1.89	0.25	0.23	0.22	0.22	0.21
Hexene	8.78	1.17	1.16	1.08	1.08	1.09
Hexane	0.49	0.08	0.08	0.07	0.07	0.07
Iso C6	0.00	0.00	0.00	0.00	0.00	0.00
Heptene	1.10	0.14	0.12	0.11	0.11	0.12
Heptanal	6.73	0.93	0.87	0.80	0.80	0.74
7-Tridecanone	0.93	0.89	0.97	1.00	1.00	0.86

Reaction condition: W/F 20 g·h/mol, $T_{reaction}$ 350 °C, $T_{activate}$ 550 °C, T_{reduce} 500 °C, Flow H_2 100 ml/min, atmospheric pressure.

Table F6 The heptanoic acid conversion and yield of products over 5%Co/SiO_2 at 400°C

	Time on stream (min)					
	30	60	90	120	150	180
Conversion	50.06	25.99	20.34	15.67	11.50	8.15
Yield (%)						
C1	4.85	3.22	2.41	2.14	1.47	0.99
C2	1.75	0.76	0.00	0.00	0.00	0.01
C3	2.42	1.10	0.71	0.49	0.28	0.17
C4	2.48	1.04	0.79	0.53	0.28	0.15
C5	5.91	2.57	1.87	1.27	0.69	0.38
Hexene	22.81	10.47	7.87	5.55	3.20	1.77
Hexane	1.55	0.85	0.87	0.74	0.49	0.31
Iso C6	0.00	0.00	0.00	0.00	0.00	0.00
Heptene	2.27	1.01	0.76	0.54	0.27	0.17
Heptanal	3.69	2.53	2.04	1.44	0.95	0.54
7-Tridecanone	2.32	2.45	3.02	2.97	3.88	3.65

Reaction condition: W/F 20 g·h/mol, $T_{reaction}$ 400 °C, $T_{activate}$ 550 °C, T_{reduce} 500 °C, Flow H_2 100 ml/min, atmospheric pressure.

Table F7 The heptanoic acid conversion and yield of products over 5%Co/SiO_2 at 425°C

	Time on stream (min)					
	30	60	90	120	150	180
Conversion	56.84	35.34	28.49	22.68	20.51	17.99
Yield (%)						
C1	9.33	10.10	9.70	5.24	5.50	4.82
C2	1.42	0.00	0.23	0.01	0.01	0.01
C3	2.24	0.88	0.55	0.22	0.21	0.15
C4	2.41	0.95	0.57	0.20	0.14	0.07
C5	5.90	2.03	0.98	0.07	0.31	0.24
Hexene	18.96	7.19	3.61	1.34	1.10	0.84
Hexane	2.62	2.28	1.86	0.87	0.81	0.64
Iso C6	1.01	0.30	0.23	0.12	0.10	0.09
Heptene	1.28	0.58	0.30	0.10	0.11	0.07
Heptanal	5.36	3.17	2.26	1.05	0.99	0.73
7-Tridecanone	6.32	7.86	8.19	11.40	10.21	8.48

Reaction condition: W/F 20 g·h/mol, $T_{reaction}$ 425 °C, $T_{activate}$ 550 °C, T_{reduce} 500 °C, Flow H_2 100 ml/min, atmospheric pressure.

3. Effect of cobalt loading

Table F8 The heptanoic acid conversion and yield of products over 2%Co/SiO_2

	Time on stream (min)											
	30	60	90	120	150	180	210	240	270	300	330	360
Conversion	95.76	57.15	40.45	31.50	19.20	22.06	20.41	19.71	13.88	15.26	16.70	12.51
Yield (%)												
C1	4.15	2.96	2.28	2.12	1.36	1.72	1.96	2.18	1.55	1.58	1.25	1.18
C2	2.38	1.16	0.19	0.15	0.03	0.05	0.05	0.21	0.00	0.00	0.00	0.00
C3	3.39	1.66	0.98	0.70	0.38	0.38	0.35	0.40	0.22	0.24	0.14	0.20
C4	4.41	2.02	1.26	0.83	0.39	0.44	0.36	0.32	0.21	0.22	0.13	0.12
C5	11.38	5.50	3.53	2.36	1.20	1.34	1.19	0.00	0.67	0.66	0.44	0.41
Hexene	58.05	29.41	19.43	14.36	7.69	8.34	7.65	6.60	4.53	4.21	3.26	2.72
Hexane	2.60	1.34	0.98	0.84	0.56	0.58	0.51	0.73	0.38	0.39	0.28	0.34
Iso C6	2.22	0.00	0.00	0.00	0.00	0.00	0.00	0.20	0.00	0.00	0.00	0.00
Heptene	4.53	2.44	1.63	1.13	0.60	0.63	0.69	0.60	0.34	0.33	0.29	0.23
Heptanal	2.65	4.16	3.40	2.60	1.61	1.81	1.34	1.30	1.17	0.94	0.95	0.87
7-Tridecanone	0.00	6.50	6.77	6.40	5.38	6.78	0.69	6.11	4.80	6.69	9.96	6.44

Reaction condition: W/F 82 g·h/mol, W/F basis on Co 1.6 g·h/mol, $T_{reaction}$ 400 °C, $T_{activate}$ 600 °C, T_{reduce} 600 °C, Flow H_2 100 ml/min, atmospheric pressure.

Table F9 The heptanoic acid conversion and yield of products over 5%Co/SiO_2

	Time on stream (min)											
	30	60	90	120	150	180	210	240	270	300	330	360
Conversion	100.00	84.73	74.95	66.47	59.71	48.58	47.02	39.21	36.72	34.99	35.42	37.36
Yield (%)												
C1	5.43	4.70	4.28	3.82	3.39	2.79	2.59	2.24	1.97	2.00	1.99	2.04
C2	2.39	1.75	1.52	1.18	0.99	0.78	0.71	0.58	0.48	0.49	0.49	0.46
C3	3.17	2.34	2.12	1.69	1.45	1.11	1.02	0.84	0.77	0.72	0.74	0.83
C4	4.45	2.85	2.35	2.36	1.50	1.33	1.22	1.00	1.11	0.77	0.78	1.12
C5	12.48	7.48	6.52	5.73	4.78	3.78	3.45	0.00	2.74	2.48	2.36	2.41
Hexene	60.02	46.42	39.45	34.08	30.41	23.76	22.59	18.76	16.30	15.97	15.69	15.33
Hexane	2.53	2.21	1.93	1.72	1.54	1.24	1.22	0.93	0.96	0.81	0.82	0.82
Iso C6	3.78	2.16	1.49	1.47	0.61	0.48	0.48	0.00	0.73	0.00	0.00	0.00
Heptene	4.66	3.63	3.21	2.79	2.45	1.93	1.78	1.54	1.34	1.26	1.30	1.27
Heptanal	1.10	3.54	2.98	2.81	2.54	2.01	2.37	1.59	1.86	1.35	1.33	1.29
7-Tridecanone	0.00	7.66	9.09	8.81	10.03	9.38	1.78	8.83	8.47	9.14	9.91	11.80

Reaction condition: W/F 33 g·h/mol, W/F basis on Co 1.6 g·h/mol, $T_{reaction}$ 400 °C, $T_{activate}$ 600 °C, T_{reduce} 600 °C, Flow H_2 100 ml/min, atmospheric pressure.

Table F10 The heptanoic acid conversion and yield of products over 10%Co/SiO_2

	Time on stream (min)											
	30	60	90	120	150	180	210	240	270	300	330	360
Conversion	100.00	78.58	56.41	48.80	40.34	38.10	53.85	46.95	47.95	30.22	29.38	23.66
Yield (%)												
C1	2.06	0.78	0.57	0.49	0.45	0.58	0.80	0.99	1.07	0.28	0.40	0.31
C2	1.24	0.62	0.43	0.33	0.31	0.33	0.56	0.57	0.59	0.19	0.22	0.20
C3	1.59	0.73	0.47	0.38	0.35	0.40	0.60	0.65	0.67	0.24	0.29	0.22
C4	2.06	1.22	0.75	0.55	0.62	0.66	0.63	1.17	0.72	0.19	0.28	0.21
C5	7.41	6.15	3.77	2.89	2.37	2.29	4.01	0.00	3.64	1.14	1.32	1.03
Hexene	54.40	53.73	33.92	26.79	21.05	19.52	34.03	28.72	29.40	11.08	11.69	8.75
Hexane	3.22	1.39	0.82	0.68	0.59	0.56	1.00	0.85	0.67	0.41	0.43	0.26
Iso C6	19.80	4.79	1.60	1.36	1.03	0.96	1.16	0.55	0.00	0.49	0.32	0.00
Heptene	3.21	3.54	2.27	1.75	1.34	1.07	2.22	1.86	1.88	0.59	0.64	0.48
Heptanal	0.00	0.60	1.84	1.48	1.30	1.17	1.89	1.47	1.64	1.08	1.03	0.83
7-Tridecanone	0.00	5.02	9.98	12.11	10.94	10.56	2.22	6.61	7.66	14.52	12.78	11.36

Reaction condition: W/F 17 g·h/mol, W/F basis on Co 1.6 g·h/mol, $T_{reaction}$ 400 °C, $T_{activate}$ 600 °C, T_{reduce} 600 °C, Flow H_2 100 ml/min, atmospheric pressure.

Table F11 The heptanoic acid conversion and yield of products over 15%Co/SiO_2

	Time on stream (min)											
	30	60	90	120	150	180	210	240	270	300	330	360
Conversion	100.00	78.58	56.41	48.80	40.34	38.10	53.85	46.95	47.95	30.22	29.38	23.66
Yield (%)												
C1	2.06	0.78	0.57	0.49	0.45	0.58	0.80	0.99	1.07	0.28	0.40	0.31
C2	1.24	0.62	0.43	0.33	0.31	0.33	0.56	0.57	0.59	0.19	0.22	0.20
C3	1.59	0.73	0.47	0.38	0.35	0.40	0.60	0.65	0.67	0.24	0.29	0.22
C4	2.06	1.22	0.75	0.55	0.62	0.66	0.63	1.17	0.72	0.19	0.28	0.21
C5	7.41	6.15	3.77	2.89	2.37	2.29	4.01	0.00	3.64	1.14	1.32	1.03
Hexene	54.40	53.73	33.92	26.79	21.05	19.52	34.03	28.72	29.40	11.08	11.69	8.75
Hexane	3.22	1.39	0.82	0.68	0.59	0.56	1.00	0.85	0.67	0.41	0.43	0.26
Iso C6	19.80	4.79	1.60	1.36	1.03	0.96	1.16	0.55	0.00	0.49	0.32	0.00
Heptene	3.21	3.54	2.27	1.75	1.34	1.07	2.22	1.86	1.88	0.59	0.64	0.48
Heptanal	0.00	0.60	1.84	1.48	1.30	1.17	1.89	1.47	1.64	1.08	1.03	0.83
7-Tridecanone	0.00	5.02	9.98	12.11	10.94	10.56	2.22	6.61	7.66	14.52	12.78	11.36

Reaction condition: W/F 17 g·h/mol, W/F basis on Co 1.6 g·h/mol, $T_{reaction}$ 400 °C, $T_{activate}$ 600 °C, T_{reduce} 600 °C, Flow H_2 100 ml/min, atmospheric pressure.

4. Deactivation

Table F12 The heptanoic acid conversion and yield of products over 10%Co/SiO_2

	Time on stream (min)											
	30	60	90	120	150	180	210	240	270	300	330	360
Conversion	100.00	78.58	56.41	48.80	40.34	38.10	53.85	46.95	47.95	30.22	29.38	23.66
Yield (%)												
C1	2.06	0.78	0.57	0.49	0.45	0.58	0.80	0.99	1.07	0.28	0.40	0.31
C2	1.24	0.62	0.43	0.33	0.31	0.33	0.56	0.57	0.59	0.19	0.22	0.20
C3	1.59	0.73	0.47	0.38	0.35	0.40	0.60	0.65	0.67	0.24	0.29	0.22
C4	2.06	1.22	0.75	0.55	0.62	0.66	0.63	1.17	0.72	0.19	0.28	0.21
C5	7.41	6.15	3.77	2.89	2.37	2.29	4.01	0.00	3.64	1.14	1.32	1.03
Hexene	54.40	53.73	33.92	26.79	21.05	19.52	34.03	28.72	29.40	11.08	11.69	8.75
Hexane	3.22	1.39	0.82	0.68	0.59	0.56	1.00	0.85	0.67	0.41	0.43	0.26
Iso C6	19.80	4.79	1.60	1.36	1.03	0.96	1.16	0.55	0.00	0.49	0.32	0.00
Heptene	3.21	3.54	2.27	1.75	1.34	1.07	2.22	1.86	1.88	0.59	0.64	0.48
Heptanal	0.00	0.60	1.84	1.48	1.30	1.17	1.89	1.47	1.64	1.08	1.03	0.83
7-Tridecanone	0.00	5.02	9.98	12.11	10.94	10.56	2.22	6.61	7.66	14.52	12.78	11.36

Reaction condition: W/F 17 g·h/mol, W/F basis on Co 1.6 g·h/mol, $T_{reaction}$ 400 °C, $T_{activate}$ 600 °C, T_{reduce} 600 °C, Flow H_2 100 ml/min, atmospheric pressure.

Table F13 The heptanoic acid conversion and yield of products over 10%Co/SiO_2 (after regenerated)

	Time on stream (min)					
	30	60	90	120	150	180
Conversion	76.29	46.93	43.82	27.73	25.98	20.99
Yield (%)						
C1	1.38	0.88	0.91	0.36	0.34	0.28
C2	0.84	0.51	0.54	0.07	0.09	0.06
C3	1.00	0.64	0.63	0.28	0.28	0.20
C4	1.66	1.04	0.89	0.32	0.31	0.24
C5	5.10	4.14	3.70	1.68	1.67	1.11
Hexene	36.05	31.34	27.82	13.47	13.00	8.85
Hexane	1.22	1.00	0.93	0.00	0.42	0.26
Iso C6	0.69	1.35	1.13	0.00	0.00	0.00
Heptene	2.41	2.31	1.94	0.89	0.91	0.55
Heptanal	2.23	1.96	1.99	0.99	0.81	0.68
7-Tridecanone	0.00	1.76	3.33	9.69	8.13	8.76

Reaction condition: W/F 17 g·h/mol, W/F basis on Co 1.6 g·h/mol, $T_{reaction}$ 400 °C, $T_{activate}$ 600 °C, T_{reduce} 600 °C, Flow H_2 100 ml/min, atmospheric pressure.

5. Effect of cobalt metal bimetallic

Table F14 The heptanoic acid conversion and yield of products over 5%Co/SiO_2

	Time on stream (min)											
	30	60	90	120	150	180	210	240	270	300	330	360
Conversion	100.00	84.73	74.95	66.47	59.71	48.58	47.02	39.21	36.72	34.99	35.42	37.36
Yield (%)												
C1	5.43	4.70	4.28	3.82	3.39	2.79	2.59	2.24	1.97	2.00	1.99	2.04
C2	2.39	1.75	1.52	1.18	0.99	0.78	0.71	0.58	0.48	0.49	0.49	0.46
C3	3.17	2.34	2.12	1.69	1.45	1.11	1.02	0.84	0.77	0.72	0.74	0.83
C4	4.45	2.85	2.35	2.36	1.50	1.33	1.22	1.00	1.11	0.77	0.78	1.12
C5	12.48	7.48	6.52	5.73	4.78	3.78	3.45	0.00	2.74	2.48	2.36	2.41
Hexene	60.02	46.42	39.45	34.08	30.41	23.76	22.59	18.76	16.30	15.97	15.69	15.33
Hexane	2.53	2.21	1.93	1.72	1.54	1.24	1.22	0.93	0.96	0.81	0.82	0.82
Iso C6	3.78	2.16	1.49	1.47	0.61	0.48	0.48	0.00	0.73	0.00	0.00	0.00
Heptene	4.66	3.63	3.21	2.79	2.45	1.93	1.78	1.54	1.34	1.26	1.30	1.27
Heptanal	1.10	3.54	2.98	2.81	2.54	2.01	2.37	1.59	1.86	1.35	1.33	1.29
7-Tridecanone	0.00	7.66	9.09	8.81	10.03	9.38	1.78	8.83	8.47	9.14	9.91	11.80

Reaction condition: W/F 33 g·h/mol, W/F basis on Co 1.6 g·h/mol, $T_{reaction}$ 400 °C, $T_{activate}$ 600 °C, T_{reduce} 600 °C, Flow H_2 100 ml/min, atmospheric pressure.

Table F15 The heptanoic acid conversion and yield of products over 5%Co+0.5%Pt/SiO_2

	Time on stream (min)											
	30	60	90	120	150	180	210	240	270	300	330	360
Conversion	100.00	100.00	95.02	81.25	93.97	88.31	86.60	85.08	88.49	79.49	78.30	74.44
Yield (%)												
C1	3.54	1.33	1.30	0.97	1.28	1.25	0.82	1.26	1.20	1.20	0.93	0.85
C2	0.55	0.51	0.42	0.27	0.42	0.39	0.06	0.40	0.36	0.40	0.30	0.37
C3	2.21	1.33	1.26	0.95	1.32	1.19	1.15	1.19	1.22	1.00	0.97	1.01
C4	3.59	1.57	1.48	1.27	1.63	1.44	1.47	1.41	1.55	1.30	1.26	1.00
C5	8.63	6.49	5.93	5.03	5.58	5.80	4.59	0.00	4.86	4.17	4.04	3.90
Hexene	28.59	54.41	49.07	42.40	48.83	45.39	45.63	44.10	46.43	40.75	39.89	38.36
Hexane	22.25	17.87	15.65	11.25	15.24	12.68	12.49	12.01	12.86	10.94	10.67	10.22
Iso C6	29.58	14.33	10.56	7.03	10.25	8.19	7.12	6.69	7.07	6.21	5.59	5.08
Heptene	1.06	2.16	1.95	1.89	2.09	2.10	2.05	2.05	2.12	1.90	1.85	1.85
Heptanal	0.00	0.00	4.10	5.91	3.87	5.49	5.81	5.83	5.80	5.94	6.16	5.86
7-Tridecanone	0.00	0.00	3.29	4.27	3.45	4.40	2.05	5.56	5.03	5.67	6.63	5.95

Reaction condition: W/F 34 g·h/mol, $T_{reaction}$ 400 °C, $T_{activate}$ 600 °C, T_{reduce} 600 °C, Flow H_2 100 ml/min, atmospheric pressure.

Table F16 The heptanoic acid conversion and yield of products over 5%Co+0.5%Pd/SiO_2

	Time on stream (min)											
	30	60	90	120	150	180	210	240	270	300	330	360
Conversion	100.00	75.75	65.82	55.79	39.20	58.16	42.41	36.17	44.59	36.73	31.86	32.88
Yield (%)												
C1	2.97	1.52	1.38	1.08	0.68	1.41	0.81	0.67	0.91	0.72	0.53	0.56
C2	1.20	0.81	0.77	0.58	0.38	0.66	0.42	0.34	0.43	0.31	0.28	0.28
C3	1.58	1.04	1.02	0.79	0.55	0.84	0.58	0.49	0.60	0.46	0.39	0.38
C4	1.91	1.25	1.11	1.13	0.61	0.98	0.77	0.62	0.70	0.64	0.49	0.49
C5	7.06	4.47	3.97	3.10	2.11	3.21	2.35	0.00	2.26	1.76	1.48	1.56
Hexene	48.89	36.64	31.68	25.13	17.24	25.80	18.84	15.43	18.70	14.69	12.42	12.81
Hexane	11.39	3.35	2.20	1.67	1.16	1.65	1.20	1.01	1.18	0.97	0.84	0.89
Iso C6	6.37	1.54	1.16	0.89	0.34	0.92	0.91	0.51	0.40	0.69	0.55	0.44
Heptene	2.82	2.29	2.01	1.43	1.22	1.57	1.21	1.04	1.26	0.96	0.80	0.84
Heptanal	13.06	15.28	11.65	9.34	7.59	7.63	6.99	6.12	6.20	5.35	4.94	5.14
7-Tridecanone	2.74	7.57	8.88	10.63	7.32	13.50	1.21	8.03	11.95	10.19	9.15	9.49

Reaction condition: W/F 34 g·h/mol, $T_{reaction}$ 400 °C, $T_{activate}$ 600 °C, T_{reduce} 600 °C, Flow H_2 100 ml/min, atmospheric pressure.

Table F17 The heptanoic acid conversion and yield of products over 5%Co+0.5%Ru/SiO_2

	Time on stream (min)											
	30	60	90	120	150	180	210	240	270	300	330	360
Conversion	96.83	57.48	50.31	35.93	27.90	43.40	28.26	19.93	19.96	22.70	21.18	22.71
Yield (%)												
C1	3.81	1.70	1.77	1.38	1.06	2.29	1.26	0.86	0.85	1.09	1.04	0.87
C2	1.42	0.66	0.53	0.34	0.27	0.41	0.25	0.17	0.17	0.23	0.20	0.16
C3	1.75	0.87	0.69	0.47	0.39	0.63	0.36	0.24	0.24	0.33	0.26	0.26
C4	2.32	1.24	0.91	0.68	0.43	0.88	0.40	0.28	0.28	0.32	0.29	0.25
C5	7.81	4.27	3.23	2.18	1.52	2.41	1.41	0.00	1.05	1.16	1.06	0.91
Hexene	67.26	37.20	30.27	21.22	15.49	24.95	14.82	10.23	10.23	11.36	10.31	8.81
Hexane	2.14	1.03	0.99	0.70	0.54	0.88	0.61	0.41	0.41	0.46	0.41	0.36
Iso C6	6.09	1.20	1.29	0.84	0.61	1.14	0.75	0.45	0.45	0.45	0.45	0.40
Heptene	4.22	2.07	1.87	1.05	0.84	1.35	0.76	0.52	0.52	0.57	0.59	0.47
Heptanal	0.00	2.99	2.36	1.40	1.20	1.60	1.23	0.79	0.79	0.75	0.72	0.65
7-Tridecanone	0.00	4.25	6.38	5.67	5.55	6.85	0.76	4.97	4.97	5.97	5.85	5.25

Reaction condition: W/F 34 g·h/mol, $T_{reaction}$ 400 °C, $T_{activate}$ 600 °C, T_{reduce} 600 °C, Flow H_2 100 ml/min, atmospheric pressure.

Table F18 The heptanoic acid conversion and yield of products over 5%Co+0.5%Au/SiO_2

	Time on stream (min)											
	30	60	90	120	150	180	210	240	270	300	330	360
Conversion	100.00	69.11	56.97	47.89	37.28	48.68	35.71	31.74	25.52	24.23	23.97	23.66
Yield (%)												
C1	2.62	1.86	1.66	1.29	1.02	1.58	0.96	0.80	0.66	0.61	0.62	0.63
C2	1.67	1.19	0.96	0.71	0.58	0.70	0.50	0.39	0.34	0.30	0.35	0.31
C3	2.25	1.83	1.33	1.10	0.81	1.10	0.75	0.63	0.53	0.48	0.58	0.57
C4	2.96	2.17	1.75	1.39	1.01	1.31	0.94	0.83	0.64	0.68	0.56	0.57
C5	9.73	6.13	4.60	3.84	2.80	3.79	2.61	0.00	1.79	1.72	1.61	1.56
Hexene	66.08	39.14	30.90	24.81	18.98	25.02	17.78	15.51	12.10	11.09	10.45	10.31
Hexane	2.27	1.55	1.29	1.17	0.91	1.20	0.91	0.85	0.73	0.65	0.72	0.63
Iso C6	5.68	1.84	1.34	1.09	0.75	0.77	0.54	0.55	0.46	0.44	0.47	0.32
Heptene	4.32	2.80	2.23	1.76	1.44	1.70	1.25	1.07	0.79	0.77	0.74	0.72
Heptanal	0.00	3.08	2.67	2.34	1.65	2.02	1.58	1.42	1.12	1.12	0.93	0.98
7-Tridecanone	0.00	7.52	8.23	8.37	7.34	9.48	1.25	7.53	6.37	6.37	6.95	7.05

Reaction condition: W/F 34 g·h/mol, $T_{reaction}$ 400 °C, $T_{activate}$ 600 °C, T_{reduce} 600 °C, Flow H_2 100 ml/min, atmospheric pressure.

6. Effect of preparation method CoPt bimetallic

Table F19 The heptanoic acid conversion and yield of products over 5%Co+0.5%Pt/SiO_2

	Time on stream (min)											
	30	60	90	120	150	180	210	240	270	300	330	360
Conversion	100.00	100.00	95.02	81.25	93.97	88.31	86.60	85.08	88.49	79.49	78.30	74.44
Yield (%)												
C1	3.54	1.33	1.30	0.97	1.28	1.25	0.82	1.26	1.20	1.20	0.93	0.85
C2	0.55	0.51	0.42	0.27	0.42	0.39	0.06	0.40	0.36	0.40	0.30	0.37
C3	2.21	1.33	1.26	0.95	1.32	1.19	1.15	1.19	1.22	1.00	0.97	1.01
C4	3.59	1.57	1.48	1.27	1.63	1.44	1.47	1.41	1.55	1.30	1.26	1.00
C5	8.63	6.49	5.93	5.03	5.58	5.80	4.59	0.00	4.86	4.17	4.04	3.90
Hexene	28.59	54.41	49.07	42.40	48.83	45.39	45.63	44.10	46.43	40.75	39.89	38.36
Hexane	22.25	17.87	15.65	11.25	15.24	12.68	12.49	12.01	12.86	10.94	10.67	10.22
Iso C6	29.58	14.33	10.56	7.03	10.25	8.19	7.12	6.69	7.07	6.21	5.59	5.08
Heptene	1.06	2.16	1.95	1.89	2.09	2.10	2.05	2.05	2.12	1.90	1.85	1.85
Heptanal	0.00	0.00	4.10	5.91	3.87	5.49	5.81	5.83	5.80	5.94	6.16	5.86
7-Tridecanone	0.00	0.00	3.29	4.27	3.45	4.40	2.05	5.56	5.03	5.67	6.63	5.95

Reaction condition: W/F 34 g·h/mol, $T_{reaction}$ 400 °C, $T_{activate}$ 600 °C, T_{reduce} 600 °C, Flow H_2 100 ml/min, atmospheric pressure.

Table F20 The heptanoic acid conversion and yield of products over 5%Co+0.5%Pt/SiO_2 (SIP) after calcine catalyst

	Time on stream (min)											
	30	60	90	120	150	180	210	240	270	300	330	360
Conversion	100.00	100.00	93.92	90.53	81.07	76.23	71.45	64.98	58.57	58.02	59.11	63.07
Yield (%)												
C1	2.69	3.12	2.57	2.54	2.28	2.24	1.91	1.92	1.69	1.67	1.83	1.90
C2	1.80	1.79	1.53	1.41	1.28	1.24	1.01	0.95	0.85	0.85	0.89	0.94
C3	2.52	2.38	2.12	2.04	1.73	1.69	1.52	1.42	1.24	1.20	1.30	1.32
C4	2.12	2.20	2.05	2.14	1.94	1.86	1.67	1.50	1.33	1.30	1.34	1.61
C5	6.65	6.73	6.21	5.95	5.14	5.10	4.64	0.00	3.87	3.85	3.70	4.07
Hexene	49.69	52.49	49.66	47.23	42.81	39.90	38.12	33.92	30.15	29.70	30.45	32.90
Hexane	15.61	15.00	12.73	11.43	9.73	8.83	7.87	6.98	6.04	5.84	6.10	6.45
Iso C6	16.60	11.62	8.82	7.25	5.85	5.12	4.12	4.06	3.41	3.14	3.20	3.16
Heptene	2.32	2.61	2.20	2.44	2.26	2.14	2.03	1.87	1.64	1.68	1.76	1.85
Heptanal	0.00	2.06	3.87	5.50	5.66	5.56	6.23	6.02	5.61	6.02	6.39	7.07
7-Tridecanone	0.00	0.00	2.15	2.62	2.39	2.56	2.03	2.27	2.75	2.77	2.17	1.80

Reaction condition: W/F 34 g·h/mol, $T_{reaction}$ 400 °C, $T_{activate}$ 600 °C, T_{reduce} 600 °C, Flow H_2 100 ml/min, atmospheric pressure.

Table F21 The heptanoic acid conversion and yield of products over 5%Co+0.5%Pt/SiO_2 (SIP) non-calcine catalyst

	Time on stream (min)											
	30	60	90	120	150	180	210	240	270	300	330	360
Conversion	100	100	100	100	100	100	100	100	100	100	100	100
Yield (%)												
C1	1.44	1.05	0.89	0.81	0.85	0.92	0.80	0.76	0.73	0.76	0.72	0.74
C2	0.44	0.42	0.37	0.39	0.40	0.43	0.42	0.39	0.44	0.40	0.40	0.40
C3	0.46	0.47	0.45	0.46	0.45	0.46	0.47	0.49	0.49	0.45	0.45	0.49
C4	0.54	0.45	0.47	0.47	0.43	0.48	0.43	0.43	0.49	0.50	0.40	0.53
C5	0.96	0.88	0.85	0.86	0.84	0.91	0.86	0.00	0.88	0.87	0.89	0.87
Hexene	7.13	6.86	6.94	7.77	8.02	7.77	9.49	9.70	10.77	11.69	12.33	12.53
Hexane	73.32	71.90	70.77	69.62	69.11	67.98	68.87	69.50	68.37	69.23	68.59	67.80
Iso C6	2.65	2.53	2.57	2.89	3.02	3.00	3.68	3.63	4.12	4.35	4.71	4.81
Heptene	0.00	0.00	0.00	0.00	0.00	0.00	0.00	0.00	0.00	0.00	0.00	0.00
Heptanal	2.40	3.23	3.95	3.72	3.98	4.51	3.02	2.90	2.59	1.84	1.83	1.99
7-Tridecanone	0.00	0.00	0.00	0.00	0.00	0.00	0.00	0.00	0.00	0.00	0.00	0.00

Reaction condition: W/F 34 g·h/mol, $T_{reaction}$ 400 °C, $T_{activate}$ 600 °C, T_{reduce} 600 °C, Flow H_2 100 ml/min, atmospheric pressure.

7. Effect of platinum loading

Table F22 The heptanoic acid conversion and yield of products over 5%Co+0.25%Pt/SiO_2

	Time on stream (min)											
	30	60	90	120	150	180	210	240	270	300	330	360
Conversion	100.00	95.67	85.05	74.10	69.54	66.44	56.14	58.71	53.11	51.83	50.39	45.80
Yield (%)												
C1	3.35	2.39	2.20	1.92	1.71	1.63	1.32	1.41	1.11	1.07	0.81	1.13
C2	1.59	1.41	1.23	1.02	0.93	0.87	0.68	0.73	0.24	0.23	0.35	0.53
C3	2.03	2.00	1.65	1.41	1.26	1.19	1.02	0.99	0.92	0.84	0.85	0.80
C4	2.18	2.45	1.94	1.63	1.51	1.54	1.18	1.19	0.93	1.03	1.01	0.96
C5	6.38	6.64	5.74	4.87	4.54	4.39	3.56	0.00	3.29	3.20	3.18	2.82
Hexene	52.14	52.39	46.53	40.22	37.64	35.38	30.36	31.31	28.91	27.90	27.45	23.74
Hexane	13.62	11.02	9.47	7.34	6.58	6.06	5.03	5.15	4.71	4.73	4.35	3.80
Iso C6	16.31	10.39	7.17	5.20	4.32	4.36	2.88	3.19	2.58	2.35	2.18	2.37
Heptene	2.40	2.62	2.34	2.13	2.04	1.86	1.62	1.70	1.57	1.47	1.45	1.32
Heptanal	0.00	2.92	3.75	4.44	4.84	4.85	4.52	5.01	4.65	4.81	4.75	4.26
7-Tridecanone	0.00	1.45	3.03	3.91	4.18	4.30	1.62	4.38	4.20	4.21	4.03	4.07

Reaction condition: W/F 34 g·h/mol, $T_{reaction}$ 400 °C, $T_{activate}$ 600 °C, T_{reduce} 600 °C, Flow H_2 100 ml/min, atmospheric pressure.

Table F23 The heptanoic acid conversion and yield of products over 5%Co+0.5%Pt/SiO_2

	Time on stream (min)											
	30	60	90	120	150	180	210	240	270	300	330	360
Conversion	100.00	100.00	95.02	81.25	93.97	88.31	86.60	85.08	88.49	79.49	78.30	74.44
Yield (%)												
C1	3.54	1.33	1.30	0.97	1.28	1.25	0.82	1.26	1.20	1.20	0.93	0.85
C2	0.55	0.51	0.42	0.27	0.42	0.39	0.06	0.40	0.36	0.40	0.30	0.37
C3	2.21	1.33	1.26	0.95	1.32	1.19	1.15	1.19	1.22	1.00	0.97	1.01
C4	3.59	1.57	1.48	1.27	1.63	1.44	1.47	1.41	1.55	1.30	1.26	1.00
C5	8.63	6.49	5.93	5.03	5.58	5.80	4.59	0.00	4.86	4.17	4.04	3.90
Hexene	28.59	54.41	49.07	42.40	48.83	45.39	45.63	44.10	46.43	40.75	39.89	38.36
Hexane	22.25	17.87	15.65	11.25	15.24	12.68	12.49	12.01	12.86	10.94	10.67	10.22
Iso C6	29.58	14.33	10.56	7.03	10.25	8.19	7.12	6.69	7.07	6.21	5.59	5.08
Heptene	1.06	2.16	1.95	1.89	2.09	2.10	2.05	2.05	2.12	1.90	1.85	1.85
Heptanal	0.00	0.00	4.10	5.91	3.87	5.49	5.81	5.83	5.80	5.94	6.16	5.86
7-Tridecanone	0.00	0.00	3.29	4.27	3.45	4.40	2.05	5.56	5.03	5.67	6.63	5.95

Reaction condition: W/F 34 g·h/mol, $T_{reaction}$ 400 °C, $T_{activate}$ 600 °C, T_{reduce} 600 °C, Flow H_2 100 ml/min, atmospheric pressure.

Table F24 The heptanoic acid conversion and yield of products over 5%Co+0.75%Pt/SiO_2

	Time on stream (min)											
	30	60	90	120	150	180	210	240	270	300	330	360
Conversion	100.00	100.00	94.12	93.29	86.40	85.62	84.15	80.19	80.38	74.98	75.71	73.42
Yield (%)												
C1	2.35	1.97	1.71	1.73	1.58	1.49	1.47	1.40	1.16	1.05	1.12	0.83
C2	1.15	1.11	1.01	1.05	0.99	0.89	0.92	0.85	0.28	0.26	0.10	0.33
C3	1.58	1.46	1.39	1.40	1.30	1.24	1.21	1.14	1.17	1.05	0.99	1.05
C4	1.48	1.50	1.59	1.53	1.21	1.30	1.36	1.22	1.25	1.12	1.10	1.08
C5	4.75	5.36	5.10	4.76	4.29	4.29	4.18	0.00	3.86	3.50	3.41	3.28
Hexene	48.98	52.17	48.48	48.71	44.64	45.06	44.45	41.40	42.51	39.10	39.06	38.59
Hexane	19.69	17.36	15.49	15.17	14.01	13.56	13.19	12.69	12.88	11.58	12.25	11.59
Iso C6	18.30	14.13	12.11	10.40	9.97	8.54	7.96	7.88	7.37	6.86	7.27	6.02
Heptene	1.72	2.02	1.90	1.97	1.83	1.82	1.78	1.68	1.66	1.57	1.46	1.49
Heptanal	0.00	2.91	3.82	4.69	4.95	5.83	6.22	6.19	6.36	6.78	6.60	7.10
7-Tridecanone	0.00	0.00	1.53	1.87	1.62	1.58	1.78	1.77	1.88	2.12	2.36	2.06

Reaction condition: W/F 34 g·h/mol, $T_{reaction}$ 400 °C, $T_{activate}$ 600 °C, T_{reduce} 600 °C, Flow H_2 100 ml/min, atmospheric pressure.

8. Effect of contact time

Table F25 The heptanoic acid conversion and yield of products over 5%Co+0.5%Pt/SiO_2 (W/F = 12 g·h/mol)

	Time on stream (min)											
	30	60	90	120	150	180	210	240	270	300	330	360
Conversion	100.00	61.35	46.43	44.61	41.68	39.43	37.62	38.26	35.74	34.21	32.36	34.52
Yield (%)												
C1	0.68	0.30	0.25	0.22	0.24	0.17	0.07	0.09	0.24	0.24	0.15	0.24
C2	0.62	0.35	0.29	0.20	0.32	0.27	0.26	0.23	0.23	0.24	0.24	0.26
C3	1.55	0.74	0.64	0.61	0.57	0.52	0.55	0.60	0.55	0.58	0.46	0.50
C4	1.67	0.80	0.55	0.39	0.40	0.50	0.36	0.49	0.47	0.30	0.43	0.32
C5	6.88	3.44	2.42	2.28	2.12	2.02	1.92	0.00	1.87	1.76	1.72	1.83
Hexene	65.66	35.45	24.94	23.20	21.15	19.23	18.36	18.67	17.23	16.08	15.16	16.32
Hexane	8.37	3.54	2.55	2.42	2.19	1.99	1.89	1.88	1.66	1.60	1.44	1.58
Iso C6	11.47	2.69	1.44	1.25	1.16	1.38	1.24	0.93	0.81	0.77	0.65	0.65
Heptene	3.11	1.69	1.12	1.00	0.98	0.87	0.86	0.89	0.86	0.78	0.76	0.85
Heptanal	0.00	3.59	3.26	3.34	3.07	2.96	2.83	2.92	2.71	2.55	2.45	2.68
7-Tridecanone	0.00	8.78	8.98	9.71	9.48	9.53	0.86	9.55	9.12	9.32	8.89	9.29

Reaction condition: W/F 12 g·h/mol, $T_{reaction}$ 400 °C, $T_{activate}$ 600 °C, T_{reduce} 600 °C, Flow H_2 100 ml/min, atmospheric pressure.

Table F26 The heptanoic acid conversion and yield of products over 5%Co+0.5%Pt/SiO_2 (W/F = 17 g·h/mol)

	Time on stream (min)											
	30	60	90	120	150	180	210	240	270	300	330	360
Conversion	100.00	67.49	53.68	49.49	49.80	45.03	50.17	41.15	35.20	38.78	41.48	38.79
Yield (%)												
C1	0.95	0.39	0.59	0.45	0.45	0.44	0.41	0.34	0.45	0.41	0.42	0.20
C2	0.82	0.44	0.52	0.24	0.27	0.13	0.36	0.21	0.41	0.25	0.29	0.26
C3	1.39	0.89	0.69	0.73	0.66	0.67	0.70	0.57	0.53	0.54	0.65	0.54
C4	1.70	1.18	1.04	0.76	0.77	0.68	0.73	0.63	0.45	0.61	0.93	0.88
C5	6.34	3.77	2.83	2.74	2.83	2.52	2.79	0.00	2.02	2.11	2.31	2.21
Hexene	62.80	38.02	28.10	26.82	26.55	24.19	26.53	21.66	18.09	20.01	20.85	19.41
Hexane	10.05	5.69	4.12	3.90	3.69	3.34	3.70	2.98	2.37	2.68	2.78	2.58
Iso C6	13.14	4.72	3.45	2.44	2.25	1.95	2.47	1.93	1.50	1.66	1.76	1.58
Heptene	2.80	1.79	1.31	1.25	1.29	1.13	1.28	1.06	0.94	1.00	1.04	0.98
Heptanal	0.00	4.32	3.98	3.78	4.06	3.79	4.38	3.58	3.11	3.44	3.71	3.62
7-Tridecanone	0.00	6.28	7.07	6.39	6.98	6.18	1.28	5.90	5.32	6.08	6.74	6.54

Reaction condition: W/F 17 g·h/mol, $T_{reaction}$ 400 °C, $T_{activate}$ 600 °C, T_{reduce} 600 °C, Flow H_2 100 ml/min, atmospheric pressure.

Table F27 The heptanoic acid conversion and yield of products over 5%Co+0.5%Pt/SiO_2 (W/F = 22 g·h/mol)

	Time on stream (min)											
	30	60	90	120	150	180	210	240	270	300	330	360
Conversion	100.00	85.48	74.89	71.29	72.10	64.66	61.11	57.53	58.53	69.08	50.59	49.50
Yield (%)												
C1	1.95	1.60	1.41	1.27	1.35	0.79	0.72	1.13	1.17	1.67	1.09	0.97
C2	1.39	1.09	0.92	0.83	0.87	0.37	0.37	0.81	0.69	0.89	0.58	0.53
C3	1.86	1.48	1.24	1.16	1.20	1.08	0.98	1.00	0.97	1.19	0.85	0.81
C4	1.93	1.77	1.47	1.20	1.41	1.26	1.15	1.10	1.60	1.23	0.94	0.77
C5	6.59	5.34	4.48	4.30	4.26	3.92	3.62	0.00	3.49	4.00	2.77	2.95
Hexene	58.92	47.64	40.24	38.48	38.23	34.74	31.77	29.48	30.11	36.92	25.86	25.68
Hexane	12.75	9.15	7.73	7.00	6.93	6.00	5.48	4.91	5.41	6.48	4.78	4.56
Iso C6	12.01	6.73	5.48	4.52	4.38	3.50	3.67	2.84	2.83	4.04	2.39	2.60
Heptene	2.60	2.32	1.96	1.94	1.92	1.87	1.70	1.55	1.61	2.13	1.42	1.30
Heptanal	0.00	4.56	4.82	5.53	5.83	5.75	6.12	5.43	6.27	7.76	5.50	5.32
7-Tridecanone	0.00	3.82	5.14	5.08	5.72	5.39	1.70	5.66	4.38	2.77	4.41	4.01

Reaction condition: W/F 22 g·h/mol, $T_{reaction}$ 400 °C, $T_{activate}$ 600 °C, T_{reduce} 600 °C, Flow H_2 100 ml/min, atmospheric pressure.

Table F28 The heptanoic acid conversion and yield of products over 5%Co+0.5%Pt/SiO_2 (W/F = 34 g·h/mol)

	Time on stream (min)											
	30	60	90	120	150	180	210	240	270	300	330	360
Conversion	100.00	100.00	95.02	81.25	93.97	88.31	86.60	85.08	88.49	79.49	78.30	74.44
Yield (%)												
C1	3.54	1.33	1.30	0.97	1.28	1.25	0.82	1.26	1.20	1.20	0.93	0.85
C2	0.55	0.51	0.42	0.27	0.42	0.39	0.06	0.40	0.36	0.40	0.30	0.37
C3	2.21	1.33	1.26	0.95	1.32	1.19	1.15	1.19	1.22	1.00	0.97	1.01
C4	3.59	1.57	1.48	1.27	1.63	1.44	1.47	1.41	1.55	1.30	1.26	1.00
C5	8.63	6.49	5.93	5.03	5.58	5.80	4.59	0.00	4.86	4.17	4.04	3.90
Hexene	28.59	54.41	49.07	42.40	48.83	45.39	45.63	44.10	46.43	40.75	39.89	38.36
Hexane	22.25	17.87	15.65	11.25	15.24	12.68	12.49	12.01	12.86	10.94	10.67	10.22
Iso C6	29.58	14.33	10.56	7.03	10.25	8.19	7.12	6.69	7.07	6.21	5.59	5.08
Heptene	1.06	2.16	1.95	1.89	2.09	2.10	2.05	2.05	2.12	1.90	1.85	1.85
Heptanal	0.00	0.00	4.10	5.91	3.87	5.49	5.81	5.83	5.80	5.94	6.16	5.86
7-Tridecanone	0.00	0.00	3.29	4.27	3.45	4.40	2.05	5.56	5.03	5.67	6.63	5.95

Reaction condition: W/F 34 g·h/mol, $T_{reaction}$ 400 °C, $T_{activate}$ 600 °C, T_{reduce} 600 °C, Flow H_2 100 ml/min, atmospheric pressure.

AURTHER BIOGRAPHY

Name	Ms. Ploynisa Phichitsurathaworn
Date of Birth	28 January 1993
Address	668 Moo 6 Sukhumvit Rd. Samrong Nua, Mueang, Samut Prakan 10270

Education

2010 Senior Higher School in Science and Mathermatics from Assumption Samutprakarn School GPA 3.29.

2014 Bachelor of Science in Industrial Chemistry from King Mongkut's Institute of Technology Ladkrabang GPA 3.32.

Work experience

Mar – April 2014 Internship at Thai Mitsui Specialty Chemicals Co., Ltd.

2015 – 2017 Teacher Assistant, King Mongkut's Institute of Technology Ladkrabang.

International Conferences

2017 Ploynisa Phichitsurathaworn, Tawan Sooknoi and Kittisak Choojun, "*Deoxygenation of heptanoic acid over cobalt supported silica catalysts*", Poster presentation, Pure and App;ied Chemistry International Conference 2017 (PACCON 2017), February 2 -3, 2017, Centra Government Complex Hotel & Convention Centre Cheng Watthana, Bangkok, Thailand.

Publication

2017 Ploynisa Phichitsurathaworn, Tawan Sooknoi and Kittisak Choojun, "*Deoxygenation of heptanoic acid over cobalt supported silica catalysts*", PACCON 2017 Conference proceedings: 1316 – 1320.

Publication

Deoxygenation of heptanoic acid over cobalt supported silica catalysts

Ploynisa Phichitsurathaworn[1], Kittisak Choojun[1,2,*], and Tawan Sooknoi[1,2,**]

[1]Department of Chemistry, Faculty of Science, KMITL, Bangkok, 10520, Thailand
[2]Catalytic Chemistry Research Unit, Faculty of Science, KMITL, Bangkok, 10520, Thailand

*e-mail: kittisak.ch@kmitl.ac.th, **e-mail: kstawan@gmail.com

Abstract: The concern of the depletion of petroleum leads to the tremendously research to supply the needs of energy and petrochemicals. Plant oils are an alternative renewable feedstock because their fatty acid composition could convert to alpha olefins. In this work, we investigate the transformation of fatty acids to alpha olefins using heptanoic acid as a model compound via metal supported silica catalysts. At similar condition at 350 °C, the conversion of heptanoic acid using 5%wt. of various metal catalysts is in the order of Co > Ni > Cu > Cr. In term of selectivity, the results show that Co/SiO_2 and Ni/SiO_2 were selectively towards 1-hexene, which could derive from the decarbonylation reaction. Upon the increasing the reaction temperature from 350-425 °C, the conversion of heptanoic acid is enhanced. The optimal reaction temperature yielding the highest hexene selectivity is at 400 °C. Nevertheless, all of catalysts showed deactivation due to the strong adsorption of heptanoic acid and coke formation.

1. Introduction

Linear alpha olefins (LAOs) is the important chemicals widely used in industry. LAOs is commonly used as a co-monomer in the production of polyethylene. Moreover, it is also applied in detergent, synthetic lubricant, and plasticizer manufactures. Industrially, linear alpha olefins are commonly produced by two main routes. The first pathway is the oligomerization of ethylene and by Fischer-Tropsch synthesis. Another route is the dehydration of alcohols. However, these two processes depend on the non-renewable feedstock which is mostly from petrochemicals. The decarbonylation of fatty acids is an interesting alternative approach to subsidize those two processes since fatty acids is derived from renewable sources.

The use of fatty acid as chemical feedstocks is of interest in an agricultural country like Thailand. Conversion of fatty acids to oxygen-free hydrocarbons can be converted using catalysts via several reactions, such as, dehydration[1], ketonization[2], decarbonylation[3], and decarboxylation.[3,4] All of those reactions are classified as deoxygenation involving the production of linear alkane or alkene combining with CO_2 and or CO from fatty acids.

Metals over silica support, such as, platinum[5], palladium[6] and rhodium, are normally used as catalyst for this conversion. However, the yield of alkane is higher than the yield of alkene due to rapid hydrogenation of the olefins primarily formed.[7] Furthermore, those metals are somewhat expensive.

In this work, Co, Ni, Cr, and Cu supported on silica support as a catalyst for the deoxygenate reaction of heptanoic acid (a model compound of fatty acids) were investigated. The effect of reaction temperature and the stability of the catalyst were also evaluated.

2. Materials and Methods

2.1 Chemicals and materials

Heptanoic acid, purity 95.0%, Sigma-Aldrich. n-Octane, purity 99.0%, Carlo Erba. Cobalt (II) nitrate hexahydrate, purity 99.8%, Rankem. Copper (II) nitrate trihydrate, purity 99.5%, QREC. Nickel (II) nitrate hexahydrate, purity 99.0%, Carlo Erba. Chromium (III) nitrate nonahydrate, purity 97%, Fluka. Silicon dioxide, purity 99.0%, Carlo Erba.

2.2 Catalysts preparation

All of catalysts, silica was calcined in muffle oven by ramping to 600 °C at the heating rate of 5 °C/ minutes and holding for 1 hour. 2.5%wt Co/SiO_2 , 5%wt Cu/SiO_2 , 5%wt Ni/SiO_2 and 5%wt Cr/SiO_2 were prepared by wet impregnation (IMP). The solid was dried in oven at 100 °C for 24 hours. Then, the dried catalyst was calcined in tube furnace under a flow of air zero (60 mL/min) at 600 °C for 1 hour with a heating rate 5 °C/min.

2.3 Characterization

Temperature-programmed reduction by H_2 gas (H_2-TPR) was performed in a quartz tube connected with a thermal conductivity detector (VICI). Prior to analysis, the samples (0.1 g) were activated in air (flow rate of 30 mL/min) at a heating rate 10 °C /min up to 600 °C, followed by an isothermal treatment at 600 °C for 1 h. Subsequently, the system was naturally cooled down in the atmosphere of nitrogen gas (flow rate of 30 mL/min) to room temperature. Finally, the temperature reduction profile was recorded using 10% H_2 in Argon at the heating rate 5 °C/min, from 50 to 900 °C. The TCD signal was calibrated employing a known mass of CuO as a standard, considering that CuO is reduced stoichiometrically and completely to Cu and H_2O.

2.4 Catalytic activity testing

Deoxygenation of heptanoic acid was investigated at atmospheric pressure in a continuous fixed-bed reactor made with quartz tube (6.3 mm O.D.). Before the catalytic testing, the catalyst was activated by heating at 5 °C/min to its calcination temperature (600 °C) and was hold at that temperature for 1 hour under the stream of air zero (100 mL/min). Then H_2 gas for reduction with a heating of 5 °C/min to 600 °C and hold for 3 hours. After that the reaction was run at 350-425 °C for 6 hour. A solution of reactant, 10%wt heptanoic acid in octane, was fed to the reactor by a 10mL syringe connected to a syringe-pump. In each run, the catalyst bed under a 100 mL/min flow of H_2. Products were analyst by online gas chromatograph (Varian 3800). The gas sample was collected in gas sampling loop, then periodically injected into GC column (MXT-1, 60 m length, 0.25 mm internal diameter, 0.5 μm film thickness) connected to flame ionized detectors (FID). Each peak areas from the chromatogram was measured and calculated. Then each peak was identified by comparing with standard and the composition of each products was determined by calibration of standard.

3. Results & Discussion

3.1 Catalysts characterization

TPR profile of all catalysts included 5% wt monometallic; Cu, Cr, Ni, Co supported on SiO_2 are collected in Figure 1. Only 5%Cu/SiO_2 shows a sharp reduction peak at 250 °C corresponding to the reduction of Cu^{2+} to Cu^0. However, the others are observed two humps where the reduction temperature is higher than that of the Cu. 5%Cr loaded catalyst is reduced around 300-400 °C due to Cr^{6+} become Cr^{3+} lattice. The reduction of Ni^{2+} to Ni^0 takes place at 300-400 °C as well but the second peak has higher intensity than that of Cr. For the

cobalt catalyst, two peaks at 350 °C and 450 °C are attributed to the reduction of Co^{3+} to Co^{2+} species and Co^{2+} to Co^{0}, respectively. However, some weak reduction peak is found at high temperature (750-850 °C). At this high reduction temperature could be the result of strong interaction of Co-O with silica or cobalt silicates.

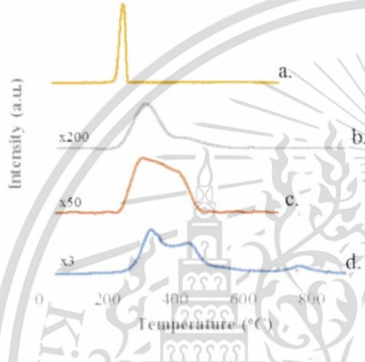

Figure 1. TPR profiles of 5%Cu/SiO_2 (a), 5%Cr/SiO_2 (b), 5%Ni/SiO_2 (c) and 5%Co/SiO_2 (d).

3.2 Catalysts activity

Aim of the olefin production,

heptanoic acid is represented as feed model because of its availability and handling. In general, the possible reactions of heptanoic acid are shown in Figure 2. The conversions of heptanoic acid over various catalysts under atmospheric H_2 at 350 °C are shown in Table1.

Table 1. Catalytic performance on deoxygenation of various metal over silica catalysts

Catalyst	Conversion (%)	Hexene yield (%)	Heptanal yield (%)	C1-5 yield (%)	7-tridecanone yield (%)	Hexane yield (%)
5%Co/SiO_2	15.4	5.4	4.8	3.1	1.0	0.3
5%Ni/SiO_2	5.3	2.0	1.5	0.6	0.5	0.2
5%Cu/SiO_2	2.9	0.1	1.2	0.1	1.6	0.0
5%Cr/SiO_2	2.2	0.1	1.1	0.1	1.0	0.0

Condition 10%Heptanoic acid in octane, contact time 20 g·h/mol, reaction temperature 350 °C, activation temperature 550 °C and reduction temperature 500 °C

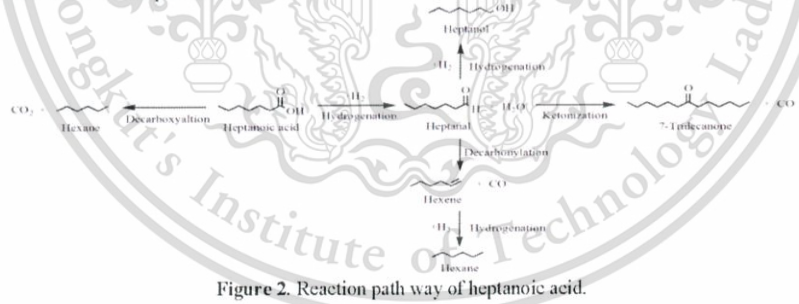

Figure 2. Reaction path way of heptanoic acid.

The conversion and products are evaluated at 30 min. before the deactivation. Concisely, it can be seen that catalysts' activity is in the order of Co > Ni > Cu > Cr. According to the product distribution, we can classified catalysts into two types where Cu and Cr are in the same group, Co and Ni are in the other group. For Cu and Cr the two main products are heptanal and 7-tridecanone. This means that Cu and Cr are favorable towards to hydrogenation forming heptanal and subsequently ketonization forming 7-tridecanone. So, Cu and Cr are not active towards decarbonylation since very low amount of hexene was observed. Interestingly, they does not hydrogenation heptanal to heptanol but rather active to ketonization. Considering Co and Ni, both of them gave the hexene as the main product which results from decarbonylation yielding the desired olefins. Interestingly, the decarboxylation does not occur so that the alkene or unsaturated product can be obtained. Additionally, 7-tridecanone was observed indicating the ketonization. These results can be assumed that the high oxophilic metal site, such as, Cr tends to form oxo-intermediate which is facile the hydrogenation. In the same word, metal with high oxophilicity does not appropriate for olefin production. Moreover, we observed some cracking product in the form of light hydrocarbon in range C1-5. The cracking depends on Lewis acid character of each metal sites. From this result cobalt was choosen to investigate other parameters throughout this work.

The effect of reaction temperature for deoxygenation of heptanoic acid was studied from 350 to 425 °C referred to thermodynamic behavior of decarbonylation. The results are presented in Figure 3.

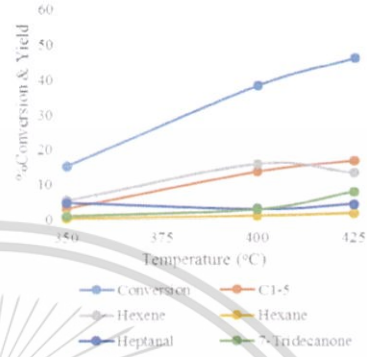

Figure 3. The effect of the reaction temperature on the conversion of heptanoic acid and yield of products from the deoxygenation of heptanoic acid over 5%Co SiO_2. Reaction conditions: 10% Heptanoic acid in octane, contact time 20 g·h mol, temperature 350-425 °C, 30 min., 1 atm, and 100 ml/ min of H_2.

As expected, the conversion is enhanced upon the increasing reaction temperature from 15% conversion at 350 °C to 50% conversion at 425 °C. The decarbonylation product, hexene, was also increased with the raising the temperature but it was decreased when the temperature changed from 400 °C to 425 °C. This could be the result of the ketonization reaction which is promoted at 425 °C, so that, heptanal is converted to 7-tridecanone faster than decarbonylation. Upon increasing the temperature, ketonization and cracking reaction were promoted due to the themodynamic favorable.

Since, the temperature at 400 °C gave the highest hexene with the fair conversion. So, the longer reaction time at 400 °C using 5%Co/SiO_2 was investigated to study the stability of the catalysts. The result is shown in Figure 4.

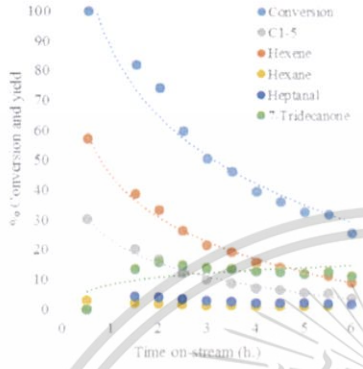

Figure 4. The deoxygenation activity of 5%Co/SiO_2. Reaction condition: 10%Heptanoic acid in octane, contact time 1.64 g.h/mol, basis on Co, temperature 400°C, 30 min, 1 atm, and 100 mL/min of hydrogen gas.

As can be seen, the conversion was decreased from 100% at 30 min. to 20% at 6 hours. This indicates the deactivation of the catalyst which could due to the heptanoic acid and product adsorption. Furthermore, it could be the result of coke formation leading to the lower metal active site. Interesting, hexene product from the decarbonylation was the main product at all time.

4. Conclusion

Co supported on SiO_2 showed the highest activity towards heptanoic acid reaction and mainly yielded hexene via decarbonylation. Ni is the second best among Co, Ni, Cu, and Cr to produce hexene. In contrast, Cu and Cr favor the hydrogenation producing heptanal and ketonization producing 7-tridecanone. When the reaction performed at 400 °C, the selectivity of hexene is highly promoted with fairly compromising cracking. However, the catalysts' deteriorate could be found in long period of time due to strong adsorption of heptanoic acid and carbon deposition.

Acknowledgements

This research was supported by Basic Research Grant (BRG 5680007, to T.S.) of the Thailand Research Fund and King Mongkut's Institute of Technology Ladkrabang, Department of Chemistry, Faculty of Science.

References.

1. Hachemi, A. N. I.; Jeništová, K.; Mäki-Arvela P.; Kumar, N.; Eränen K.; Hemminge J.; and Murzin, D.Y. *Catal. Sci. Tech* **2016**, *00*, 1-3.
2. Nagashima, O.; Sato, S.; Takahashi, R.; Sodesawa, T. *Journal of Molecular Catalysis A: Chemical* **2005**, *227*,231–239.
3. Santillan-Jimenez, E.; and Crocker, M. *J Chem Technol Biotechnol* **2012**, *87*, 1041–1050.
4. Na, J.G.; Yi, B.E.; Kim, J.N.; Yi, K.B.; Park, S.Y.; Park, J.H.; Kim, J.n.; Ko, C.H. *Catalysis Today* **2010**, *156*, 44–48.
5. Lopez-Ruiz, A.J.; and Davis, J.R. *Green Chem* **2014**, *16*,683.
6. Sari, E.; Kim, M.; Salley, O.S.; Ng, S.K.Y. *Applied Catalysis A: General* **2013**, *467*, 261–269.
7. Snåre, M.; Kubičková, I.; Mäki-Arvela, P.; Eränen, K.; and Murzin, Y.D. *Ind. Eng. Chem. Res* **2006**, *45*, 5708-5715.